Wnt/β–catenin Signaling Defines Organizing Centers That Orchestrate Growth and Differentiation of the Regenerating Zebrafish Caudal Fin

D I S S E R T A T I O N

zur Erlangung des Doktorgrades

Doctor rerum naturalium

(Dr. rer. nat.)

der Fakultät für Naturwissenschaften der Universität Ulm

vorgelegt von

Daniel Wehner

geb. in Ludwigshafen, Deutschland

Ulm, 2013

Amtierender Dekan:	Prof. Dr. Joachim Ankerhold
1. Gutachter:	Prof. Dr. Michael Kühl
2. Gutachter:	Prof. Dr. Thomas Wirth
Tag der Promotion:	11.02.2014

Table of Contents

List of Figures 2
List of Tables 4
Abbreviations 5
List of Publications Based on Doctoral Studies 8
Summary 9
Zusammenfassung 11

1 Introduction 14

1.1 Motivation 14
1.2 Cellular Mechanisms of Tissue Regeneration 15
1.3 Appendage Regeneration in the Teleost *Danio Rerio* 17
1.4 Wnt Signal Transduction Pathways 20
1.4.1 Wnt Genes and Proteins 21
1.4.2 The β–catenin-Dependent Wnt Signaling Pathway 22
1.5 Wnt β–catenin Signaling in Tissue Regeneration 25

2 Aims of the Study 27

3 Material and Methods 29
3.1 Materials 29
3.1.1 Technical Equipment 29
3.1.2 Chemicals and Consumables 30
3.1.3 Reagents and Buffers 30
3.1.4 Molecular Biology / Biochemistry Kits 31
3.1.5 Antibodies 32
3.1.6 Plasmids and Constructs 32
3.1.7 Oligos 35
3.1.8 Transgenic Zebrafish Lines 36

3.2 Methods 37
3.2.1 Fish Husbandry and Fish Transgenesis 37
3.2.2 Fin Amputations, Heat Shocks, Drug Treatments, Irradiation and Regenerate Length Measurements 38
3.2.3 Synthesis of Capped Sense RNA and Labeled RNA Probes 39
3.2.4 RNA Whole Mount in situ Hybridization (ISH) and Cryosectioning 39
3.2.5 Immunohistochemistry 41
3.2.6 Detection of cell death 42
3.2.7 BrdU Incorporation 43
3.2.8 Tissue Histology 43
3.2.9 Preparation of Fin Regenerate Lysates and Immunoblotting 43
3.2.10 Dissociation of Fin Regenerates and Flow Cytometry 44
3.2.11 RNA Extraction and cDNA Synthesis 44
3.2.12 RT-PCR 45
3.2.13 Genotyping 45
3.2.14 Microarray Analysis 45
3.2.15 Weighted Gene Expression Correlation Network Analysis 47
3.2.16 Statistics 49
3.2.17 Nomenclature 49

4 Results 50
4.1 Transgenic Wnt Reporter Lines Reveal Spatiotemporal Dynamics of Pathway Activation 50
4.2 Tcf/Lef Transcription Factor Expression in the Regenerating Caudal Fin 53
4.3 The Wound Epidermis is Not Competent to Respond to Wnt Ligands Activating β–catenin Signaling 56
4.4 Frizzled Receptor Expression in the Regenerating Caudal Fin 59
4.5 Wnt/β–catenin Signaling is Active in Different Blastemal Compartments with Distinct Proliferative Properties and Wnt Co-Receptor Expression 60
4.6 Tissue-Specific Pathway Manipulation Indicates That Wnt/β–catenin Signaling in the Proximal Blastema, in Committed Osteoblasts, or the Wound Epidermis Has no Role in Regulating Regenerative Cell Proliferation 66
4.7 Wnt/β–catenin Signaling in the Actinotrichia-Forming Cells is Required for Osteoblast Differentiation 72
4.8 Identification of the Wnt Targetome in the Regenerating Caudal Fin 74
4.9 Wnt/β–catenin Signaling is Required for Expression of Ligands, Pathway Components and Target Genes of Numerous Signaling Pathways Involved in Regeneration 76
4.10 Wnt/β–catenin Signaling Receives Little Reciprocal Input from the Signaling Pathways it Regulates 80

4.11 Wnt/β–catenin Signaling Indirectly Regulates Epidermal Patterning Through Fgf and Bmp Signaling 82
4.12 Wnt/β–catenin Signaling Regulates Maintenance of the Wound Epidermis via a Retinoic Acid/Igf-Signaling Axis 85
4.13 Blastemal Cell Proliferation is Regulated by β–catenin Pathway via Hedgehog and Retinoic Acid Signaling 86
4.14 Amputation-Induced Jnk Activity, ROS Production or Immune System Activation is Dispensable for Wnt/β-catenin Pathway Activation During Caudal Fin Regeneration 89

5 Discussion 91
5.1 A Model for Wnt/β–catenin Signaling Functions During Caudal Fin Regeneration 91
5.2 Signaling Pathway Interactions during vertebrate Appendage Regeneration 94
5.3 Wound Signals Activating Wnt/β–catenin Signaling During Caudal Fin Regeneration 95
5.4 Tcf1/Lef11 Function in the Wound Epidermis 96
5.5 Parallels and Differences to Amniote Limb Development 96
5.6 Wnt Signaling in Osteoblast Differentiation 97

6 References 100

7 Acknowledgements 109

8 Curriculum Vitae 110

9 Erklärung (Statement of Original Contribution) 111

10 Supplemental Information 112

List of Figures

Fig. 1.1. Cellular mechanisms of tissue regeneration 15
Fig. 1.2. The zebrafish caudal fin 28
Fig. 1.3. Stages of caudal fin regeneration 18
Fig. 1.4. Tissue compartments in the regenerating caudal fin 20
Fig. 1.5 The β–catenin-dependent Wnt signaling pathway 23
Fig. 3.1. Plasmid maps of constructs used for generation of *7xTCF-Xla.Siam*: 3xKaede and *ubiquitin:*irTAM2(3F)-p2A-AmCyan transgenic lines 34
Fig. 4.1. The *7xTCF*:mCherry transgenic reporter line reveals Wnt/β–catenin pathway activation during caudal fin regeneration 51
Fig. 4.2. *axin2* is expressed in the *7xTCF*:mCherry-positive blastema where it depends on Wnt/β–Catenin signaling 52
Fig. 4.3. *6xTCF*:dGFP and *Top*:dGFP transgenic reporter lines reveal Wnt/β–catenin pathway activation during fin regeneration 53
Fig. 4.4. Tcf/Lef transcription factor expression during caudal fin regeneration 55
Fig. 4.5. *lef1* expression depends on Wnt/β–catenin signaling during caudal fin regeneration 56
Fig. 4.6. *lrp5* and *lrp6* co-receptor expression during caudal fin regeneration 57
Fig. 4.7. *her4.3*:EGFP reporter activity is confined to the proliferative zone of the proximal medial blastema 57
Fig. 4.8. The wound epidermis is not competent to respond to Wnt ligands activating β–catenin signaling 58
Fig. 4.9. Frizzled receptor expression during caudal fin regeneration 59
Fig. 4.10. Tissue compartments in a caudal fin regenerate at 72 hpa 60
Fig. 4.11. Wnt activity in the proximal blastema is confined to the actinotrichia-forming cells 61-62
Fig. 4.12. Wnt/β–catenin signaling is active in the distal-most blastema 62
Fig. 4.13. The Wnt-receiving cells in the distal-most blastema define a scarcely-proliferative cell population 63
Fig. 4.14. The Wnt-receiving cells in the distal-most blastema retain their relative localization during regenerative growth 64
Fig. 4.15. *6xTCF*:dGFP reporter activity in the regenerating caudal fin at 72 hpa 65
Fig. 4.16. *lrp5* and *lrp6* co-receptors are distinctly expressed in the blastema during regenerative outgrowth of the caudal fin 65

Fig. 4.17. Systemic overexpression of *axin1* strongly inhibits blastemal cell proliferation and regenerative growth 66
Fig. 4.18. The TetON system is suitable for studying the tissue-specific role of Wnt/β–catenin signaling during caudal fin regeneration 68
Fig. 4.19. Wnt/β–catenin signaling is not required in the wound epidermis during caudal fin regeneration 69
Fig. 4.20. Wnt/β–catenin signaling is not required in committed osteoblasts during caudal fin regeneration 70
Fig. 4.21. Wnt/β–catenin signaling in the proximal medial blastema is not essential for regenerative growth during caudal fin regeneration 71
Fig. 4.22. Wnt/β–catenin signaling in the medial proximal blastema has little role in regulating blastemal cell proliferation 71
Fig. 4.23. Wnt/β–catenin signaling in the medial proximal blastema is required for differentiation of adjacently located osteoblasts 73
Fig. 4.24. Genes of WGCNA modules 26, 21 and 3 are co-expressed under conditions of Wnt inhibition 75
Fig. 4.25. *wnt10a* and *sost* expression depends on Wnt/β–catenin signaling during caudal fin regeneration 76
Fig. 4.26. Wnt/β–catenin signaling is required for expression of ligands, pathway components and target genes of many signaling pathways involved in regeneration of the zebrafish caudal fin 78
Fig. 4.27. *bmp4* and *actβB* are expressed in the Wnt-receiving cells 79
Fig. 4.28. Wnt/β–Catenin signaling receives little reciprocal input from other developmental signaling pathways during caudal fin regeneration 81-82
Fig. 4.29. Epidermal *lef1* expression is regulated via Bmp and Fgf signaling independently of Wnt/β–catenin signaling 84
Fig. 4.30. Wnt/β–catenin signaling regulates epidermal *pea3* and *erm* expression via Fgf/Ras signaling 84
Fig. 4.31. Wnt/β–catenin signaling regulates Igf signaling via retinoic acid signaling 86
Fig. 4.32. Wnt/β–catenin signaling regulates Hedgehog signaling 87
Fig. 4.33. Wnt/β–catenin signaling regulates blastemal cell proliferation via Hedgehog signaling 87
Fig. 4.34. Wnt/β–catenin signaling regulates blastemal cell proliferation via retinoic acid signaling 88-89
Fig. 4.35. Amputation-induced Jnk activity, ROS production or immune system activation is dispensable for activation of Wnt/β–catenin signaling during caudal fin regeneration 90
Fig. 5.1. A model for Wnt/β–catenin function during caudal fin regeneration 93

List of Tables

Table 3.1. Antibodies used 32
Table 3.2. Constructs used for generation of capped sense RNA 32
Table 3.3. Constructs used for synthesis of *in situ* hybridization probes 33
Table 3.4. Constructs used for generation of transgenic zebrafish lines 33
Table 3.5. RT-PCR Primer used for expression analysis of FACS-sorted cells 35
Table 3.6. Primer used for genotyping 35
Table 3.7. Primer used for generation of *7xTCF-Xla.Siam*:3xKaede and *ubiquitin:*irTAM2(3F)-p2A-AmCyan constructs 35
Table 3.8. Primer used for generation of *in situ* hybridization probe templates 35
Table 3.9. Transgenic zebrafish lines used 36
Table 3.10. Experimental design for identification of the Wnt targetome during caudal fin regeneration 46
Table 3.11. WGCNA modules significantly enriched for biological process and pathways as determined by DAVID Bioinformatics resource 48
Table 4.1. Gene composition of WGCNA modules 26, 21 and 3 75

Abbreviations

+	Positive
–	Negative
AER	Apical ectodermal ridge
Alk4	Activin receptor-like kinase receptor 4
AmpR	Ampicillin resistance
Ap	Alkaline phosphatase
Apc	Adenomatous polyposis coli
Ck	Casein kinase
BCIP	5-Brom-4-chlor-3-indolylphoshpat
Bmp	Bone morphogenetic protein
bp	Base pairs
BrdU	5-bromo-2-deoxyuridine
BSA	Bovine serum albumin
β–Trcp	β–Transducin repeat containing protein
bzw	beziehungsweise
°C	Degrees celcius
CDS	Coding sequence
Da	Dalton
Dkk	Dickkopf
Dapi	6-diamidino-2-phenylinodole
DIG	Digoxigenin
DMSO	Dimethylsulfoxid
DNA	Deoxyribonucleic acid
DOX	Doxycycline
dNTP	Deoxyribonucleotide triphosphate
dpa	Days post amputation
Dvl	Dishevelled
ECM	Extracellular matrix
EDTA	Ethylendiaminetetraacetic acid
e.g.	Exempli gratia (for example)
EGFP	Enhanced green fluorescent protein
ER	Endoplasmatic reticulum
EtOH	Ethanol
Fgfr	Fgf receptor

FACS	Fluorescence-activated cell sorting
Fgf	Fibroblast growth factor
Fig	Figure
Fzd	Frizzled
g	Gram or gravity
GFP	Green fluorescent protein
Gsk3	Glycogen synthase kinase 3
h	Hours
Hdac	Histone deacetylase
Hh	Hedgehog
H3P	Phospho-histone 3
hpa	Hours post amputation
Hrp	Horseradish peroxidase
Igf	Insulin-like growth factor
Igf1r	Insulin-like growth factor 1 receptor
Igfbp4	Insulin-like growth factor binding protein 4
INT	Iodonitrotetrazolium chloride
ISH	*In situ* hybridization
Jnk/Sapk	c-Jun N-terminal kinase/Stress-activated protein kinase
l	Liter
Lef	Lymphoid enhancer factor
Lrp5/6	Low-density lipoprotein receptor-related protein 5/6
m	Meter
M	Molare
Mapk	Mitogen-activated protein kinase
MeOH	Methanol
min	Minutes
mRNA	Messenger RNA
N	Normal
n.a.	No information available
NBT	Nitro Blue Tetrazolium
NCS	Newborn calf serum
Nicd	Notch intracellular domain
n.s.	Not significant
o/n	Over night
Osx	Osterix
PBS	Phosphate-buffered saline
Pcna	Proliferative cell nuclear antigen
PCR	Polymerase chain reaction
Pdgf	Platelet-derived growth factor
PFA	Paraformaldehyde
Pkc	Protein kinase C

Pod	Peroxidase
RA	retinoic acid
RNA	Ribonucleic acid
ROS	Reactive oxygen species
RT	Room temperature
RT-PCR	Reverse transcription PCR
s	Second
SAG	Smoothened agonist
SDS	Sodium dodecyl sulfate
sFrp	Secreted frizzled-related protein
Sost	Sclerostin
Suppl.	Supplemental
Tcf	T cell factor
TetA	TetActivator
TetRE	TetResponder
Tgfβ	Transforming growth factor β
TFM	Tissue freezing medium
Tle	Transducin-like enhancer of split
U	Unit
v/v	Volume per volume
WGCNA	Weighted gene expression correlation network analysis
WPI	World precision instruments
w/v	Weight per volume
wt	Wild type
YFP	Yellow fluorescent protein

List of Publications Based on Doctoral Studies

Wehner, D., Haase, C., Özhan, G. Vasudevaro, M., Kagermeier-Schenk, B., Röder, A., Moro, R., Argenton, F., and Weidinger, G. "Wnt/β–catenin signaling defines organizing centers that orchestrate growth and differentiation of the regenerating zebrafish caudal fin". Dev. Cell*, under revision.*

Özhan, G, Sezgin, E., **Wehner, D**., Pfister, A., Kühl, S. J., Kagermeier-Schenk, B., Kühl, M., Schwille, P., and Weidinger, G. (2013). "Lypd6 enhances Wnt/β–catenin signaling by promoting LRP6 phosphorylation in raft plasma membrane domains". Dev. Cell, *accepted.*

Grotek, B.*****, **Wehner, D**.*****, and Weidinger, G. (2013). "Notch signaling coordinates cellular proliferation with differentiation during zebrafish fin regeneration". Development *140*, 1412-1423. ***these authors contibuted equally to this work**

Kagermeier-Schenk, B., **Wehner, D**., Özhan-Kizil, G., Yamamoto, H., Li, J., Kirchner, K., Hoffmann, C., Stern, P., Kikuchi, A., Schambony, A.*, et al.* (2011). "Waif1/5T4 inhibits Wnt/beta-catenin signaling and activates noncanonical Wnt pathways by modifying LRP6 subcellular localization". Dev. Cell *21*, 1129-1143.

Parts of this thesis have been published in Grotek *et al*., 2013.

Summary

Adult mammals, including humans, have limited regenerative potential. In contrast, many other animal groups possess remarkable capabilities to fully regenerate body appendages or organs that have been lost or damaged due to injury or disease. A key goal of regeneration research is to understand the cellular and molecular mechanisms underlying naturally occurring regeneration in these organisms, which will provide clues for the development of regenerative therapies in humans.

Adult zebrafish robustly regenerate the caudal fin following amputation which provides an excellent model for studying basic mechanisms of tissue regeneration. Fin regeneration occurs via dedifferentiation of mature stump cells, which form a proliferative mass of undifferentiated precursor cells, the blastema. During regenerative outgrowth, the blastema and the overlying epidermis become compartmentalized into several zones defined by molecular markers, distinct proliferation characteristics and cell fates. Little is known about the molecular mechanisms specifying these regions and the signaling pathways mediating their interaction. This is in particular due to a lack of sensitive reporters to monitor the spatiotemporal dynamics of pathway activation, the absence of genetic tools for temporally and spatially controlled manipulation of pathway activity, and the limited knowledge about downstream target genes.

Here, I provide evidence that Wnt/β–catenin signaling has an essential role in defining two signaling centers in the blastema that orchestrate regenerative growth and cellular differentiation. Using sensitive transgenic pathway reporters I found that Wnt/β–catenin signaling is activated soon after amputation and maintained in the very distal tip of the blastema, where cells are non-proliferative, plus in proliferative proximal domains which line osteoblast precursors and which are thought to form non-mineralized skeletal elements called actinotrichia. I utilized a panel of transgenic TetON driver lines to induce expression of the Wnt pathway inhibitor *axin1* specifically in different regions of the fin to probe the tissue-specific roles of the Wnt pathway, and found that β–catenin signaling is not required in the epidermis or in committed osteoblasts for regenerative

growth or bone formation. Intriguingly, signaling in the proliferative actinotrichia-forming cells lining the osteoblasts appeared to be required for osteoblast differentiation but had little role in controlling blastemal cell proliferation, while pathway activity in the distal, non-proliferative domain was essential for regenerative growth. This strongly suggests that Wnt/β–catenin signaling controls regenerate growth and differentiation largely indirectly. To identify candidate signals that could act downstream of β–catenin signaling and thus mediate its effect on the surrounding tissue, a gene expression profiling was performed after inducible inhibition of the Wnt/β–catenin pathway. Analysis of the Wnt targetome revealed that Wnt/β–catenin signaling controls expression of ligands, pathway components and target genes of many signaling pathways required for caudal fin regeneration including Hh, Fgf, retinoic acid, Bmp, Notch, Activin and Igf. In contrast, Wnt/β–catenin signaling appears to receive little reciprocal input from the signaling pathways it regulates. Rescue experiments showed, that Wnt/β–catenin signaling acts through Fgf, Hh and retinoic acid signaling to indirectly regulate blastemal cell proliferation and gene expression in the epidermis. Thus, Wnt/β–catenin signaling orchestrates fin regeneration by forming signaling centers that instruct cellular behaviors of adjacent tissues.

Zusammenfassung

Adulte Säugetiere, so auch der Mensch, haben nur ein relativ eingeschränktes Regenerationspotenzial. Im Gegensatz dazu gibt es Tiere, die eine beachtliche Fähigkeit besitzen, Körperteile und Organe vollständig zu regenerieren, welche krankheits- bzw. verletzungsbedingt beschädigt oder verloren gegangen sind. Ein Schwerpunkt der Regenerationsforschung ist daher die Aufklärung zellulärer und molekularer Mechanismen, die diesen natürlich auftretenden Regenerationsphänomenen zugrunde liegen. Neue Erkenntnisse können einen wichtigen Beitrag zur Entwicklung regenerativer Therapien für den Menschen liefern.

Die sich nach Amputation vollständig regenerierende Schwanzflosse adulter Zebrafische (Zebrabärblinge) eignet sich besonders gut zur Erforschung grundlegender Mechanismen der Gewebsregeneration. Zebrafischflossenregeneration erfolgt durch die Bildung eines Blastems, einer Population von proliferierenden Vorläuferzellen, die durch Dedifferenzierung ausdifferenzierter Zellen des Stumpfgewebes hervorgehen. Während des regenerativen Flossenwachstums werden das Blastem und die Blastem umgebende Wundepidermis in Zonen untergliedert, die durch bestimmte molekulare Marker, verschiedene proliferative Eigenschaften und Zellschicksale definiert sind. Über die molekularen Mechanismen, die für die Spezifikation dieser Regionen verantwortlich sind, sowie über Signale, die die Interaktionen zwischen diesen Zonen vermitteln, ist erst wenig bekannt. Gründe dafür sind der Mangel an sensitiven Reportergensystemen zum Nachweis räumlicher und zeitlicher Aktivierung von Signaltransduktionswegen, das Fehlen von genetischen Werkzeugen zur räumlich und zeitlich kontrollierten Manipulation von Signaltransduktionswegen und begrenztes Wissen über Zielgene der beteiligten Signaltransduktionswege.

Die in der vorliegenden Arbeit präsentierten Ergebnisse liefern Hinweise für eine essentielle Rolle des Wnt/β–catenin-Signalweges in der Etablierung zweier blastemaler Signalzentren, welche regeneratives Wachstum und zelluläre Differenzierung regulieren. Mittels sensitiver, transgener Wnt-Reportergene konnte gezeigt werden, dass der

Wnt/β–catenin-Signalweg bereits sehr früh nach der Flossenamputation aktiviert wird, und während des weiteren Regenerationsprozesses in der nicht-proliferativen distalen Spitze des Blastems, sowie in proliferativen, proximalen Domänen, welche die Osteoblastenvorläuferzellen säumen und vermutlich für die Bildung von Actinotrichien (nicht-mineraliserten Stützelementen) verantwortlich sind, aktiv bleibt. Darüber hinaus wurde die gewebespezifische Rolle des Wnt/β–catenin-Signalweges in der regenerierenden Flosse durch regionsspezifische Expression des Wnt/β–catenin-Signalweg-Inhibitors *axin1* mittels transgener TetON-Transaktivatorlinien untersucht. Dabei konnte gezeigt werden, dass der Wnt/β–catenin-Signalweg weder in der Wundepidermis noch in nicht differenzierten Osteoblastenvorläufern für regeneratives Wachstum oder Knochenreifung notwendig ist. Interessanterweise ist die Aktivierung des Wnt/β–catenin-Signalweges in den proliferativen Actinotrichien-bildenden Zellen, welche neben den Osteoblastenvorläuferzellen lokalisiert sind, notwendig, hat gleichzeitig aber wenig Bedeutung für die Regulierung der blastemalen Proliferation. Dagegen ist die Aktivierung des Wnt/β–catenin-Signalweges in der nicht-proliferativen, distalen Spitze des Blastems essentiell für regeneratives Wachstum. Daraus lässt sich schließen, dass der Wnt/β–catenin-Signalweg regeneratives Wachstum, sowie Differenzierung weitestgehend indirekt reguliert. Um Signale zu identifizeren, welche durch den Wnt/β–catenin-Signalweg aktiviert werden und somit diese Effekte in den angrenzenden Geweben vermittlen könnten, wurde eine Genexpressionsanalyse nach induzierbarer Inhibition des Wnt/β–catenin-Signalweg durchgeführt. Die Auswertung der Genexpressionsaten zeigte, dass der Wnt/β–catenin-Signalweg die Expression von Liganden, Signalwegkomponenten und Zielgenen von vielen für die Flossenregeneration essentiellen Signalwegen reguliert. Dazu gehören der Hh-, Fgf-, Retinsäure-, Bmp-, Notch-, Activin- und Igf-Signalweg. Im Gegensatz dazu deutet sich an, dass die durch den Wnt/β–catenin-Signalweg-regulierten Signalwege nur wenig reziproken Einfluss auf die Aktivierung des Wnt/β–catenin-Signalweges haben. Rettungsversuche zeigten, dass die Wnt/β–catenin-Signalweg-abhängige Regulation blastemaler Zellproliferation sowie Genexpression in der Epidermis indirekt erfolgt und durch Fgf-, Hh- und Retinsäure-Signalwege vermittelt wird. Zusammenfassend lässt sich sagen, dass der Wnt/β–catenin-Signalweg die

Flossenregeneration durch die Bildung von Signalzentren organisiert, welche das zelluläre Verhalten und damit die Entwicklung benachbarter Gewebe instruiert.

1 Introduction

1.1 Motivation

Within the animal kingdom the ability to regenerate organs or appendages that have been lost or severely damaged due to injury or disease varies greatly. With a few exceptions, adult mammals including humans, have limited regenerative potential and most tissues respond to severe injury by formation of fibrotic scar tissue which is poorly organized and lacks functionality. In contrast, certain lower vertebrates, such as urodele amphibians (newts and salamanders) or the teleost *Danio rerio* (zebrafish), possess an elevated regenerative capacity and efficiently restore complex organs and body structures upon injury throughout lifetime. A thorough understanding of the cellular and molecular mechanisms underlying naturally occurring regeneration in these organisms will provide valuable clues for the development of regenerative therapies in humans.

Central goals of regeneration research are to identify the cellular source(s) of tissue restoration, and to characterize the molecular signals, which 1) initiate the regenerative program in response to injury, and 2) control the regenerative program until tissue integrity and functionality is restored. While studies on several regenerating systems, foremost the zebrafish caudal fin, have revealed a number of signals that are required for complete regeneration, our knowledge about their exact cellular functions during these processes remains incomplete. Hence, further efforts are needed to elucidate their tissue specific functions and how do they incorporate into complex signaling networks that guide regeneration. Therefore, this study was conducted to gain a more detailed understanding of the molecular mechanisms underlying regeneration in the vertebrate appendage.

1.2 Cellular Mechanisms of Tissue Regeneration

Successful tissue regeneration requires a series of instructive signals and a source of cells that restore the damaged tissue. While many signals are shared between naturally regenerating systems, it has become apparent that the cellular source of newly formed, regenerated tissue differs. Possible modes are (Fig. 1.1) (King and Newmark, 2012; Zhang *et al*., 2013): 1) the activation of resident stem cells, which self-renew and generate a differentiated daughter cell (*e.g.* skeletal muscle), 2) proliferation of lineage-restricted progenitor cells that are derived via dedifferentiation of mature cells (*e.g.* osteoblasts in the zebrafish caudal fin), 3) proliferation of differentiated, mature cells (*e.g.* hepatocytes after partial hepatectomy of the mammalian liver), or 4) transdifferentiation of mature cells into another cell type, either directly or via dedifferentiation to a progenitor cell (*e.g.* newt lens).

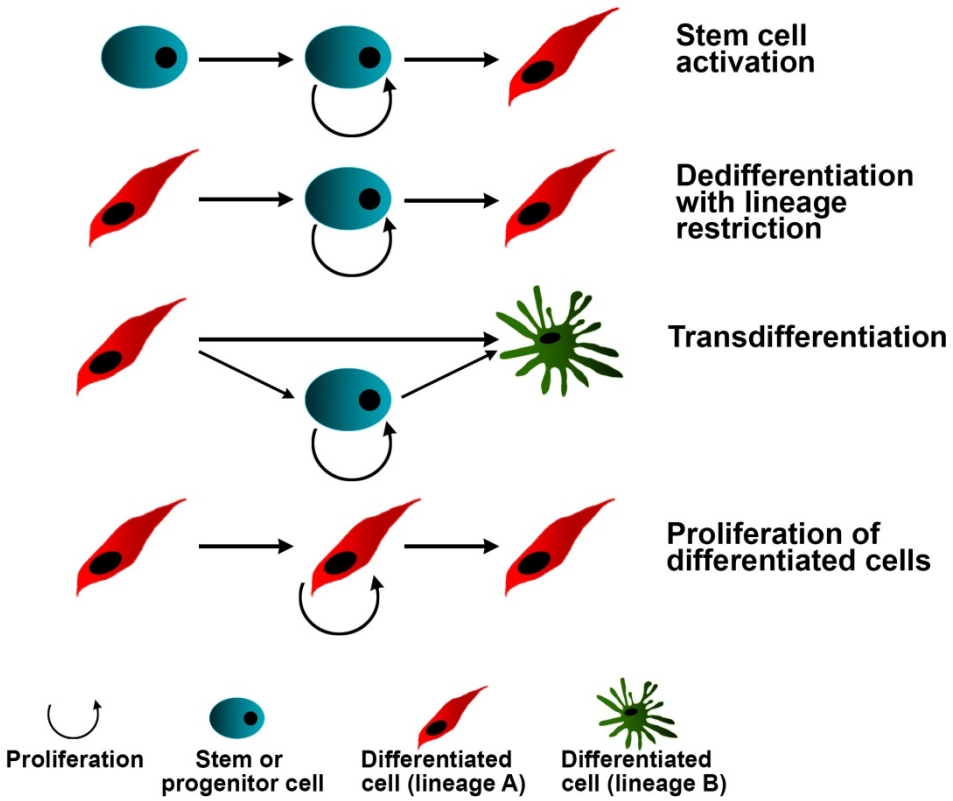

Fig. 1.1. Cellular mechanisms of tissue regeneration (adapted and modified from Günes Özhan and Gilbert Weidinger)**.** Tissue regeneration can involve different cellular mechanisms: 1) activation of resident stem cells, which self-renew and generate one or more differentiating daughter cells, 2) dedifferentiation of mature, differentiated cells into cells with progenitor-like status, which however remain lineage restricted, 3) transdifferentiation of mature, differentiated cells into another cell type, which can occur either directly or involves dedifferentiation to a progenitor cell, and 4) proliferation of mature, differentiated cells.

The regenerative capacity among metazoan species can be categorized by their scale. Certain invertebrates such as planarian flatworms and the freshwater polyp *Hydra* are capable of regenerating large body parts from small pieces of tissue (Gierer *et al*., 1972; Salo, 2006). When a planarian's head or tail is amputated, resident pluripotent stem cells (called neoblasts) form a mass of undifferentiated cells, the blastema, which provides a source for all cell types required to restore the missing body part (Reddien and Sanchez Alvarado, 2004). Head regeneration in *Hydra,* following midgastric bisection (at 50 % of the body length), likewise occurs through activation of stem cells (Tanaka and Reddien, 2011). Though less efficiently than planarians and the *Hydra*, lower vertebrates including frogs (*Xenopus laevis*) at tadpole stage, adult urodele amphibians (newts and salamanders) and adult teleosts (*e.g.* zebrafish) can robustly regenerate lost appendages and in the case of newts, salamanders and teleosts also many internal organs (Poss, 2010). During zebrafish heart regeneration, mature cardiomyocytes provide a source for precursor cells, which proliferate and restore the damaged heart muscle (Jopling *et al*., 2010). Appendage regeneration occurs via establishment of a blastema, a heterogeneous population of undifferentiated, proliferative cells, which are however unlike the planarian's neoblasts lineage restricted (King and Newmark, 2012). Solid evidence has recently been provided that these progenitor cells are derived via dedifferentiation of mature, differentiated cells as it is the case during bone regeneration in the zebrafish caudal fin (Stoick-Cooper *et al*., 2007a¸ Knopf *et al.*, 2011; Tu and Johnson, 2011). Some evidence exists, which suggests that many other lineages likewise regenerate via dedifferentiation of mature cells in fish and salamander appendages (Tanaka and Reddien, 2011). Although dedifferentiation of mature cells to a progenitor-like status appears to be an important mechanism for many cellular lineages during vertebrate appendage regeneration, activation of resident stem cells has also been identified as a possible mode for regeneration of some cellular lineages in the vertebrate appendage, in particular muscle (Morrison *et al*., 2006).

Regeneration of complex tissues in mammals, including humans, is very limited. Examples of tissues with elevated regenerative potential are the liver and skeletal muscle. While regeneration of skeletal muscle is based on myogenic precursor cells, liver regeneration can occur via different cellular mechanisms that involve progenitor cells or proliferation of mature hepatocytes (Duncan *et al*., 2009; Poss, 2010). Mammals are also able to regenerate their digits after amputation, which involves the concerted action of nerve stem cells and

populations of fate-restricted mesenchymal progenitors (Lehoczky *et al*., 2011; Rinkevich *et al*., 2011; Takeo *et al*., 2013).

1.3 Appendage Regeneration in the Teleost *Danio Rerio*

The zebrafish *Danio rerio* is of central biomedical interest since it is amenable to large-scale drug screens and has the remarkable ability to fully regenerate its appendages and several internal organs, including the retina, brain, spinal cord, heart and kidney (Poss, 2010; Stoick-Cooper *et al*., 2007a). In the recent past the zebrafish caudal fin has emerged as a highly successful model for studying basic mechanisms of tissue regeneration due to its easy access to surgery, rapid and robust regeneration, apparently unlimited regenerative potential (Azevedo *et al*., 2011), relatively simple tissue architecture and largely transparent appearance (Fig. 1.2).

The caudal fin consists of 16-18 bifurcated, bony rays, the lepidotrichia, which extend along the whole length of the fin and are separated by soft interray tissue (Fig. 1.2A-B). Each fin ray consist of two concave, segmented hemirays, which enclose blood vessels, nerves, pigment cells and fibroblast-like cells (Fig. 1.2B-C) (Poss *et al*., 2003). A monolayer of bone-secreting cells, the osteoblasts, covers on both surfaces the calcified lepitodrichia bone which is formed via intramembranous ossification without a cartilage intermediate (Mari-Beffa *et al*., 2007; Poss *et al*., 2003). Additionally to the lepitodrichia bone, rigid, non-calcified, collagenous, skeletal elements are found at the distal tip of each ray, the actinotrichia (Fig. 1.2B) which provide further support to the fin edge and are thought to be specific to fish fins (Duran *et al*., 2011; Zhang *et al*., 2010).

The caudal fin completely regenerates following partial amputation (Fig. 1.2). The regenerative process can be grossly divided into three phases (Fig. 1.3; Stoick-Cooper *et al*., 2007a): 1) wound healing, 2) blastema formation, and 3) regenerative outgrowth and regeneration termination. During the early wound healing phase (1-3 hours post amputation; hpa) epidermal cells migrate over the wound edges and cover the wound (Stoick-Cooper *et al*., 2007a). When fish are kept at 28°C, wound healing continues until 24-36 hpa giving rise to a multi-layered wound epidermis, whose basal layer is composed of characteristic cuboidal-shaped cells (Stoick-Cooper *et al*., 2007a). Until 48 hpa

populations of lineage-restricted proliferative mesenchymal progenitor cells are established via dedifferentiation of mature stump cells distally to each ray, called blastema (Stoick-Cooper *et al*., 2007a, Knopf *et al.*, 2011; Tu and Johnson, 2011). Once the blastema has been formed the regenerative outgrowth phase is initiated leading to restoration of the fin within two to three weeks.

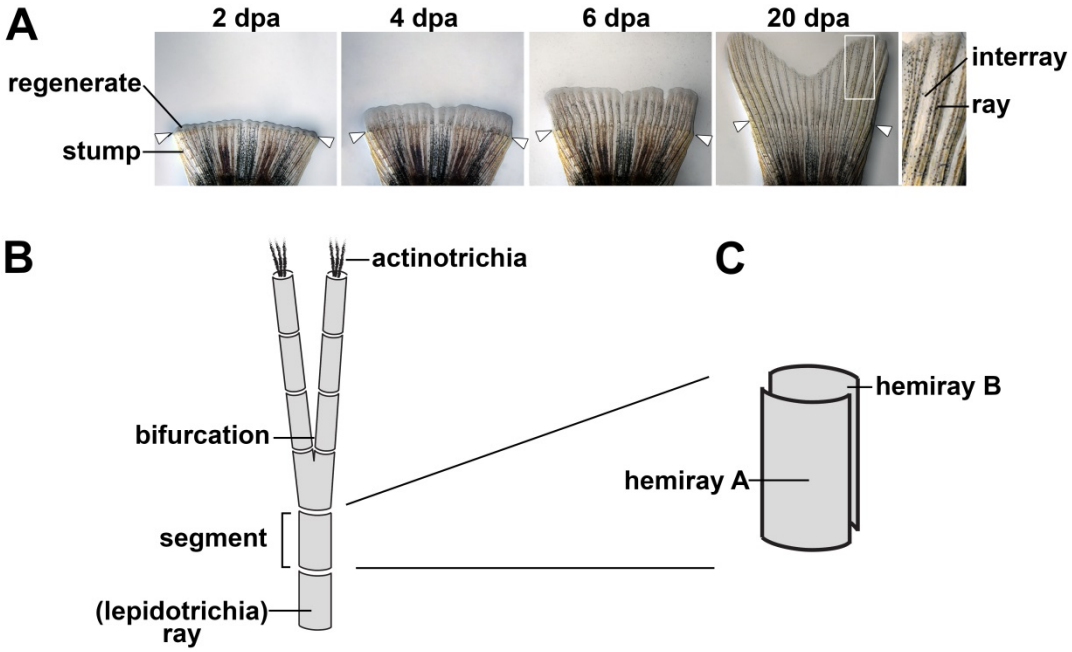

Fig. 1.2. The zebrafish caudal fin. (A) A regenerating caudal fin at 2, 4, 6 and 20 days post amputation (dpa)**.** The caudal fin is composed of bony rays and soft interray tissue, and regenerates completely within ~2-3 weeks following partial resection. Arrowheads: amputation plane. **(B)** Cartoon representing the (uninjured) fin ray skeleton comprising bifurcated, segmented lepidotrichia bone and distally-located actinotrichia (adapted and modified from Quint *et al*., 2002). **(C)** Cartoon of a fin ray segment which composed of a pair of mineralized hemirays.

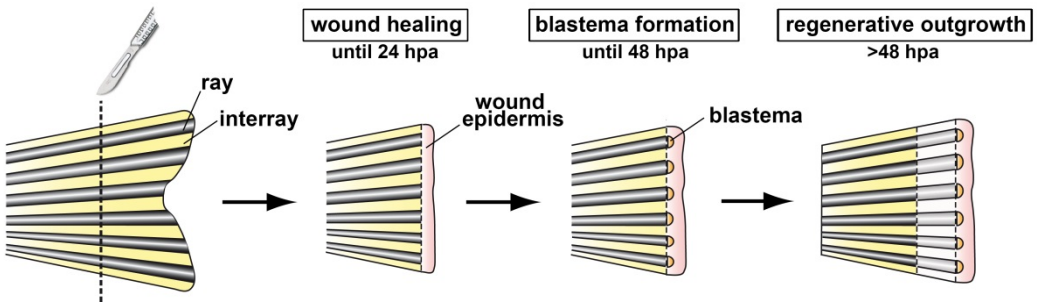

Fig. 1.3. Stages of caudal fin regeneration (modified from Stoick-Cooper *et al*., 2007a). Within 24 following amputation (hpa) the wound is covered by epidermal cells and a multilayered wound epidermis is formed. Dedifferentiation of mature stump cells form populations of proliferative, lineage-restricted progenitor cells, the blastema, distally to each fin ray. Blastema formation is completed at 48 hours post amputation (hpa) and followed by the regenerative outgrowth phase leading to restoration of the fin within 2-3 weeks. The time frame applies when fish are kept at 28°C.

During regenerative outgrowth, the regenerate is organized into several tissue compartments as revealed on longitudinal sections (Fig. 1.4). The blastemal mesenchyme comprises at least four domains: 1) the distal-most, scarcely proliferative blastema, characterized by expression of *aldh1a2* (*raldh2*), the synthesis rate-limiting enzyme in retinoic acid synthesis (Mathew *et al*., 2009; Nechiporuk and Keating, 2002), 2) the medial proximal blastema which is rapidly proliferating and positive for the mitotic checkpoint kinase *ttk* (*mps1*) (Poss *et al*., 2002), and for readouts of Notch signaling (*her6* and the transgenic reporter *her4.3:*EGFP^{y83}; Grotek *et al*., 2013), 3) highly proliferative bilateral zones containing *runx2b, sp7* (*osterix*, *osx*) and Zns5-positive osteoblast progenitors (Brown *et al*., 2009), and 4) domains directly medial to the osteoblast progenitors. These mediolaterally located cells constitute a subset of the Notch signaling-positive medial proximal blastema, are positive for *and1/2* transcripts, and are thought to be required for formation of actinotrichia (Zhang *et al*., 2010). The wound epidermis overlying the blastemal mesenchyme likewise comprises different regions. In particular, a subdomain of the basal epidermal layer that abuts the *runx2b*/*sp7*-positive mesenchyme expresses the transcription factor *lef1* and the Hedgehog (Hh) ligand *shh,* and is thought to instruct the underlying osteoblast progenitors to differentiate (Laforest *et al*., 1998; Lee *et al*., 2009).

Recent studies have revealed the requirement of a number of signaling pathways for caudal fin regeneration, including Activin (Jazwinska *et al*., 2007), Bone morphogenetic protein (Bmp; Smith *et al*., 2006), Fibroblast growth factor (Fgf; Poss *et al*., 2000b; Whitehead *et al*., 2005), Hedgehog (Hh; Quint *et al*., 2002), Insulin-like growth factor (Igf; Chablais and Jazwinska, 2010), Notch (Grotek *et al*., 2013; Munch *et al*., 2013), retinoic acid (RA; Blum and Begemann, 2012) and Wnt/β–catenin (Kawakami *et al*., 2006; Stoick-Cooper *et al*., 2007b). All of these pathways have been shown to promote proliferation of the blastemal progenitor cells and/or are essential for formation of the blastema. However, our understanding of how these signals regulate regeneration is incomplete. Little is known about their tissue-specific roles or how different pathways interact to regulate distally-oriented growth during fin regeneration.

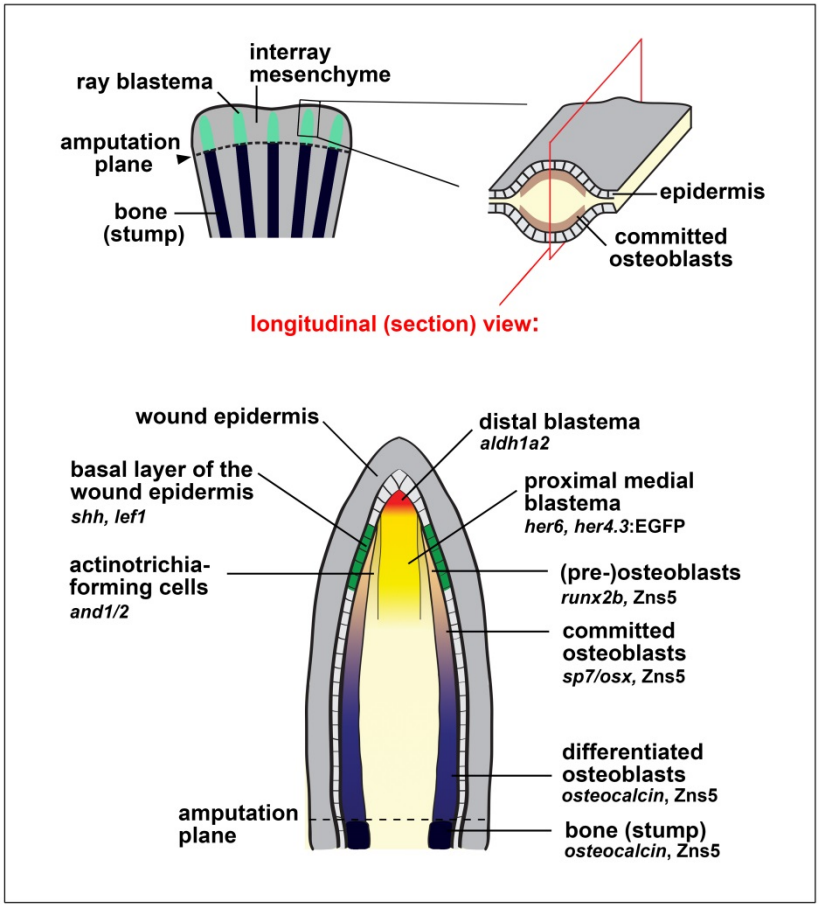

Fig. 1.4. Tissue compartments in the regenerating caudal fin. Cartoons summarizing relevant anatomical structures and expression domains of a caudal fin regenerate during the outgrowth phase. Whole mount and longitudinal section views are shown.

1.4 Wnt Signal Transduction Pathways

A fundamental property of all multicellular organisms is the ability of individual cells or cell populations to communicate and thus to coordinate their spatiotemporal directed response to environmental changes. Communication between cells is achieved by the activation of different signal transduction pathways, either by direct cell-cell contact in adjacent cells or through secreted signaling molecules, which allow information to be spread over short and long distance. Once activated, these pathways elicit a specific cellular response including cell fate decisions, cell differentiation, proliferation, apoptosis, or changes in cell polarity and morphology. Complex biological phenomena including embryogenesis and tissue regeneration are governed by the concerted action of multiple signaling pathways tightly coordinated in space and time.

Among the many pathways identified, those that are initiated by members of the highly conserved Wnt family of secreted proteins are of central importance. This is due to their ability to regulate a multitude of cellular mechanisms, including cell proliferation, migration, cell polarity, and cell fate determination during embryonic development and tissue homeostasis (Logan and Nusse, 2004; MacDonald *et al*., 2009). Importantly, Wnt signaling also appears to play critical roles in essentially all naturally regenerating systems studied to date, ranging from hydra and planarian whole body regeneration to organ and tissue regeneration in lower vertebrates and mammals (Poss, 2010; Stoick-Cooper *et al*., 2007; Whyte *et al*., 2012). Hence, the following chapters will provide a brief introduction and background on Wnt signaling.

1.4.1 Wnt Genes and Proteins

Wnt proteins are encoded by the large family of *wnt* genes of which the first, *wnt1*, was discovered more than three decades ago in mouse (Nusse and Varmus, 1982). Today up to 19 different *wnt* genes are known to be present in mammalian genomes (Willert and Nusse, 2012). *wnt* genes are expressed in all metazoan species ranging from simple cnidarians and sponges to humans (Holstein, 2012; Kusserow *et al*., 2005; Nichols *et al*., 2006; Willert and Nusse, 2012). In contrast, they are not found within genomes of single-cell organisms, which led to the hypothesis that the Wnt signaling pathway has been instrumental in the evolution of multicellularity (Clevers and Nusse, 2012). Genes of the *wnt* family code for cysteine-rich secreted growth factor proteins of approximately 40 kDa in size, which act as signaling molecules over short and long distances (Clevers and Nusse, 2012; Holstein, 2012). The latter however likely requires association with additional factors such as the Swim protein or lipoprotein particles (Bartscherer and Boutros, 2008; Mulligan *et al*., 2012). Several posttranslational modifications have been reported for Wnt proteins of which acylation (palmitoylation) on a highly conserved cysteine residue and several glycosylation events are crucial for Wnt secretion and signaling activity (Fung *et al*., 1985; Komekado *et al*., 2007; Kurayoshi *et al*., 2007; Willert *et al*., 2003; Willert and Nusse, 2012). Following procession through endoplasmic reticulum (ER) and Golgi, Wnt proteins are secreted with the help of the Wntless protein into the extracellular space where they

bind to cell-surface receptors of target cells (Banziger *et al*., 2006; Bartscherer *et al*., 2006; Goodman *et al*., 2006).

Historically Wnt proteins have been categorized into two groups based on their ability to induce formation of a secondary body axis in *Xenopus laevis* embryos and to morphologically transform cells of the mouse mammary epithelial cell line C57MG (Du *et al*., 1995; McMahon and Moon, 1989; Wong *et al*., 1994). Wnt proteins with these capacities were classified as transforming or "canonical" Wnts, while Wnt proteins that lacked the former were categorized as non-transforming or "non-canonical" Wnts (Du *et al*., 1995; van Amerongen, 2012). The transforming ability of canonical Wnts was soon discovered to be attributable to an increase in the cellular levels of the transcriptional co-activator β–catenin (Shimizu *et al*., 1997). By contrast non-canonical Wnts ligands employ alternative, β–catenin-independent signaling mechanisms including intracellular calcium release and activation of protein kinase C (Pkc), small and heterotrimeric G proteins, or the c-Jun N-terminal kinase (Jnk) (van Amerongen, 2012). It has become apparent however, that whether the canonical, β–catenin-dependent signaling pathway is triggered or whether non-canonical, β–catenin-independent signaling pathways are employed in a particular system, is not determined by the Wnt protein, but rather by the cellular context and the presence of specific combinations of Wnt receptors (van Amerongen, 2012; Willert and Nusse, 2012).

1.4.2 The β–catenin-Dependent Wnt Signaling Pathway

Of the various signaling pathways triggered by Wnt ligands, the β–catenin dependent pathway is the best characterized. Wnt/β–catenin signaling has important functions during embryonic development and adult tissue homeostasis by controlling many biological processes including cell fate determination and cell proliferation. Since this pathway is highly regulated at many levels with still growing complexity, only the signaling steps and components that are most relevant for this study will be introduced (Fig. 1.5) (Clevers and Nusse, 2012; MacDonald *et al*., 2009): The central signaling molecule of the β–catenin-dependent Wnt pathway is the transcriptional co-activator β–catenin, whose stability is tightly controlled. In the absence of a Wnt ligand, cytoplasmic β–catenin is bound by a so

called “destruction complex”, which is a multi-protein complex consisting of the scaffolding protein Axin, the tumor suppressor Adenomatous polyposis coli (Apc), and two serine-threonine kinases (Glycogen synthase kinase 3, Gsk3α/β and Casein kinase 1 α/β, Ck1α/β). Both kinases sequentially phosphorylate β–catenin at N-terminal serine/threonine residues. Phosphorylated β–catenin is then ubiquitinated and thereby targeted for degradation by the proteasome pathway (Fig. 1.5A). Thus, in the absence of a Wnt signal very low levels of β–catenin are present in the cytoplasm, which are insufficient to trigger signaling. Additionally, in the nucleus proteins of the T cell factor/Lymphoid enhancer family (Tcf/Lef) bind to regulatory sequences of Wnt target genes and recruit co-repressors (*e.g.* Histone deacetylases, Hdacs and Transducin-like enhancer of split, Tle) to inhibit gene expression.

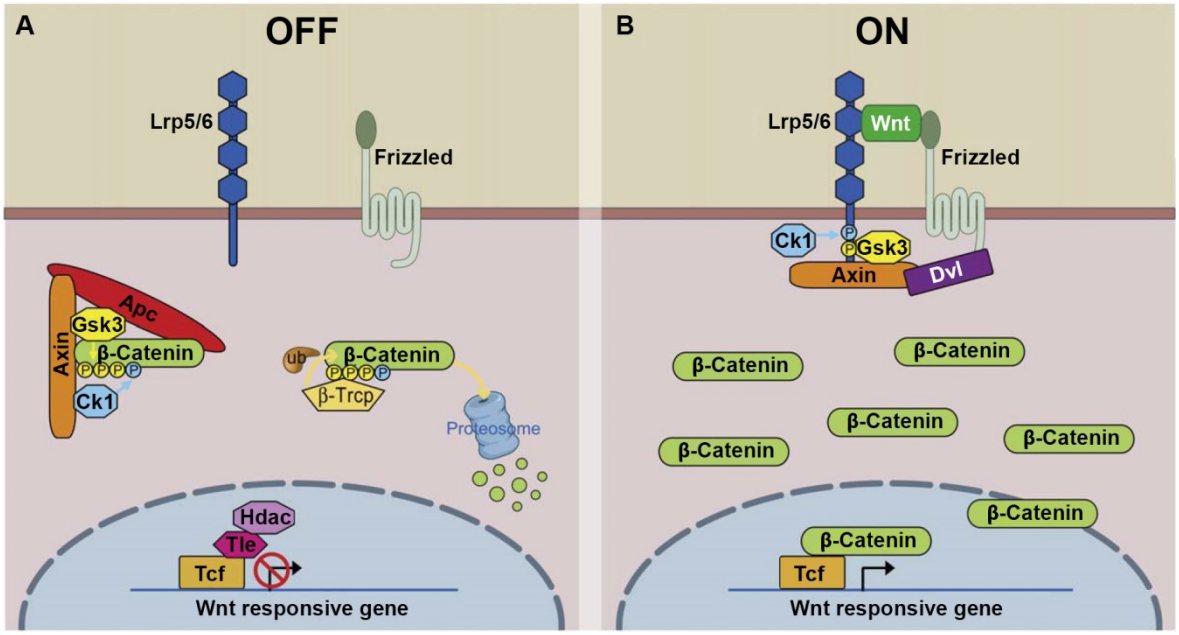

Fig. 1.5. The β–catenin-dependent Wnt signaling pathway (modified from MacDonald *et al*., 2009). Shown is a simplified overview of signaling events and protein interactions in the absence (A) or in the presence (B) of Wnt ligands activating β–catenin signaling. **(A)** In the absence of a Wnt ligand, β–catenin is bound by a multi-protein “destruction” complex composed of Axin, Apc, Gsk3 and Ck1 which phosphorylates β–catenin. Phosphorylated β–catenin is recognized by β–Trcp, a subunit of the E3 ubiquitin ligase complex, subsequently ubiquitinated and targeted for degradation by the proteasome. Transcriptional repressor complexes in the nucleus prevent activation of Wnt target genes. **(B)** Wnt ligand binding to Frizzled receptors and Lrp5/6 co-receptors results in Lrp5/6 phosphorylation and Axin recruitment to Lrp5/6, which inactivates the destruction complex. Subsequently, newly synthesized β–catenin accumulates, translocates to the nucleus and activates transcription of target genes together with transcription factors of the Tcf/Lef family. The scaffolding protein Dvl is thought to facilitate Lrp5/6 phosphorylation.

Wnt/β–catenin signaling is initiated by binding of a Wnt ligand to a seven-pass transmembrane receptor of the Frizzled (Fzd) family and its single-pass co-receptor low-density lipoprotein receptor-related protein 5 or 6 (Lrp5/6) (Fig. 1.5B). Subsequently, the scaffolding protein Dishevelled (Dvl) is recruited to the receptor complex and Lrp5/6 is phosphorylated on multiple conserved sites (PPPSPxS motifs) in its intracellular domain by the concerted action of Gsk3β and Ck1γ. Phosphorylated Lrp5/6 then serves as docking site for the recruitment of the cytoplasmic scaffolding protein Axin, which renders the destruction complex inactive. Consequently, newly synthesized β–catenin accumulates and translocates to the nucleus. Binding of nuclear β–catenin to Tcf/Lef proteins and recruitment of additional cofactors converts the Tcf/Lef repressor complex into a transcriptional activator which initiates transcription of target genes. While many target genes are cell-type specific due to the numerous biological processes regulated by the Wnt/β–catenin pathway, a number of genes such as the negative feedback inhibitor *axin2* are considered to represent common targets and thus are frequently used as readout for active signaling (Jho *et al*., 2002; Lustig *et al*., 2002; Weidinger *et al.*, 2005).

Due to its pivotal role in development and tissue homeostasis it is not surprising that the β–catenin pathway activity is tightly regulated by a wide range of modifiers whose number is still growing. These effectors act in a promoting or antagonizing manner at different levels in the signaling cascade including intracellularly to modulate components of the signal transduction machinery, or extracellularly to modulate ligand-receptor interactions (reviewed in Cruciat and Niehrs, 2013; MacDonald *et al*., 2009). Among the secreted antagonists which include Frizzled-related proteins (sFRPs), Dickkopf (Dkk) proteins, Wise/Sost proteins, Cerberus and insulin-like growth factor binding protein 4 (Igfbp4), proteins of the Dickkopf (Dkk) family are the best characterized (Cruciat and Niehrs, 2013). The founding member of the Dkk family, Dkk1, inhibits Wnt/β–catenin signaling by binding to Lrp5/6 co-receptors which disrupts the Wnt-induced Wnt/Lrp/Fzd complex and additionally induces cell surface removal of Lrp6 (Yamamoto *et al*., 2008). Crucial cytoplasmic regulators of Wnt/β–catenin signaling are Apc and Axin, which promote β–catenin phosphorylation and degradation. Ectopic expression of *dkk1* or *axin1* has become a frequently used strategy to efficiently interfere with Wnt/β–catenin signaling as knock-out approaches are often hindered through frequently occurring functional

redundancy of Wnt/β–catenin pathway components, and β–catenin's additionally role in regulating cell-cell adhesion.

1.5 Wnt/β–catenin Signaling in Tissue Regeneration

Among the many molecular signals that have been identified to be involved in tissue regeneration, Wnt signaling has emerged as an important player in essentially all naturally regenerating systems studied to date, ranging from *Hydra* and planarian whole body regeneration to organ and tissue regeneration in lower vertebrates and mammals (Poss, 2010; Stoick-Cooper *et al*., 2007a; Whyte *et al*., 2012). Particularly, activation of the Wnt/β–catenin pathway has been found to be a crucial signal in controlling many cellular processes during tissue regeneration. The functions of β–catenin pathway activation however, if known, are diverse and include promotion of progenitor cell proliferation and maintenance, regulation of progenitor cell differentiation into mature cells and patterning of the newly formed tissue (Whyte *et al*., 2012). During regeneration in planarians β–catenin signaling has an essential role in establishment of axial tissue pattering since pathway manipulation can result in worms with two heads or two tails (Gurley *et al*., 2008). Head regeneration in *Hydra* likewise relies on Wnt/β–catenin signaling. Following midgastric bisection, apoptotic cells provide a source for ligands activating the β–catenin pathway, which promotes proliferation of interstitial stem cells (Chera *et al*., 2009). Additionally, Wnt/β–catenin signaling also plays a critical role in axial patterning during *Hydra* head regeneration via establishment of the head organizer (Bode, 2009; Broun *et al*., 2005). During zebrafish caudal fin regeneration Wnt/β–catenin pathway activation is essential for formation and proliferation of the blastema (Kawakami *et al*., 2006; Stoick-Cooper *et al*., 2007b). Similarly, interference with β–catenin pathway activation prevents complete regeneration of adult Axolotl limbs and larval *Xenopus* limbs and tails (Kawakami *et al*., 2006; Yokoyama *et al*., 2007). Importantly, Wnt/β–catenin signaling also promotes regenerative processes in mammals, including liver and muscle regeneration. Here, β–catenin pathway activation appears to not only promote cellular proliferation of the involved progenitor cells to provide the cellular source for tissue

regeneration, but it is also thought to have additional roles in directing differentiation of muscle and liver progenitors (Boulter *et al*., 2012; Brack *et al*., 2008; Nejak-Bowen and Monga, 2011; Otto *et al*., 2008). During mammalian digit regeneration Wnt/β–catenin signaling directs differentiation of nail stem cells which prerequisites complete digit regeneration (Takeo *et al*., 2013). Thus, injury-induced β–catenin signaling appears to represent a pro-regenerative signal in most regenerative systems examined, though its exact role remains to be elucidated.

2 Aims of the Study

Two independent studies have shown that β–catenin pathway activation is essential for fin regeneration to occur (Kawakami *et al*., 2006; Stoick-Cooper *et al*., 2007b). Interference with Wnt/β–catenin signaling, before or immediately after amputation through systemic overexpression of a dominant negative form of a *tcf* transcription factor or the secreted Wnt antagonist *dkk1*, prevented specification of the wound epidermis and formation of the blastema. Inhibition of Wnt/β–catenin signaling during regenerative outgrowth resulted in incomplete regeneration due to reduced cellular proliferation. Thus, Wnt/β–catenin signaling appears to be required for fin regeneration, yet the precise function of pathway activation during this regenerative process remains largely unidentified. This is due to several reasons. First, the spatiotemporal dynamics of pathway activation have not been identified due to a lack of sensitive transgenic reporter. Transcripts of the direct Wnt/β–catenin target *axin2* were detected in the blastema while *lef1* expression was detected in both, the blastema and the basal epidermal layer (Poss *et al*., 2000a; Stoick-Cooper *et al*., 2007b). However, it remains controversial whether *lef1* expression in the basal epidermal layer indeed reflects sites of active Wnt/β–catenin signaling (Poss *et al*., 2000a). Furthermore, whether β–catenin signaling is activated throughout the blastemal mesenchyme or confined to certain subregions has not been elucidated. Second, the cellular mechanisms regulated by the β–catenin pathway are essentially unknown. Third, while it has been suggested that Wnt/β–catenin signaling regulates Fgf signaling during fin regeneration (Stoick-Cooper *et al*., 2007b), its position within the molecular signaling network remains unknown. Little is known about the downstream targets that mediate the effects of pathway activation. Similarly, signals that act upstream of Wnt/β–catenin signaling have not been reported during caudal fin regeneration.

Therefore, the aim of this study was to investigate the role Wnt/β–catenin signaling plays during zebrafish caudal fin regeneration. Specifically I aimed:

i) to determine the spatiotemporal pattern of Wnt/β–catenin pathway activation

ii) to probe the tissue-specific roles of Wnt/β–catenin signaling

iii) to investigate the hierarchical relationships between Wnt/β–catenin signaling and other signaling pathways known to be required for fin regeneration.

Answering these questions will further our understanding of the molecular mechanisms underlying appendage regeneration and thus might have implications for regenerative medicine.

3 Material and Methods

3.1 Materials

3.1.1 Technical Equipment

Additional technical equipment that was used for a particular experimental procedure is found within the chapter '*3.2 Methods*' and is not listed here.

Agarose electrophoresis system:	C.B.S. Scientific CO
Ball joint holder:	WPI
Borosilicate glass capillaries:	TW100-4, WPI
Confocal microscopes:	LSM 510 Meta, Zeiss; LSM 700, Zeiss; SP5, Leica
Heat shock device:	Lauda E300, Ecoline star edition
Centrifuges:	5415R, Eppendorf, Megafuge 1.0R, Thermo Scientific; CS-15R, Beckmann
Forceps:	WPI
Incubators:	WTW TS 606 / 4-i
Magnetic Stand:	WPI
Microinjector:	PV830 Pneumatic Pico Pump with foot pedal, WPI
Micromanipulator:	KITE-R, WPI
Microscope	WF upright Olympus
Needle Puller:	Flaming/Brown P87, Sutter
Pipettes:	Eppendorf
SDS-PAGE Gel System:	X Cell XureLock Mini Cell, Invitrogen
Spectrophotometer:	Nano Drop NC-1000 Spectrophotometer, Peqlab
Stereo fluorescence microscope	MVX10, Olympus; M205FA, Leica; MZ16 FA, Leica; Axio Imager, Zeiss; CTR6000, Leica
Stereo microscope	SZ61, Olympus; SZX16, Olympus
Syringe	0.1 ml #1710, Hamilton
Thermocycler:	MyCycler Thermal Cycler, BioRad
Thermomixer:	Thermomixer comfort, Eppendorf
Water bath:	Memmert
Western blot:	XCell II Blot Module, Invitrogen

3.1.2 Chemicals and Consumables

All generally used chemicals were, if not indicated otherwise, purchased from AppliChem, Merck, Roth, Sigma or VWR. General plastic ware was purchased from Sarstedt. Additional chemicals or consumables that were used for a particular experimental procedure are found within the chapter '*3.2 Methods*' and are not listed here.

Chemicals:

Alizarin Red, Sigma
3-Aminobenzoic acid ethylester (Tricaine), Sigma
5-Brom-4-chlor-3-indolylphoshpat (BCIP), Roche
5-Bromo-2-deoxyuridine (BrdU), Sigma
Fast red TR/Naphthol AS-MX Tablets, Sigma
Iodonitrotetrazolium chloride (INT), Sigma
Nitro Blue Tetrazolium (NBT), Roche
Tissue freezing medium (TFM), Triangel Biomedical Sciences

Consumables:

Chromatography paper (3 mm), Whatmann
Scalpels, Techno Cut scalpel, HMD Healthcare, LTD
Syringe needles (different size), BD Microlance.

3.1.3 Reagents and Buffers

Additional reagents or buffers that were used for a particular experimental procedure are found within the chapter '*3.2 Methods*' and are not listed here.

Buffers:

Alizarin Red solution:	0.5 % Alizarin Red, 1 % KOH
Bleaching buffer:	0.8 % KOH, 0.6 % H_2O_2
Blocking solution (ISH):	5 % heat-inactivated sheep serum, 10 mg/ml BSA in PBT
Carnoy's Fixative:	60 % EtOH, 30 % Chloroform, 10 % Acetic Acid
E3 embryo medium:	5 mM NaCl, 0.17 mM KCl, 0.33 mM $CaCl_2 \cdot 2\ H_2O$, 0.33 mM $MgSO_4 \cdot 7\ H_2O$, 0.2 ‰ (w/v) methylene blue, pH 6.5

Hybridization buffer:	5x SSC, 500 µg/ml type VI Torula yeast RNA (Sigma), 50 µg/ml Heparin, 0.1 % Tween 20, 9 mM Citric Acid (Monohydrate), 50 % deionized formamide, pH 6.0
INT/BCIP staining buffer:	175 µg INT, 175 µg BCIP per 1ml NTMT
Mounting Medium:	75 % Glycerol in PBS
NBT/BCIP staining buffer:	350 µg NBT, 175 µg BCIP per ml NTMT
NCS-PBT:	10 % Newborn calf serum, 1 % DMSO, 89 % PBT
NTMT:	50 mM $MgCl_2$, 100mM $NaCl_2$, 100 mM Tris-HCl, pH 9.5, 0.1 % Tween 20
PBS:	1.7 mM KH_2PO_4, 5.2 mM Na_2HPO_4, 150 mM NaCl
PBT:	PBS with 0.1 % Tween 20
PBTx	PBS with 0.3 % Triton X-100
PFA 4%:	4 % (w/v) paraformaldehyde in PBS
RIPA buffer:	1 mM EGTA, 50 mM HEPES, 10 % Glycerol, 1.5 mM $MgCl_2$, 150 mM NaCl, 100 mM NaF, 0.1 % SDS, 1 % Sodiumdeoxycholate, 1 mM Sodium orthovandate, 1 % Triton X-100, pH 7.4
SDS PAGE Running buffer:	1 M MOPS, 1 M Tris Base, 69.3 mM SDS, 20.5 mM EDTA
SDS sample buffer (3x):	100 ml: 40 ml 0.5 M Tris, 228 mg EGTA, 6 g SDS, 28 ml Glycerol, 70 mg Brompehnol Blue, top up with H_2O, pH 6.8
SSC (20x):	300 mM NaCl, 200 mM Na-Citrate, pH 7
SSCT:	0.1 % Tween 20 in SSC (1x)
STOP Solution:	1 mM EDTA, 0.1 % Tween 20, 0.05 M phosphate buffer, pH 5.8
Stripping buffer (ISH):	0.1 % Tween 20 in 0.1 M Glycin-HCl, pH 2.2
Transfer buffer (10x):	0.5 M Bicine, 0.5 M Bis-Tris, 20.5 mM EDTA, 10 % MeOH
Tricaine solution (24x):	0.4 % Tricaine powder in 15 mM Tris, pH 7

Reagents:

BSA, Roche
NCS, Sigma
Horse serum, Sigma

3.1.4 Molecular Biology / Biochemistry Kits

All restriction enzymes and DNA modifying enzymes (*e.g.* T4 Ligase) were purchased from New England Biolobas (NEB) or Thermo Scientific. Additional kits that were used

for a particular experimental procedure are found within the chapter '*3.2 Methods*' and are not listed here.

Deoxynucleotide Solution MIX, NEB
Fast Plasmid Mini Kit, 5 Prime
Gene Ruler 1 kbp Plus DNA ladder, Fermentas
I-SceI, Roche
QIAquick gel extraction kit, Quiagen
Plasmid Plus Midi Kit, Quiagen
Proteinase K, Invitrogen

3.1.5 Antibodies

Table 3.1. Antibodies used. Ap: Alkaline phosphatase, BrdU: Bromdesoxyuridin, Hrp: Horseradish peroxidase, Igf1r: Insulin-like growth factor 1 receptor, Pcna: proliferative cell nuclear antigen, Pod: Peroxidase.

Name	Type	Host	Source
Anti-BrdU	monoclonal	rat	Abd seroTec
Anti-DIG Ap conjugated	polyclonal	sheep	Roche
Anti-DIG Pod conjugated	polyclonal	sheep	Roche
Anti-Fluorescein Ap conjugated	polyclonal	sheep	Roche
Anti-Fluorescein Pod conjugated	polyclonal	sheep	Roche
Anti-GFP	polyclonal	chicken	Abcam
Anti-Pcna	monoclonal	mouse	DakoCytomation
Anti-phospho Igf1	polyclonal	rabbit	SCBT
Anti-phoshpo-histone 3 (H3P)	polyclonal	rabbit	Millipore
Anti-γTubulin	monoclonal	mouse	Sigma
Anti-Zns5	monoclonal	mouse	ZIRC
Secondary Alexa fluor-conjugated antibodies were purchased from Invitrogen.			
Secondary Hrp-conjugated antibodies were purchased from Roche.			

3.1.6 Plasmids and Constructs

Amplification of DNA fragments used for generating of below listed constructs (Table 3.3 & 3.4) was performed using Advantage HF 2 PCR Kit (Clontech). Oligos that were used are listed in Table 3.7 & 3.8 (see chapter '*3.1.7 Oligos*'). All constructs were sequenced.

Table 3.2. Constructs used for generation of capped sense RNA.

Insert	Vector	Source
tol2 transposase (full CDS)	pCSP2+	(Suster *et al.*, 2009)

Table 3.3. Constructs used for synthesis of *in situ* hybridization probes. CDS indicates full coding sequence. n. a. indicates no information available.

Insert	Vector	Source
actβAa/inhβAa (cDNA fragment)	pGEM-t	generated in this study
actβB/inhβB (CDS)	pGEM-t	generated in this study
aldh1a2 (cDNA)	pCR4	M. Brand, Technische Universität Dresden
amcyan (CDS)	pCSP2+	generated in this study
and1 (CDS)	pBK-CMV	M.-A. Akimenko, University of Ottawa
axin1(mouse, cDNA fragment)	pCRII	generated in this study
axin2 (n. a.)	pSPORT1	n. a.
bambib (CDS)	pGEM-t	generated in this study
bmp2a (CDS)	pGEM-t	generated in this study
bmp4 (n. a.)	pBS	M. brand, Technische Universität Dresden
crabp1b (cDNA fragment including CDS)	pGEM-t	generated in this study
egfp, humanized (CDS)	pCSP2+	(Stoick-Cooper *et al*., 2007b)
erm (cDNA fragment)	pGEM-t	generated in this study
fgf3 (cDNA fragment including CDS)	pCSP2+	M. brand, Technische Universität Dresden
fzd9b (cDNA fragment)	pGEM-t	generated in this study
gdf6a (cDNA fragment)	pGEM-t	generated in this study
her12 (cDNA fragment including CDS)	pGEM-t	generated in this study
heyl (CDS)	pGEM-t	generated in this study
igf2b (cDNA fragment including CDS)	pCRII	A. Wood, Center for Reproductive Biology, Boston
ihha (CDS)	pCRII	generated in this study
kaede (CDS)	pCSP2+	generated in this study
lef1 (n. a.)	n. a.	(Stoick-Cooper *et al*., 2007b)
lfng (CDS)	pGEM-t	generated in this study
lrp5 (cDNA fragment)	pGEM-t	generated in this study
lrp6 (cDNA fragment)	pGEM-t	generated in this study
msxB (n. a.)	pBluescript SK	(Akimenko *et al*., 1995)
pea3(cDNA fragment)	pGEM-t	generated in this study
ptc2 (cDNA fragment)	pGEM-t	generated in this study
runx2b (n. a.)	n. a.	H. Roel, University of Sheffield
scube2 (cDNA fragment)	pGEM-t	generated in this study
shha (CDS)	pGEM-t	generated in this study
socs3b (cDNA fragment)	pCRII	generated in this study
sost (cDNA fragment)	pGEM-t	generated in this study
sp7 (n. a.)	n. a.	H. Roehl, University of Sheffield
spry4 (cDNA fragment)	pSPORT1	(Stoick-Cooper *et al*., 2007b)
tcf1 (cDNA fragment)	pGEM-t	generated in this study
tcf3a (n. a.)	pCSP2+	R. Dorsky, University of Utah
tcf3b (full CDS)	pGEM-t	generated in this study
tcf4 (cDNA fragment)	pGEM-t	generated in this study
waif1a 5'UTR + mCherry (CDS)	pCSP2+	B. Kagermeier-Schenk, Technische Universität Dresden
wnt10a	pCRII	(Stoick-Cooper *et al*., 2007b)

Table 3.4. Constructs used for generation of transgenic zebrafish lines

Construct	Source
7xTCF-Xla.Siam:3xKaede; Tol2, I-SceI, attp entry sites	generated in this study
*her4.3:*irTAM2(3F)-p2A-AmCyan; Tol2, I-SceI sites	C. Haase, Technische Universität Dresden
keratin4:irTAM2(3F)-p2A-AmCyan; Tol2, I-SceI sites	C. Haase, Technische Universität Dresden
keratin18:irTAM2(3F)-p2A-AmCyan; Tol2, I-SceI sites	C. Haase, Technische Universität Dresden
*sp7:*irTAM2(3F)-p2A-Cerulean; Tol2, I-SceI sites	C. Haase, Technische Universität Dresden
ubiquitin:irTAM2(3F)-p2A-Cerulean; Tol2, I-SceI sites	generated in this study

The *7xTCF-Xla.Siam*:3xKaede construct was created by cloning the *7xTCF-Xla.Siam* regulatory sequence (Moro *et al*., 2012) upstream of 3 in-frame fused Kaede (Ando *et al*., 2002) CDS which were separated via a linker sequences containing either a SmaI (5'-CTGGAGGAAGCGGACCCGGGGGA-3') or ApaI (5'-CCTGGAGGAAGCGGGCCC GGCGGA-3') restriction site (Fig. 3.1A).

The *ubiquitin:*irTAM2(3F)-p2A-AmCyan construct was generated by cloning the previously described regulatory sequence of the *ubiquitin* gene (Mosimann *et al*., 2011) upstream of the doxycycline (DOX)-inducible transcriptional activator [irtTAM2(3F)] tagged with p2a and AmCyan (Knopf *et al*., 2010) (Fig. 3.1B). The remaining TetActivator constructs were generated by Christa Haase (Technische Universität Dresden) by cloning the previously described regulatory sequences of the *her4.3* (Yeo *et al*., 2007), *sp7/osx* (Spoorendonk *et al*., 2008), *keratin4* (Gong *et al*., 2002) or *keratin18* (Wang *et al*., 2006) genes upstream of the doxycycline (DOX)-inducible transcriptional activator [irtTAM2(3F)] tagged with p2a and AmCyan or Cerulean (Knopf *et al*., 2010).

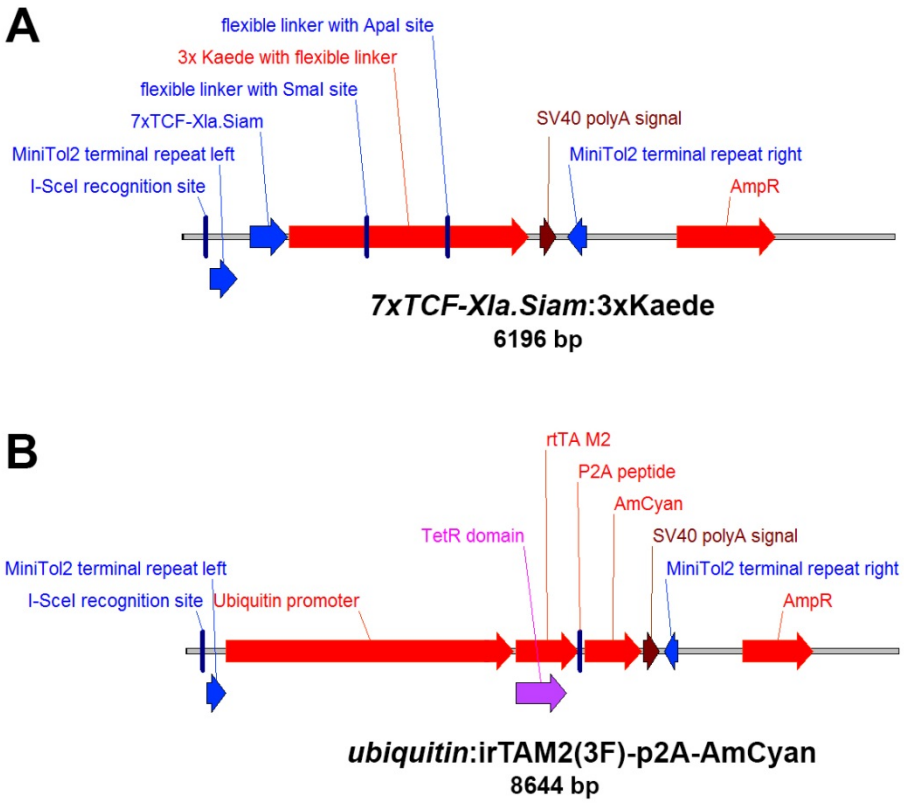

Fig. 3.1. Plasmid maps of constructs used for generation of *7xTCF-Xla.Siam*:3xKaede (A) and *ubiquitin:*irTAM2(3F)-p2A-AmCyan (B) transgenic lines.

3.1.7 Oligos

Table 3.5. RT-PCR Primer used for expression analysis of FACS-sorted cells.

Gene	RefSeq	Forward primer	Reverse primer
axin2	NM_131561	GTGACCCCGGAAATCCTAAT	GGCTATCAACTGTGCTGCAA
β-actin1	NM_131031	GAAGGAGATCACCTCTCTTGCTC	GTTCTGTTTAGAAGCACTTCCTGTG
lrp5	NM_001177458	CAGCATGGTAAAGGGATATCATGT	CATGTAGTACTTGTTGCTTTTCCAGC
lrp6	NM_001134684	TCGTCCAGCACTAAAGGAGCAT	GCTAGCGTAGCCTTTAGCAGCA
spry4	NM_131826	CAGCCGCGTTCCCTACGGAC	ATGGAGCTAGGCCGACCGCT

Table 3.6. Primer used for genotyping.

Transgenic line	Forward primer	Reverse primer
***hsp70l*:cyp26a1^{kn1}**	CAGCAGGAGGTGAAGAGC	GAGCAAAGGTCTGGAGGA
HG21C	GTGTTTCCAAACATGTATGAGT	GACTGTTTGTTAGTTTGAGGCT
***hsp70l*:noggin3^{fr14}**	CGCAGGAAAGAACATGTGAGC	CGGGTTGGACTCAAGACGATAG

Table 3.7. Primer used for generation of *7xTCF-Xla.Siam*:3xKaede and *ubiquitin:*irTAM2(3F)-p2A-Am Cyan constructs.

Construct	Forward primer	Reverse primer
7xTCF-Xla.Siam: 3xKaede	**7xTCF-Xla.Siam:** TTATTTCTCGAGGAATTCGATTAAGGACCTCAGAATCATCAAAGGACC **3xKaede:** **(A)**TTATTTACGCGTCCACCATGGTGAGTCTGATTAAACCAGA **(B)**CCTGGAGGAAGCGGACCCGGGGGAATGGTGAGTCTGATTAAACCAGAAATGAAGATC **(C)**CCTGGAGGAAGCGGGCCCGGCGGAATGGTGAGTCTGATTAAACCAGAAATGAAGATC	**7xTCF-Xla.Siam:** TTTATTACGCGTCTTGCAAGCTTATCTCTGTCTCCCAAAATGTTGG **3xKaede:** **(A)**TTTATTTCCCCCGGGTCCGCTTCCTCCAGGCTTGACGTTGTCCGGCAATCCAG **(B)**TCCGCCGGGCCCGCTTCCTCCAGGCTTGACGTTGTCCGGCAATCCAG **(C)**TTTATTGACGTCAAAAAACCTCCCACACCTCCCCC
*ubiquitin:*irTAM2(3F)-p2A-Cerulean	TTATTTGGGCCCACCAGCAAAGTTCTAGAATTTGTCGAAACATTTATG	TTTATTGGCCGGCCCTGTAAACAAATTCAAAGTAAGATTAGCAATCACACATTTC

Table 3.8. Primer used for generation of *in situ* hybridization probe templates.

Gene	RefSeq/ Source	Forward primer	Reverse primer
actβAa/ inhβAa	NM_130916	GGGATCCTCCTGCTGCTAATCCG	GTGGAGTGGAAGGACAGCGAGTTG
actβB/ InhβB	NM_131068	ATGGACACGATATTTATGAAAATGAGCGT	TCAGGCACAGCCGCACTCCT
amcyan	Clonetech	TTATTTGAATTCCCACCATGGCCCTGTCCAACAAGTTCATC	TTTATTCTCGAGCTAGAAGGGCACCACGGAGGTGAT

–Table 3.8., continued–

Gene	RefSeq/ Source	Forward primer	Reverse primer
axin1 (mouse)	TetRE:Axin1-YFP	Excised from *TetRE*:Axin-YFP construct (Knopf *et al.*, 2010) and ligated into pCRII Topo	
bambib	NM_001002189	ATGCAGCGGAACAGCAGTCTCG	TCACACAAACTCCAGCTTTCCTCG
bmp2a	NM_131359	ATGGTCTCGTCCACCGCCGC	TCAGCGGCACCCGCATCCCT
crabp1b	NM_001001842	AAAAGGGGTTGACACTGTAGTATAGACCGA	ACAATCAAATGTCTTTATTATTACATGCATGTAACA
erm	NM_131205	TGCCATCAGCCCAAACACAGAC	TCAGGGAACCTGCAGACTATCAGGC
fzd9b	NM_131511	ATGGGAAGCTCACCTCTGCAAATTG	CTGCTGCTAGAAACCAAGTAAGGGTGAG
gdf6a	NM_001159994	CATGGTGGTAGAACAGTGTGGCTGC	ACGCTCCTTCCAGAGTACTTGGACAG
her12	NM_205619	ATGGCACCCCACTCAGCCAC	CAGTTTATTAAGCAAGTAAAAAAACAGGGGT
heyl	NM_181736	ATGAAGAGACCTCATGACTACAGTTCTCCA	TCAAAACGCCCCTATCTCTGTGC
ihha	NM_001034993	ATGCGTCTCCCCGTGGTGTTT	TCATCTATCATTGTCCATCATGCTCCA
kaede	(Ando *et al.*, 2002)	TTATTTGAATTCCCACCATGGTGAGTCTGATTAAACCAGAAATGAAGA	TTTATTCTCGAGCTACTTGACGTTGTCCGGCAATCCA
lfng	NM_130971	ATGTTGAAAACATATCGCGGAAAAGTC	TTAGTAGGCAACCTGAGGAGGGCAC
lrp5	NM_001177458	AACTGTCCCATCTGCTCCAAACTGCA	TCATGAGGAGTCTGTGCAGGGCG
lrp6	NM_001134684	TTCCAGTGTGACAGCCGGCAG	TCAGGAGGAGTCTGTGCAGGGC
pea3	NM_131425	TTAGTACATGTAGCCTTTGGAGTAGGGCTG	CTATGAGCAGAAGAGAGCAGCCGTG
ptc2	NM_130988	ATCTACCTGACAGTATGGGTCAGTAATGATCC	CGTTTCAGATTAGTATTCAGAGTCAGAAGTCTCA
scube2	NM_001014813	ATCCTGTTTCACATGCGGAGGAAG	GACAAGAACGCTCAACAATATCTGTTCCA
shha	NM_131063	ATGCGGCTTTTGACGAGAGTGC	TCAGCTTGAGTTTACTGACATCCCCA
socs3b	NM_213304	GCTCCCATCTAGCCCTCTCTCC	ACTGCGGTCATCAGACCAGACC
sost	XM_001340647	AAGAGAAGAAAACTGGTCGAAGTTTGCC	TCAGTATGAATTGCTGTTGATGGACGG
tcf1	NM_001012389	GTCTTGAGAAAGTTTGGATCATGCCG	CTTTGGAGAGCCAGGCCCTGTACT
tcf3b	AY221031	ATGCCGCAGCTTAACGGAGGC	TCAGTCGCTGGATTTGGTGACCAG
tcf4	NM_131259	CGGGCTATCCATTTATAATGATTCCCG	TCAAAGACTGCTTGTATTAGAACAGAAAGACAAGA

3.1.8 *Transgenic Zebrafish Lines*

Table 3.9. Transgenic zebrafish lines used.

Line	Abbreviation	Source
***6xTCF/lef-miniP*:2dGFP**	*6xTCF*:dGFP	(Shimizu *et al.*, 2012)

–Table 3.9., continued–

Line	Abbreviation	Source
***7xTCF-Xla.Siam*:3xKaede**	*7xTCF*:3xKaede	generated in this study
***7xTCF-Xla.Siam*:nlsmCherry^{la5}**	*7xTCF*:mCherry	(Moro *et al.*, 2012)
***her4.3*:EGFP^{y83}**	*her4.3*:EGFP	(Yeo *et al.*, 2007)
***her4.3*:irtTAM2(3F)-p2a-AmCyan**	*her4.3*:TetA AmCyan	C. Haase, Technische Universität Dresden, G. Weidinger (Ulm University)
HG21C	-	(Nagayoshi *et al.*, 2008)
***hsp70l*:Mmu.Axin1-YFP^{w35}**	*hs*:Axin1	(Kagermeier-Schenk *et al.*, 2011)
***hsp70l*:cyp26a1^{kn1}**	*hs*:cyp26a1	(Blum and Begemann, 2012)
***hsp70l*:dkk1-GFP^{w32}**	*hs*:dkk1	(Stoick-Cooper *et al.*, 2007b)
***hsp70l*:dnfgfr1-EGFP^{pd1}**	*hs*:dnfgfr1	(Lee *et al.*, 2005)
***keratin4*:irtTAM2(3F)-p2a-AmCyan**	*keratin4*:TetA AmCyan	C. Haase, Technische Universität Dresden, G. Weidinger (Ulm University)
***keratin18*:irtTAM2(3F)-p2a-AmCyan**	*Keratin18*:TetA AmCyan	generated in this study
***hsp70l*:noggin3^{fr14}**	*hs*:nog3	(Chocron *et al.*, 2007)
***hsp70l*:vHRAS,cryaa:DsREDEx^{pd8}**	*hs*:v-ras	(Lee *et al.*, 2009)
***hsp70l*:wnt8-GFP^{w34}**	*hs*:wnt8	(Weidinger *et al.*, 2005)
***sp7*:irtTAM2(3F)-p2a-Cerulean**	*sp7:*TetA Cerulean	C. Haase Technische Universität Dresden, G. Weidinger (Ulm University)
***Top*:dGFP^{w25}**	*Top*:dGFP	(Dorsky *et al.*, 2002)
***TetRE*:Axin1-YFP^{tud1}**	*TetRE*:Axin1-YFP	(Knopf *et al.*, 2010)
***ubiquitin*:irtTAM2(3F)-p2a-AmCyan**	Ubiquitin:TetA AmCyan	generated in this study

3.2 Methods

3.2.1 Fish Husbandry and Fish Transgenesis

Transgenic and wild type zebrafish (strains: AB, WIK, GOL, ALBINO, PANTHER) were raised and maintained under standard laboratory conditions in a 14-hour on/10-hour off light/dark cycle at 26-27°C and pH 7.5 (Westerfield, 2000). Embryos were kept for 6 days in E3 embryo medium at 28.5°C followed by maintenance under standard conditions. Transgenic fish lines created in this study were either established by Tol2-mediated transgenesis (*keratin18*:TetA AmCyan, *7xTCF*:3xKaede) or using the I-SceI meganuclease technique (*ubiquitin*:TetA AmCyan) (Suster *et al.*, 2009; Thermes *et al.*, 2002). The *her4.3*:TetA AmCyan, *keratin4*:TetA AmCyan, and *sp7*:TetA Cerulean transgenic fish lines were generated by Christa Haase (Technische Universiät Dresden) using the I-SceI meganuclease technique. 50 pg plasmid DNA of interest, containing either an I-SceI meganuclease site or Tol2 transposable elements, was injected into fertilized eggs together

with I-SceI protein for I-SceI-mediated transgenesis or capped sense RNA coding for *Tol2* transposase for transposon-mediated transgenesis, respectively. Germ-line integration was assessed by outcross and appearance of fluorescence.

3.2.2 Fin Amputations, Heat Shocks, Drug Treatments, Irradiations and Regenerate Length Measurements

For fin amputations, fish were anesthetized in 1x Tricaine solution and approximately 50 % of the caudal fin was removed with a scalpel as previously described (Poss *et al*., 2000a), after which fish were returned to 28.5°C water.

Heat shocks were performed for 1 h at 37°C or for 1 h at 38°C for *hsp70l*:cyp26a1 transgenic fish, according to the schematic timelines shown with each experiment. Water temperature was raised to 37°C or 38°C within 10 min.

Drug treatments were performed by incubating fish in fish system water containing the drugs except for retinoic acid treatments. Fish were kept in the dark and water was exchanged daily. Doxycycline (DOX; Sigma) was dissolved in 50 % EtOH and used at 25 µg/ml. 10 µM Alk4/5/7 inhibitor SB431542 (Tocris), 5 µM Igf1r inhibitor NVP-AEW541 (Selleck), 10 µM γSecretase inhibitor LY411575 (Selleck), 5 µM Smoothened agonist (SAG; Calbiochem), 5 µM Jnk inhibitor SP60125 (Tocris), 50 µM Smoothened inhibitor Cyclopamine (Sigma) or 12 µM Axin stabilizer IWR-1 (Sigma) was used as previously described (Chablais and Jazwinska, 2010; Grotek *et al*., 2013; Ishida *et al*., 2010; Jazwinska *et al*., 2007; Lee *et al*., 2009; Lu *et al*., 2009). NADPH-oxidase inhibitor VAS-2780 (Enzo life science) was dissolved in DMSO at 20 µM and used at 0.5 µM. 10 µl of 3 mM retinoic acid (Sigma) were administered by repeated intraperitoneal injections as described (Blum and Begemann, 2012).

Sublethal irradiation of zebrafish was performed in collaboration with Nona Shayegi (CRTD, Dresden). In brief, fish were transferred to plastic bags containing 1 l of fish system water, placed in a ^{137}Cesium source irradiator (Gammacell 3000 Elan) and exposed until a total dosage of 40 Gy was achieved.

Regenerate length and calcified bone length measurements were performed using ImageJ software. The regenerate length or calcified bone length of the 2nd, 3rd and 4th lateral ray of each lobe was determined.

3.2.3 Synthesis of Capped Sense RNA and Labeled RNA Probes

Capped sense RNA was synthesized *in vitro* from 0.5-1 µg of linearized plasmid DNA of interest using mMessage mMachine Kits (Ambion) according to manufacturer instruction. Subsequently, DNA template was removed using DNaseI (Promega), and RNA was purified using RNeasy Mini Kit (Quiagen) following the instruction manual. Correct integrity of purified RNA was confirmed by agarose gel electrophoresis and RNA was stored at -80°C.

DIG- or Fluorescein-labeled antisense RNA probes were *in vitro* synthesized from 1 µg linearized plasmid DNA of interest using SP6/T7/T3 RNA polymerases (Promega) and either DIG-labeled or Fluorescein-labeled Nucleotides (Roche). Reaction was performed according to SP6/T7/T3 RNA Polymerase instruction manuals. Following probe synthesis reaction mix was further processed as described for synthesis of capped sense RNA. Purified RNA probes were mixed with 100 µl Hybridization buffer and stored at -20°C.

3.2.4 RNA Whole Mount in situ Hybridization (ISH) and Cryosectioning

All ISHs were performed on whole mount regenerates and stained samples were subsequently cryosectioned. For chromogenic whole mount ISH, fins were fixed overnight (o/n) at 4°C in 4 % PFA. Next day fins were washed twice in PBT and stepwise dehydrated by successive incubation 5 min each in 25 % MeOH-PBT, 50 % MeOH-PBT, 75 % MeOH-PBT, 100 % MeOH, and stored until needed in 100 % MeOH at -20°C. When required, fins were rehydrated at room temperature (RT) by successive incubation 5 min each in 75 % MeOH-PBT, 50 % MeOH-PBT and 25 % MeOH-PBT followed by 4 washes 5 min each in PBT. Subsequently, fins were incubated at RT for 20 min in PBT containing 20 µg/ml Proteinase K (Invitrogen) followed by 2 brief washes in PBT to stop the digest. Fins were re-fixed at RT for 20 min in 4 % PFA followed by 5 washes 5 min each in PBT. Thereafter, fins were incubated at 65°C for >1 hour (h) in pre-warmed Hybridization buffer. Hybridization buffer was replaced with ISH probes diluted in Hybridization buffer (1:100-1:200; pre-warmed to 72°C for 10 min) and incubated o/n at 65°C. The next day

fins were washed at 65°C 20 min each once in Hybridization buffer, 3 times in 50 % 2xSSCT / 50 % deionized Formamide, and twice in 2xSSCT, followed by 4 washes at 65°C 30 min each in 0.2x SSCT. Thereafter, fins were washed twice at RT 5 min each in PBT and incubated for >1 h in Blocking solution under slow agitation. Subsequently, fins were incubated at 4°C o/n in Blocking solution containing anti-DIG-Ap antibody (1:4000). The next day fins were washed 6 times at RT 20 min each in PBT, followed by 3 washes at RT 5 min each in NTMT. Blue colour reaction was performed by incubating fins at RT in NBT/BCIP staining buffer in the dark until signal had reached the desired intensity. The staining reaction was terminated by washing fins several times in PBT and/or STOP solution. Background staining was cleared by incubating fins 2 times 15 min each in 100 % EtOH, once for 5 min in 50 % EtOH-PBT, followed by 5 washes 5 min each in PBT. Fins were stored in STOP solution or mounted in 75 % Glycerol-STOP solution. If required, fins were further processed for a 2nd color reaction as follows. Anti-DIG-Ap antibody was removed by washing fins 5 min each two times in Stripping buffer and five times in PBT. Afterwards fins were blocked in Blocking solution for >1 h at RT and incubated at 4°C o/n with anti-Fluorescein-Ap antibody diluted in Blocking solution (1:4000). Fins were further processed as described for 1st staining reaction using INT/BCIP (brown precipitate) staining solution or using FastRed tablets (fluorescent red precipitate).

TSA fluorescence ISH was performed using the TSA Plus System Kit (Perkin Elmer). Dual color TSA fluorescence ISH was performed as described for chromogenic dual color ISH with some modifications: 1.) Before pre-hybridization endogenous peroxidase activity was quenched by incubating fins at RT for 20 min in 1-3 % H_2O_2 followed by 5 washes 5 min each in PBS. 2.) Before incubation with anti-DIG or anti-Fluorescein antibody, fins were blocked at RT for >1 h in Blocking reagent (1 % in PBT) provided with the Kit. 3.) Antibodies used to detect labeled RNA hybrids were anti-DIG-Pod or anti-Fluorescein-Pod diluted 1:500 in Blocking reagent. 4.) Color reaction was performed at RT for 5-30 min in Amplification buffer containing Tyramid substrate (1:500) provided with the Kit, followed by 6-8 washes 20 min each in PBT.

For cryosectioning, fins were incubated at 4°C o/n in 0.5 mM EDTA in PBS. The next day, fins were incubated at RT in 10 % sucrose-PBS, 20 % sucrose-PBS, 30 % sucrose-PBS and 30 % sucrose-PBS:tissue freezing medium (TFM; Triangel Biomedical Sciences) at 1:1 for 30 min each. Subsequently, fins were incubated at 4°C for >2 h in

tissue freezing medium. Fins were frozen in cryomolds and 12-14 µm cryosections were obtained with a Cryostat HM560 (Microm) and stored at -20°C until needed.

3.2.5 Immunohistochemistry

For immunohistochemistry on fin sections, sections were treated with 100 % MeOH (chilled to -20°C) for >30 min to improve adherence to the microscope slides followed by two washes at RT 5 min each in PBT. Sections were blocked at 37°C for 1 h in NCS-PBT containing 2.5 % horse serum, and incubated o/n at 4 °C with primary antibody of interest (1:300-1:500) diluted in NCS-PBT. The next day, sections were washed at RT 4 times 10 min each with PBT and incubated for 2 h at RT with secondary antibody of interest diluted 1:400 in NCS-PBT. Thereafter, sections were washed 10 min each two times in with PBT and one times in PBS. Subsequently, sections were incubated for 10 min with 4', 6-diamidino-2-phenylinodole (Dapi; Sigma) to visualize nuclei followed by two washes 10 min each in PBS. Fin section were re-fixed for 7.5 min in 4 % PFA, washed two times 5 min each in PBS and mounted in Mounting medium.

Simultaneous detection of transcripts and proliferative nuclear antigen protein (Pcna) in whole mount regenerates was performed as described previously (Nechiporuk and Keating, 2002). During sample incubation with anti-DIG-Ap antibody (see chapter '*3.2.4 RNA Whole Mount in Situ Hybridization (ISH) and Cryosectioning*') an anti-Pcna antibody (1:100) was added. The next day, fins were washed at RT 8 times 20 min each in PBT and incubated o/n at 4 °C with secondary Alexa Fluor-conjugated antibody of interest (1:200 in Blocking solution). The next day, fins were washed at RT 8 times 20 min each in PBT and processed for ISH staining reaction using FastRed tablets.

For simultaneous detection of transcripts and BrdU-labeled DNA, ISH-stained whole mount regenerates where subsequently washed twice in 2 N HCl-PBTx and incubated at RT for 30 min in 2 N HCl-PBTx to retrieve antigen. Fins were further processed as described below for whole mount H3P staining. Anti-BrdU antibody was used at 1:100.

Whole mount phospho-histone 3 (H3P) staining and imaging of H3P+ cells was performed as described previously (Lee *et al*., 2005; Poss *et al*., 2002). Fin regenerates were harvested and fixed o/n at 4 °C in Carnoy's fixative. Next day fins were washed at

RT twice in 100 % MeOH and stepwise rehydrated by successive incubation 5 min each in 75 % MeOH-PBTx, 50 % MeOH-PBTx, 25 % MeOH-PBTx and PBTx. Subsequently fins were briefly washed at RT twice in 2 N HCl-PBTx and incubated for 30 min in 2 N HCl-PBTx to retrieve antigen. Fins were washed several times in PBTx, blocked at RT for 4 h in PBTx containing 0.25 % BSA and incubated o/n at 4 °C with anti-H3P antibody (1:200 in 0.25 % BSA-PBTx). Next day fins were washed at RT 8 times 20 min each in 0.25 % BSA-PBTx and incubated o/n at 4 °C with secondary Alexa Fluor-conjugated antibody of interest (1:200 in 0.25 % BSA-PBTx). Next day fins were washed at RT 8 times for 20 min each in PBS, mounted in Mounting medium and blastemal H3P+ cells were imaged using a Zeiss 510 Meta confocal microscope. Following H3P staining, the epidermis developed a non-specific fluorescence (unpublished observations; Lee *et al*., 2005; Poss *et al*., 2002). Thus, during the scans the confocal depth range was set between the highly stained epidermal layers. H3P+ cells in the 2nd and 3rd lateral ray of each lobe were then counted on maximum projections of confocal stacks (1 µm optical sections) covering the blastemal mesenchyme (~22-25 µm).

3.2.6 Detection of cell death

Apoptotic cells in regenerating fins were detected using the TUNEL assay. TUNEL staining on whole mount regenerates was performed using the ApopTag Red In Situ Apoptosis Detection Kit according to the manufacturer's instructions with some modifications. Regenerates were fixed, de-hydrated, re-hydrated, treated with Proteinase K and re-fixed as described in chapter '*3.2.4 RNA Whole Mount in situ Hybridization (ISH) and Cryosectioning*'. Subsequently, fins were equilibrated and incubated with TdT enzyme according to the user's manual, followed by several washes in Stop/Wash buffer. Thereafter, fins blocked for 30 min and incubated with ant-DIG-Ap diluted 1:2000 in Blocking solution provided with the Kit. Subsequently, fins were washed 20 min 6 times each in PBT and staining reaction was performed with NBT/BCIP as described in chapter '*3.2.4 RNA Whole Mount in situ Hybridization (ISH) and Cryosectioning*'. A positive control was generated by incubating the fins at RT for 10 min in 3000 U/ml DNase I in 50 mM Tris-HCl, pH 7.5.

3.2.7 BrdU Incorporation

Fish were incubated for 2 days in 1 l fish system water containing 50 µg/ml BrdU. Water was changed daily. At the end of the BrdU incubation fish were briefly rinsed in water before regenerates were harvested.

3.2.8 Tissue Histology

Alizarin Red staining of whole mount regenerates was performed as described previously (Munch *et al*., 2013). Fins were fixed o/n at 4°C in 4 % PFA. Next day fins were washed twice in PBT and rehydrated through a MeOH series as described for chromogenic ISH (see chapter '*3.2.4 RNA Whole Mount in Situ Hybridization (ISH) and Cryosectioning*'). Subsequently, fins were washed twice in distilled H_2O and bleached for 30 min in Bleaching buffer followed by two washes in distilled H_2O. Subsequently fins were incubated for 20 min in Alizarin Red solution and destained in H_2O until background staining disappeared.

Calcein staining of regenerates was performed on living fish. Fish were incubated for 30 min in fish system water containing 0.1 % Calcein (Sigma). Subsequently, fish were briefly rinsed once in fish system water and incubated for 20 min in fish system water to remove unbound excess Calcein. Calcein fluorescence was detected in the GFP channel using a Leica M205FA stereo microscope.

3.2.9 Preparation of Fin Regenerate Lysates and Immunoblotting

Fin regenerates were washed once in ice-cold PBS, transferred to RIPA buffer supplement with protease and phosphatase inhibitors (Calbiochem), snap frozen in liquid nitrogen and mechanically homogenized using a pestle. Samples were centrifuged at 4°C and 16,000 g for 5 min to pellet debris, and protein extracts were quantified by BCA protein assay (Pierce). Protein extracts were mixed with 3x SDS Page Sample buffer, separated using NuPage 10 % Bis/Tris gels (Invitrogen), transferred to Immobilion-FL PVDF membranes

(Millipore), and immunoblotted for protein of interest. Blots were developed using SuperSignal West Femto Maximum Sensitivity Substrate ECL detection (Pierce). Signals were visualized using a luminescent image analyzer LAS-3000 (Fujifilm).

3.2.10 Dissociation of Fin Regenerates and Flow Cytometry

Adult zebrafish caudal fin regenerates were harvested, briefly rinsed in PBS and incubated in 2 ml PBS containing 1 mg/ml Collagenase/Dispase mix (Roche). During incubation regenerates were mechanically dissociated by carefully pipetting them up and down using Pasteur glass pipettes with decreasing tip diameter. Cell suspension was filtered using a 20 µm Filcon (Keul GmbH) mesh. Flow cytometry was performed using a Becton Dickinson FACS ARIA II SORP (at the FACS Facility Biotec Dresden, Germany).

3.2.11 RNA Extraction and cDNA Synthesis

All centrifuge steps were performed at 4°C and 16.000 g. Zebrafish embryos, regenerates or FACS-sorted cells were incubated for 5 min in 500 µl Trizol (Gibco) and subsequently vigorously vortexed. Thereafter, samples were centrifuged for 10 min to pellet debris. Supernatant was mixed with 269 µl Chloroform, incubated for 10 min at RT and centrifuged for 15 min. The resulting upper (aqueous) phase was transferred to a new tube, mixed with 500 µl Isopropanol and centrifuged for 30 min. After decanting the Isopropanol, RNA pellet was washed in 500 µl 70 % EtOH and samples were centrifuged for 10 min. Ethanol was aspirated, RNA pellet air-dried followed by re-suspension in 20 µl RNase-free water. cDNA was synthesized from maximum 1µg RNA using ThermoScript RT-PCR system (Invitrogen) according to manufacturer's instructions.

3.2.12 RT-PCR

PCR on cDNA derived from FACS-sorted cells or zebrafish embryos was performed as follows using 10 mM of each dNTP and 10 µM of each primer: 1x (120 s, 94°C); 25-35x (30 s, 94°C; 30 s, T_m – 2°C; 30 x, 68°C); 1x (120 s, 68°C).

3.2.13 Genotyping

For isolation of genomic DNA, caudal fins were amputated and incubated at 95°C for 20 min in 120 µl 50 mM NaOH. Subsequently samples were cooled to 8°C and 14 µl 1M Tris-HCl, pH 8 was added. Samples were vortexed and centrifuged at 4°C and top speed for 5 min to pellet debris. 2 µl of each sample were used for PCR reaction. The PCR conditions for genotyping of *hs*:nog3, HG21C and *hs*:cyp26a1 transgenic fish were as follows using 10 mM of each dNTP and 10 µM of each primer: 1x (120 s, 95 °C); 25-35x (30 s, 95°C; 30 s, $T_{hs:nog3}$ = 55°C / T_{HG21C} = 58°C / $T_{hs:cyp26a1}$ = 58°C; 30 x, 68 °C); 1x (120 s, 68 °C).

3.2.14 Microarray Analysis

The microarray analysis was performed by Birgit Kagermeier-Schenk (Technische Universität Dresden) and Gilbert Weidinger (Ulm University). Probes for an Agilent 44K custom microarray were created using cDNA sequences derived from RefSeq, Unigene and ZFin databases (design LOLLSG01). Samples were prepared as detailed in Table 3.10. 10 fish were used for each sample and the regenerate plus 2 bony segments of the stump harvested for total RNA isolation using Trizol (Invitrogen), followed by a DNaseI digest and 21 subsequent purification with the NucleoSpin RNA extraction kit (Macherey & Nagel). RNA quality was analyzed using the Agilent Bioanalyzer. The Low RNA Input Fluorescent Linear Amplification Kit (Agilent) was used to obtain fluorescent cRNA. Two-color hybridizations were performed where arrays were simultaneously hybridized with 850 ng Cy3-labeled cRNA derived from one sample and a mix of Cy5-labeled cRNA

from all samples. All microarray experiments were performed with three independent biological samples.

Table 3.10. Experimental design for identification of the Wnt targetome during caudal fin regeneration. All samples were derived from caudal fins that were amputated at about 50 % of their proximodistal length. The regenerate plus 2 bony segments of stump tissue were harvested for RNA isolation. hpa, hours post amputation.

Stage of regeneration	Fish line	Manipulation	Timepoint of harvest	Sample Identifier
control	wild type	heat shock 2 h before harvest	0 hpa	0hpa_1hs_wt1/2/3
control	wild type	none	0 hpa	0hpa_no hs_wt1/2/3
wound healing	wild type	none	6 hpa	6hpa_no hs_wt1/2/3
wound healing	wild type	heat shock 2 h before harvest	6 hpa	6hpa_1hs_wt1/2/3
wound healing	*hs:*dkk1	heat shock 2 h before harvest	6 hpa	6hpa_1hs_dkk1/2/3
wound healing	*hs*:Axin1	heat shock 2 h before harvest	6 hpa	6hpa_1hs_axin1/2/3
blastema formation	wild type	none	48 hpa	48hpa_no.hs_wt1/2/3
blastema formation	wild type	heat shock 6 h before harvest	48 hpa	48hpa_1hs_wt1/2/3
blastema formation	*hs:*dkk1	heat shock 6 h before harvest	48 hpa	48hpa_1hs_dkk1/2/3
blastema formation	*hs*:Axin1	heat shock 6 h before harvest	48 hpa	48hpa_1hs_axin1/2/3
blastema formation	wild type	heat shock 2 h before amputation plus heat shocks at 10 hpa, 22 hpa, 34 hpa, 46 hpa	48 hpa	48hpa_serialhs_wt1/2/3
blastema formation	*hs:*dkk1	heat shock 2 h before amputation plus heat shocks at 10 hpa, 22 hpa, 34 hpa, 46 hpa	48 hpa	48hpa_serialhs_dkk1/2/3
blastema formation	*hs*:Axin1	heat shock 2 h before amputation plus heat shocks at 10 hpa, 22 hpa, 34 hpa, 46 hpa	48 hpa	48hpa_serialhs_axin1/2/3
regenerative growth	wild type	None	96 hpa	96hpa_no.hs_wt1/2/3
regenerative growth	wild type	heat shock 6 h before harvest	96 hpa	96dpa_1hs_wt1/2/3
regenerative growth	*hs:*dkk1	heat shock 6 h before harvest	96 hpa	96hpa_1hs_axin1/2/3
regenerative growth	*hs*:Axin1	heat shock 6 h before harvest	96 hpa	96dpa_1hs_dkk1/2/3

For annotation, probe sequences were mapped by BLASTn against Ensembl transcript sequences from version 9 of the zebrafish genome (derived via BioMart). Out of the 43219 probes that were used, 30081 probes had at least one hit using an E value cutoff < 10-9, while 13138 produced no hits. The latter probes were re-blasted against a transcript set including1000 bp genomic sequence 3´ of the predicted 3' end of the cDNA. 2334 probes produced a hit in the 3´flanking region of the cDNA set. These were assumed to represent 3'UTRs and the probes thus annotated to detect the corresponding transcript. Thus, in total, 32449 probes had at least one hit, with 1578 however being homologous to transcripts from more than 1 gene. These ambiguous probes were manually inspected and removed if they showed homology to transcripts of different genes. This resulted in a set of 31537 non-ambiguous annotated probes that have been used further (for differentially

expressed genes and co-expression analysis). Ortholog information for each transcript predicted by Ensembl was also extracted for mouse and humans.

The Agilent feature extraction software version 9.1 with all default parameters from Agilent was used to generate the feature extraction data from scans of hybridized arrays. Data analysis was performed using the Bioconductor package Limma (Smyth, 2005) for "two color" microarray with a "common reference". Feature extraction data was corrected for background using the "backgroundCorrect" function and MA values were extracted after normalization using "normalizeWithinArrays" (by loess). To make the arrays comparable with each other "normalizeBetweenArrays" function was used and the "M values" extracted for further analysis (Suppl. file *1_M_values.xlsx*). The function "lmfit" was used to get lists of fold changes and standard errors. "eBayes" was invoked for smoothing to the standard errors. A "design" was constructed based on the user guidelines in Limma Package for analysis of arrays with common reference. *axin1* and *dkk1* overexpressed samples were compared to the respective wild type controls. Since a Cy5 labeled common reference was used the design was multiplied by -1. The function "topTable" gave a list of differentially expressed genes. All probes were considered that showed absolute fold change of 1.2 and a Benjamini adjusted p-value <0.05. To remove multiple probes that were annotated to the same gene only the probe showing the biggest fold change was considered further (Suppl. *2_Differentially_expressed_genes.xlsx*).

3.2.15 Weighted Gene Expression Correlation Network Analysis

The weighted gene expression correlation network analysis (WGCNA) was performed in collaboration with Mohankrishna Dalvoy Vasudevaro and Gilbert Weidinger (Ulm University). Expression data of probes that were significantly differentially expressed (up- or downregulated) between control and *dkk1* or control and *axin1* overexpressed samples in at least 1 of the following conditions were used to perform weighted gene co-expression network analysis (WGCNA) using the WGCNA package (Langfelder and Horvath, 2008): 48 hpa single heat shock group; 48 hpa serial heat shock 22 group; 96 hpa single heat shock group. A total of 8761 probes fulfilled these criteria and were used for the analysis. A signed (bidirectional) network was constructed where only the positively correlated

genes are clustered into modules. Default values were used ("power = 6" and "mergeCutHeight =0.25"). "Module membership" for each probe was retrieved by using the "datKME" function and tabulated for all probes (Suppl. *3_Module_membership.xlsx*) Module eigengene information was extracted using the "net$MEs" function of WGCNA (Suppl. file *4_Module eigengenes.xlsx*). To visualize the expression patterns of modules using module eigengenes, the eigengene information for the "wild type heat shock", "Axin1" and "Dkk1" samples was used. Normalization was done by adjusting the values in a manner where eigengenes for the wild type samples at 0 hpa were set to zero. Averaging of the eigengenes was performed for the three biological replicates and the "Standard error of the means" calculated. The modules of our interest with respect to the pattern of expression (reduction in expression upon Wnt inhibition) were modules 26 (darkorange), 21 (darkred) and 3 (brown). To find the correlation between these modules, "eigengene adjacency" was calculated using the "cor(MEs)" function. Module 26 was found to be positively correlated with module 21 and 3 by a positive correlation co-efficient of 0.37 and 0.42 respectively (Suppl. *5_Eigengene adjacency.xlsx*).

Gene Ontology (GO) and KEGG and PANTHER Pathway enrichment analysis was performed using "DAVID Bioinformatic Resource" (Huang da *et al.*, 2009). Since functional annotation of zebrafish Ensembl gene IDs was poor in DAVID, the mouse ortholog Ensembl IDs for enrichment analysis was used. A specificity level of 5 was used for analysis of biological processes. Only those processes and pathways were considered that were composed of at least 4 genes with a Benjamini FDR corrected p value < 0.05. Out of the 33 modules clustered by WGCNA, 15 were significantly enriched for biological processes, and 14 showed enrichment for pathways (Table 3.11).

Table 3.11. WGCNA modules significantly (corrected p-value <0.05) enriched for biological process and pathways as determined by DAVID Bioinformatics resource. The Table was generously provided by Mohankrishna Dalvoy Vasudevaro (Ulm University).

Module number	Gene ontology	Benjamini corrected p-value	KEGG/Panther pathway	Benjamini corrected p-value
1	Sterol biosynthetic process	0.016	Circadian rhythm	1.16E-06
2	M phase	6.62E-42	Cell cycle	1.22E-18
3	**Heart development** **Cell morphogenesis**	**0.010** **0.01**	**None**	
4	Intracellular signaling cascade Regulation of lymphocyte differentiation	0.0090 0.020	Leukocyte transendothelial migration	2.77E-07
5	Organ morphogenesis	0.0059	Focal adhesion	3.06E-04
8	None		Proteasome	1.38E-04

-Table 3.11, continued-

Module number	Gene ontology	Benjamini corrected p-value	KEGG/Panther pathway	Benjamini corrected p-value
9	Cartilage development	2.61E-06	Tgfβ signaling pathway	3.99E-04
11	RNA metabolic process	3.72054E-19	RNA polymerase	0.019
12	Protein folding	1.57E-05	None	
13	Regulation of gene expression	1.15E-05	Wnt signaling pathway	0.058
15	RNA metabolic process	3.72E-16	None	
16	Translation	6.26E-11	Oxidative phosphorylation	7.93E-08
18	Chromatin modification	2.32E-07	Pdgf signaling pathway Prostate cancer	0.0024 0.026
21	**Tissue development**	**0.0016**	**Pathways in cancer** **Hedgehog signaling**	**9.72E-05** **4.16E-04**
26	**Organ morphogenesis**	**9.23E-06**	**Wnt signaling pathway** **Hedgehog signaling pathway**	**9.87E-05** **6.19E-05**
28	Translation	2.85E-30	Ribosome	4.09E-44

3.2.16 Statistics

Error bars shown indicate error of the mean. Significance of differences in mean regenerate/calcified bone length and number of proliferative cells was tested using Student's t-test. n.s. indicates not significant, * = $p<0.05$, ** = $p<0.01$, *** = $p<0.001$.

3.2.17 Nomenclature

The nomenclature of genes and proteins in this thesis has been simplified and is as follows: gene symbol: *dkk1* (small, italic), protein symbol: Dkk1 (1st letter is capitalized). Excluded from this rule are fluorescent proteins (*e.g.* EGFP) and transgene names of transgenic lines. Transgenic zebrafish lines were annotated according to the Zebrafish database 'ZFIN'. Abbreviations for each line used are listed in Table 3.9 (chapter '*3.1.8 Transgenic Zebrafish Lines*').

4 Results

4.1 Transgenic Wnt Reporter Lines Reveal Spatiotemporal Dynamics of Pathway Activation

It has recently been demonstrated that zebrafish caudal fin regeneration requires β–catenin-dependent Wnt signaling for both blastema formation and proliferation (Kawakami *et al*., 2006; Stoick-Cooper *et al*., 2007b). However, it has remained unexplained how Wnt signaling exerts these functions. To identify the mechanisms of Wnt action during fin regeneration, I first set out to characterize the spatiotemporal pattern of pathway activation taking advantage of sensitive transgenic reporters of β–catenin-dependent transcription. Transcripts of *7xTCF-Xla.Siam*:nlsmCherry^{ia5} (*7xTCF*:mCherry; Moro *et al*., 2012) could be detected from 6 hours post amputation (hpa) in the interray tissue extending approximately 100-200 μm proximal to the amputation plane (big arrowhead in Fig. 4.1A). Interray expression persisted by 12 hpa throughout further regeneration (big arrowhead in Fig. 4.1A). These interray domains were lost upon overexpression of the Wnt inhibitor *dickkopf-1* (*dkk1*) in *7xTCF*:mCherry; *hsp70l:*dkk1-GFP^{w32} (*hs:*dkk1; Stoick-Cooper *et al*., 2007b) double transgenic fish, indicating that they indeed reflect sites of active Wnt/β–catenin signaling (Fig. 4.1B). At 24 hpa *mCherry* transcripts were additionally detected distally to the fin ray stumps, where the blastema is forming (arrow in Fig. 4.1A). Following blastema formation, reporter activity was maintained in the distal part of the regenerate throughout the regenerative process (Fig. 4.1A and data not shown). Longitudinal sections revealed that within fin rays reporter activity was restricted to the mesenchyme of the blastema at all stages analyzed, while the epidermis was devoid of signal (asterisk in Fig. 4.1C). Similarly, the early interray expression domain was mesenchymal as well (Fig. 4.1C). mCherry fluorescence was detectable from 16 hpa and resembled that of the *mCherry* transcript expression pattern throughout the entire course of regeneration (Fig. 4.1D and data not shown).

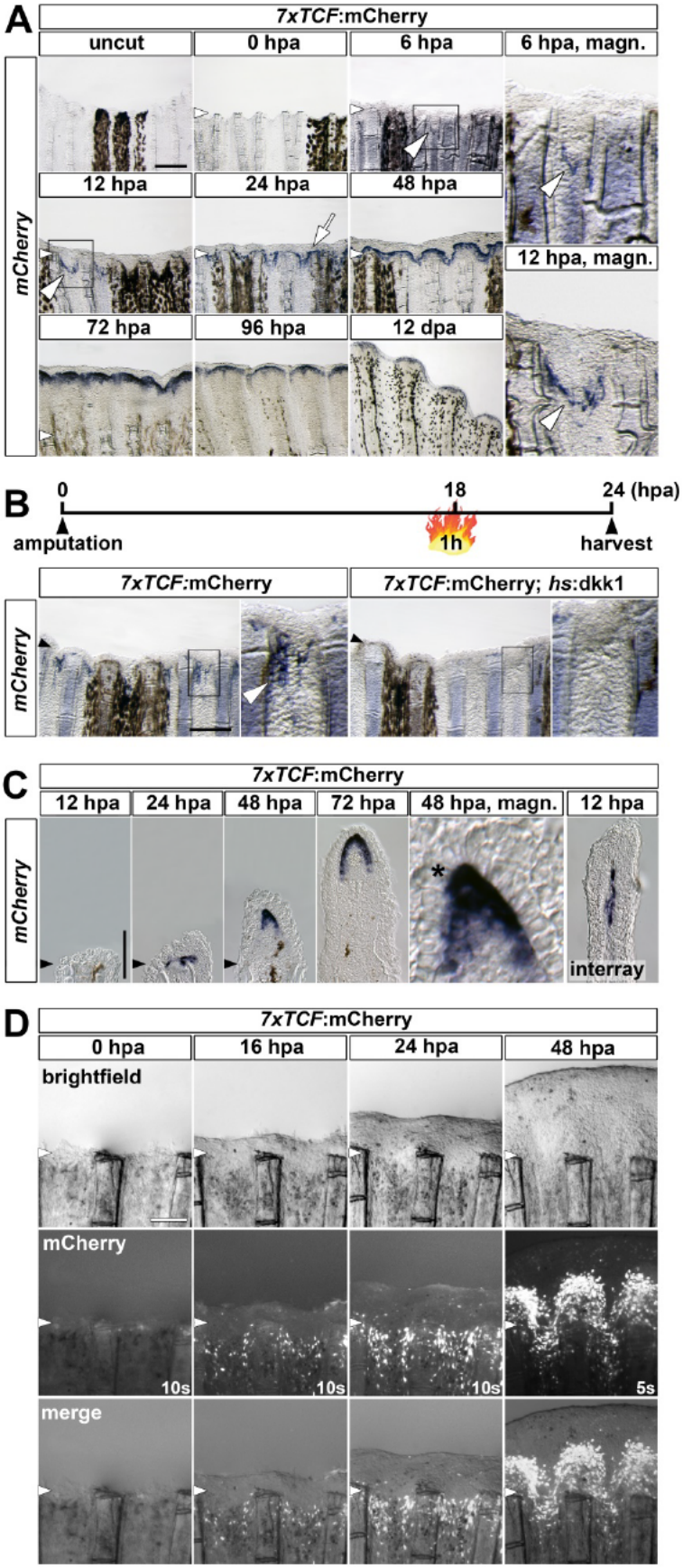

Fig. 4.1. The *7xTCF*:mCherry transgenic reporter line reveals Wnt/β–catenin pathway activation during caudal fin regeneration.
(A) *mCherry* transcripts in *7xTCF*:mCherry transgenic regenerates. Note transgene expression at 6 and 12 hpa in the interray tissue (big arrowheads). **(B)** *7xTCF*:mCherry reporter activity in the interray tissue (white arrowhead) is abolished upon *dkk1* overexpression in *7xTCF*:mCherry; *hs:*dkk1 double transgenic regenerates 6 hours post heat shock. n(*7xTCF* mCherry; *hs:*dkk1) = 11/11, n(*7xTCF*:mCherry; *hs:*dkk1) = 11/11. Heat shocks were performed according to the schematic timeline. **(C)** *mCherry* expression in *7xTCF*:mCherry transgenic regenerates is confined to the mesenchyme at all stages analyzed. The basal layer of the epidermis is devoid of staining (asterisk). **(D)** mCherry fluorescence in *7xTCF*:mCherry transgenic caudal regenerates. **(A-D)** Small arrowheads: amputation plane. Scale bars: whole mounts, 200 µm; sections, 100 µm.

Expression of the negative pathway regulator *axin2* is directly regulated by the Wnt/β–catenin pathway in many systems and thus frequently used as readout for active signaling (Jho *et al*., 2002; Lustig *et al*., 2002 and others). *axin2* expression was likewise found to be dependent on Wnt signaling in the regenerating fin as revealed by its suppression after ovexpression of the Wnt inhibitor *axin1* in *hsp70l*:Mmu.Axin1-YFP^{w35} (*hs*:Axin1; Kagermeier-Schenk *et al*., 2011) transgenic fish (Fig. 4.2A). *7xTCF*:mCherry and *axin2* expression largely co-localized in the distal blastema, supporting that the transgene reports sites of endogenous β–catenin transcriptional activity (arrowhead in Fig. 4.2B, Fig. 4.2C).

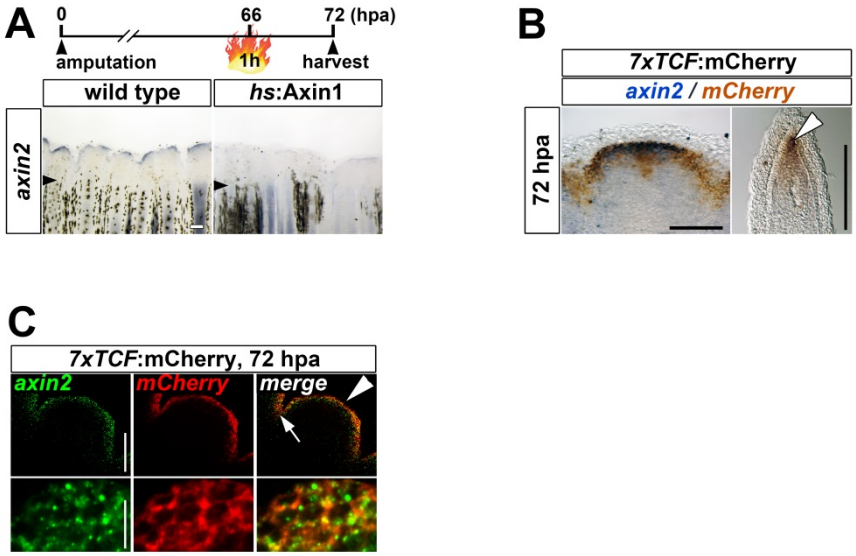

Fig. 4.2. *axin2* is expressed in the *7xTCF*:mCherry-positive blastema where it depends on Wnt/β–catenin signaling. (A) Downregulation of *axin2* expression in *hs*:Axin1 transgenic fish 6 h post heat shock. n(wild type) = 5/5, n(*hs*:Axin1) = 4/6. Heat shocks were performed according to the schematic timeline. **(B)** *axin2* (blue) and *mCherry* RNA (brown) are co-expressed in the distal blastema (arrowhead) in *7xTCF* mCherry transgenic regenerates. **(C)** *axin2* (green) and *mCherry* RNA (red) are co-expressed in distal blastema cells (arrowhead) and interray cells (arrow) in *7xTCF* mCherry transgenic regenerates. Shown is an optical section through a whole mount blastema. **(A-C)** Small arrowheads: amputation plane. Scale bars: whole mounts, 200 µm (A), 100 µm (B, C) and 10 µm (C); sections, 100 µm.

The expression pattern of a second transgenic reporter line *6xTCF/Lef-miniP*:2dGFP (*6xTCF*:dGFP; Shimizu *et al*., 2012) was similar to that of the *7xTCF*:mCherry reporter at 72 hpa (Fig. 4.3A). Expression of a third Wnt/β–catenin reporter line, *Top*:dGFP^{w25} (Dorsky *et al*., 2002) could not be detected before 24 hpa by *in situ* hybridization (ISH), which is consistent with its lower sensitivity during zebrafish embryogenesis (Moro *et al*., 2012), but expression from 24 hpa onwards likewise was confined to distal domains of the

regenerate and restricted to the blastemal mesenchyme (Fig. 4.3B). These results show that Wnt/β–catenin signaling is activated soon after fin amputation and that it is maintained in the tip of the blastemal mesenchyme throughout the course of tissue restoration.

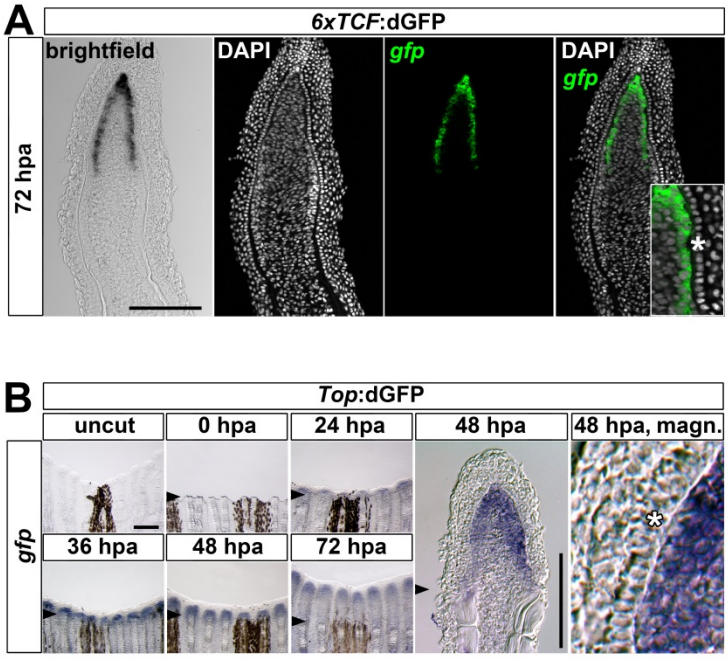

Fig. 4.3. *6xTCF*:dGFP and *Top*:dGFP transgenic reporter lines reveal Wnt/β–catenin pathway activation during fin regeneration. (A) *gfp* RNA expression in *6xTCF*:dGFP transgenic regenerates is confined to the distal and lateral blastemal mesenchyme. The basal layer of the epidermis is devoid of staining (asterisk). Shown is a confocal image of a longitudinal section. **(B)** *gfp* RNA expression in *Top*:dGFP transgenic caudal regenerates. Note transgene expression is detected in the blastemal mesenchyme while the basal epidermal layer is devoid of signal (asterisk). **(A-B)** Small arrowheads: amputation plane. Scale bars: whole mounts, 200 µm; sections, 100 µm.

4.2 Tcf/Lef Transcription Factor Expression in the Regenerating Caudal Fin

Wnt target gene expression is regulated by binding of stabilized β–catenin to transcription factors of the Tcf/Lef family that includes Lef1, Tcf1 (Tcf7), Tcf3a (Tcf7l1a), Tcf3b (Tcf7l1b) and Tcf4 (Tcf7l2). In the absence of β–catenin, Tcf/Lefs can interact with transcriptional co-repressors to repress transcription, while β–catenin binding causes recruitment of co-activators and transcriptional activation of target genes (Arce *et al*., 2006; Hoppler and Kavanagh, 2007). Genetic studies in several systems have revealed that different Tcf/Lefs mainly act as repressors (Tcf3), in an activating role (Lef1) or both (Tcf1, Tcf4) (Arce *et al*., 2006; Hoppler and Kavanagh, 2007). To further identify the

tissues responding to Wnt signals during fin regeneration, I characterized the expression patterns of the zebrafish Tcf/Lef members. ISH on 72 hpa regenerates showed that expression of all 5 Tcfs was upregulated upon amputation (Fig. 4.4A). In agreement with previous findings, *lef1* expression was detected weakly in the distal blastema (arrowhead in Fig. 4.4B) and stronger signal was observed in the proximal basal wound epidermis (Fig. 4.4B) (Poss *et al*., 2000a). *tcf1* was not only expressed in the distal blastema (arrowhead in Fig. 4.4B) and the basal epidermal layer, but also in the lateral blastema where osteoblast progenitors are located (asterisk in Fig. 4.4B). *tcf3a* and *tcf3b* were largely confined to the medial blastema, and largely absent from the (pre-)osteoblast domains (Fig. 4.4B), while *tcf4* appeared to be weakly expressed in the medial and lateral (asterisk in Fig. 4.4B) blastema. Epidermal transcripts of *tcf1* co-localized with that of *lef1* (Fig. 4.4C). *lef1*, *tcf1* and *tcf3a* were co-expressed with the *7xTCF*:mCherry reporter in the distal blastema mesenchyme (black arrowheads in Fig. 4.4D), while *tcf3b* and *tcf4* expression hardly overlapped with distal reporter activity (white arrowheads in Fig. 4.4D). Thus, β–catenin signaling seems to be only activated in a subset of cells expressing Tcf/Lef family members. Since Tcf3a acts as a transcriptional repressor in many systems (Arce *et al*., 2006; Hoppler and Kavanagh, 2007), Lef1 and Tcf1 are primary candidates for mediating the response to Wnt ligands in the *7xTCF*:mCherry reporter-positive distal blastema during fin regeneration. Interestingly, transposon-mediated loss of *tcf1*-function in the transgenic enhancer trap line HG21C did not impair regenerative growth suggesting redundant roles for Lef1 and Tcf1 during caudal fin regeneration (Fig. 4.4E), similar to pectoral fin development (Nagayoshi *et al*., 2008).

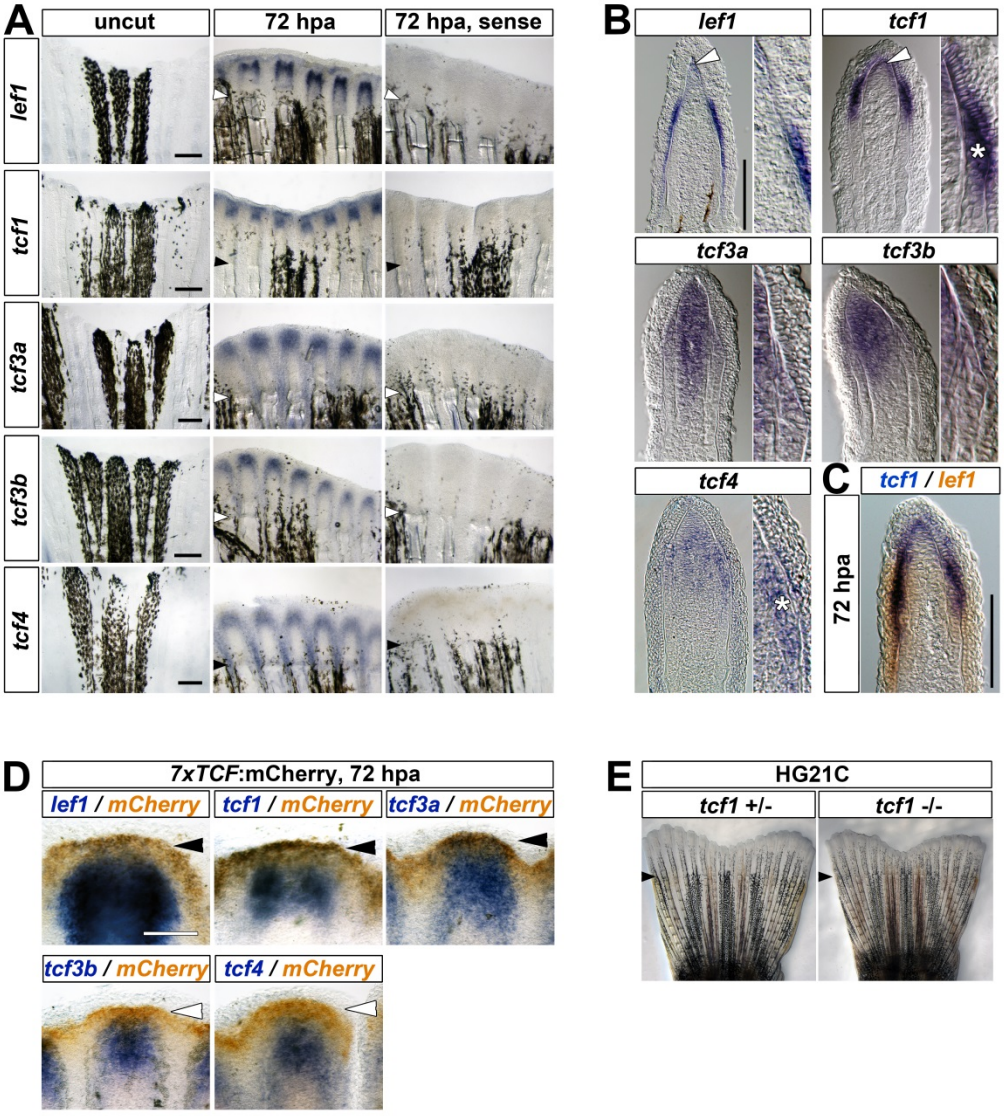

Fig. 4.4. Tcf/Lef transcription factor expression during caudal fin regeneration. (A) *lef1*, *tcf1*, *tcf3a*, *tcf3b* and *tcf4* are expressed in the regenerating fin. Hybridization with sense control probes revealed no signal. **(B)** Sections of whole mount stained regenerates shown in (A) reveal *lef1* expression in the distal blastema (arrowhead) and the basal layer of the epidermis, *tcf1* expression in the basal epidermis, lateral (asterisk) and distal blastema (arrowhead), *tcf3a, tcf3b* and *tcf4* expression in the medial and lateral (asterisk) blastema. **(C)** *tcf1* and *lef1* are co-expressed in the epidermis of the regenerating fin. **(D)** Dual color ISH of Tcf/Lef transcription factors and *mCherry* in *7xTCF*:mCherry transgenic regenerates. *tcf1, lef1* and *tcf3a* are co-expressed with *mCherry* in the distal blastema (black arrowheads), while *tcf3b* and *tcf4* are not expressed in the distal *mCherry*-positive domain (white arrowheads). **(E)** Transposon-mediated loss of *tcf1(tcf7)*-function in HG21C transgenic fish does affect fin regeneration. n($tcf1^{+/-}$) = 10/10, n($tcf1^{-/-}$) = 10/10. **(A-E)** Small arrowheads: amputation plane. Scale bars: whole mounts, 200 µm and 100 µm (D); sections, 100 µm.

4.3 The Wound Epidermis is not Competent to Respond to Wnt Ligands Activating β–catenin Signaling

lef1 does not only mediate signaling by Wnt proteins but its expression is directly activated by the pathway itself in several systems (Filali *et al*., 2002; Hovanes *et al*., 2001; Li *et al*., 2006). Furthermore, it was reported that *lef1* expression is suppressed by *dkk1* overexpression in the regenerating fin (Stoick-Cooper *et al*., 2007b) and I found it to be downregulated in all of its expression domains 6 hours after a single heat shock in *hs*:Axin1 transgenic fish as well (Fig. 4.5).

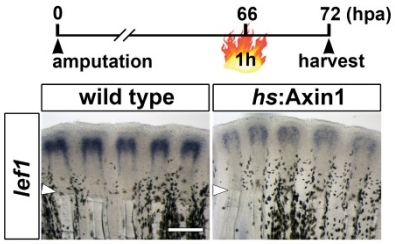

Fig. 4.5. *lef1* expression depends on Wnt/β–catenin signaling during caudal fin regeneration. Downregulation of *lef1* expression in *hs*:Axin1 fish 6 hours post heat shock. n(wild type) = 8/8, n(*hs*:Axin1) = 7/8. Heat shocks were performed according to the schematic timeline. Arrowheads: amputation plane. Scale bar: 200 µm.

Thus, *lef1* expression in the wound epidermis is regulated by Wnt signaling, yet all three of the transgenic Wnt reporter lines that I have used failed to detect pathway activation in the epidermis. To further test whether β–catenin signaling is indeed restricted to the blastemal mesenchyme, I asked whether epidermal cells express the Wnt co-receptors *lrp5* and *lrp6,* which are considered to be essential for β–catenin pathway activation by Wnt ligands (He *et al*., 2004; Wehrli *et al*., 2000). I found that both, *lrp5* and *lrp6* transcripts were upregulated upon fin amputation (Fig. 4.6A) and restricted to the blastemal mesenchyme, while the epidermis was devoid of expression (asterisk in Fig. 4.6B). To exclude that I missed potential low expression levels of *lrp5* or *lrp6* in the epidermis due to insufficient sensitivity of the employed ISH protocol, I developed a flow-cytometry approach that allowed the separation of regenerated epidermal from mesenchymal tissue. I used double transgenic fins of *7xTCF*:mCherry, which is most strongly active in the distal blastema, and *her4.3:*EGFP^{y83} (Yeo *et al*., 2007), which labels the proliferative proximal blastema but excludes the laterally located osteoblasts (Fig.

4.7A-D, Fig. 4.8A). Thus, the GFP+ mCherry+ fraction of such fins should contain blastemal cells, while the GFP– mCherry– fraction should encompass epidermal cells and other cell types.

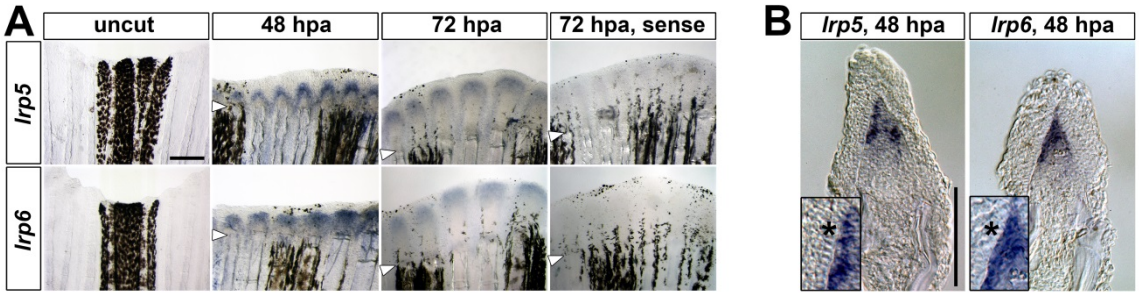

Fig. 4.6. *lrp*5 and *lrp6* co-receptor expression during caudal fin regeneration. (A) *lrp5* and *lrp6* are expressed in the regenerating fin. Hybridization with sense control probes revealed no signal. **(B)** *lrp5* and *lrp6* transcripts are detected in the blastemal mesenchyme while the basal layer of the epidermis is devoid of signal (asterisk). Arrowheads: amputation plane. Scale bar: whole mounts, 200 µm; sections, 100 µm.

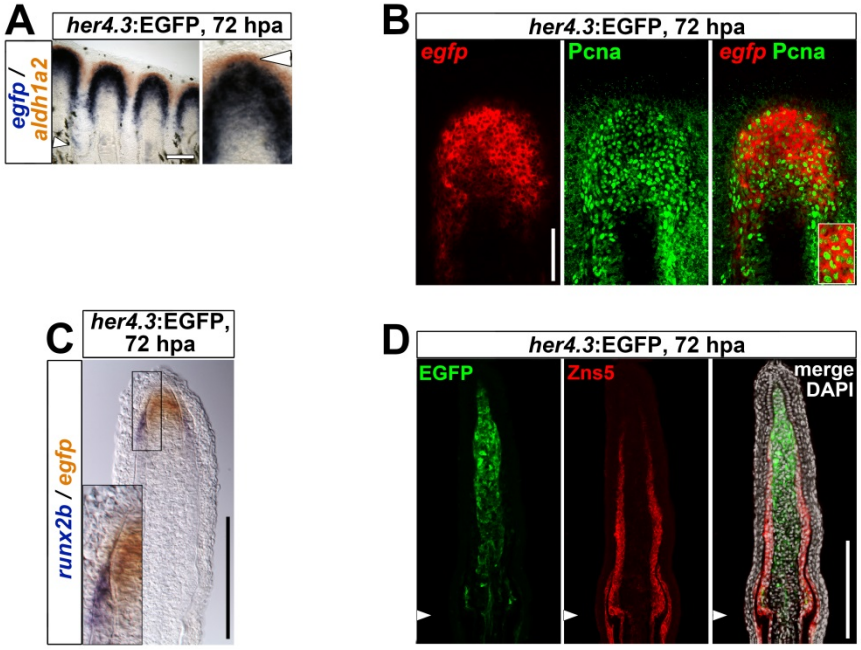

Fig. 4.7. *her4.3*:EGFP reporter activity is confined to the proliferative zone of the proximal medial blastema. (A) The *her4.3*:EGFP reporter (blue) is expressed proximally to the distal-most blastema marker *aldh1a2* (brown; big arrowhead). **(B)** *her4.3*:EGFP is active in the proliferative cell nuclear antigen (Pcna)-positive cells of the proximal blastema. Optical section through the center of a blastema stained for *egfp* transcripts and Pcna protein is shown. **(C)** *her4.3*:EGFP activity (brown) is detected medial to the *runx2b*-positive osteoblast progenitors. **(D)** Confocal image of a longitudinal section of a *her4.3*:EGFP transgenic regenerate stained with Zns5 antibody (labeling all osteoblasts) and GFP antibody show no overlap. Small arrowheads: amputation plane. Scale bar: whole mounts, 200 µm; sections, 100 µm.

By RT-PCR, transcripts of the distal blastema marker *axin2* were only detected in the GFP+ mCherry+ cell fraction while the Fgf target *spry4*, which is expressed in the blastema and the basal layer of the wound epidermis (Lee *et al*., 2005), was found in both GFP+ mCherry+ and GFP– mCherry– fractions, confirming that the cell sorting was successful (Fig. 4.8B). Importantly, *lrp5* and *lrp6* transcripts were only detectable in the GFP+ Cherry+ fraction, confirming the absence of these co-receptors in the epidermis. Furthermore, overexpression of *wnt8* was sufficient to increase Wnt reporter expression in the mesenchyme, but could not ectopically activate the reporter in the wound epidermis in *hsp70l:*wnt8-GFP^{w34} (*hs:*wnt8; Weidinger *et al*., 2005); *7xTCF*:mCherry double transgenic fish (Fig. 4.8C). Together, these data strongly suggest that Wnt/β–catenin signaling is restricted to the blastemal mesenchyme and that epidermal *lef1* expression must be indirectly regulated by β–catenin signaling.

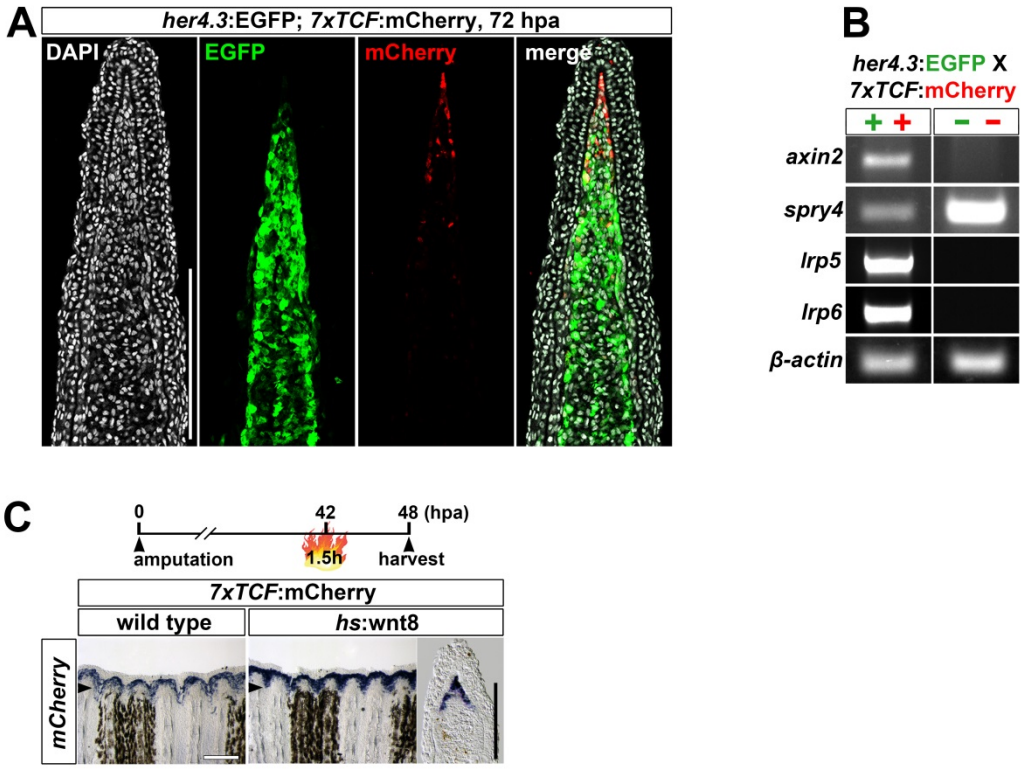

Fig. 4.8. The wound epidermis is not competent to respond to Wnt ligands activating β–catenin signaling. **(A)** Confocal image showing mCherry+ and EGFP+ cells on a longitudinal section of a *7xTCF*:mCherry; *her4.3*:EGFP double transgenic regenerate at 72 hpa. **(B)** RT-PCR of indicated genes on cDNA derived from FACS sorted *7xTCF* mCherry; *her4.3*:EGFP double transgenic regenerates at 72 hpa shown in (A). Note that endogenous *lrp5* and *lrp6* transcripts are not detected in the fluorescence-negative, blastema-free cell fraction that contains epidermal cells while *spry*4 is. **(C)** *wnt8* overexpression does not cause ectopic Wnt reporter activation in the wound epidermis in *7xTCF*:mCherry; *hs:*wnt8 double transgenic fish. Heat shocks were performed according to the schematic timeline. n(*7xTCF*:mCherry) = 8/8, n(*7xTCF*:mCherry; *hs:*wnt8) = 8/8. **(A-C)** Arrowheads: amputation plane. Scale bars: whole mounts, 200 µm; sections, 100 µm.

4.4 Frizzled Receptor Expression in the Regenerating Caudal Fin

Pathway activation by Wnt ligands requires binding to receptors of the Frizzled (Fzd) family and to Lrp5/6 co-receptors (Angers and Moon, 2009). Both *lrp5* and *lrp6* co-receptors were found to be expressed in the blastemal mesenchyme during fin regeneration (Fig. 4.6, Fig. 4.8). To identify candidate Fzd receptors that potentially mediate Wnt/β–catenin signaling in the *7xTCF*:mCherry-positive, distal blastema, deep sequencing-based gene expression profiling on mCherry+ and mCherry– cell fractions derived from 72 hpa *7xTCF*:mCherry transgenic regenerates was performed in collaboration with the Dresden Genome Center (Technische Universität Dresden). Of the 14 *fzd* genes present in the zebrafish genome (Nikaido *et al*., 2013; Ensembl Genome Browser) *fzd2, fzd7a*, *fzd7b and fzd9b* showed considerable expression levels in the samples (Fig. 4.9A). Among these, *fz9b* was found to be highly enriched (~8.5 fold) in the mCherry+ fraction relative to the mCherry– fraction (Fig. 4.9B). ISH against *fzd9b* on regenerates at 72 hpa confirmed robust *fz9b* expression in the distal domains of the regenerate (Fig. 4.9C). Thus, Fzd9b represent a candidate for mediating Wnt/β–catenin signaling in the *7xTCF*:mCherry-positive distal blastema during fin regeneration.

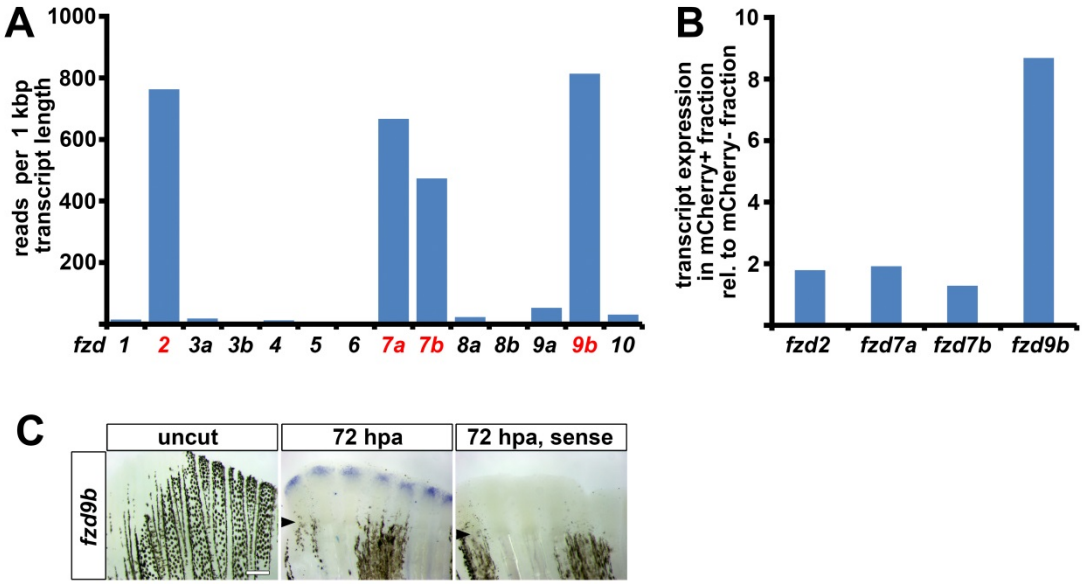

Fig. 4.9. Frizzled receptor expression during caudal fin regeneration. (A) *fzd2, fzd7a, fzd7b and fz9b* are most abundantly expressed at 72 hpa as detected by deep sequencing. Shown is the number of reads in mCherry+ and mCherry– samples per 1 kbp transcript length of the indicated genes. **(B)** *fz9b* is enriched in the *7xTCF*:mCherry-reporter-positive cells. Shown is the expression of indicated genes in the mCherry+ fraction relative to the mCherry– fraction. **(C)** *fz9b* is expressed in the distal regenerate at 72 hpa. Arrowhead: amputation plane. Scale bar: 200 µm.

4.5 Wnt/β–catenin Signaling is Active in Different Blastemal Compartments with Distinct Proliferative Properties and Wnt Co-Receptor Expression

The data presented so far strongly suggest that Wnt/β–catenin signaling is restricted to the blastemal mesenchyme. Since the blastema is organized into several domains during regenerative outgrowth (see Fig. 4.10), with distinct proliferative potential and cell fate, I next sought to map the relative spatial localization of the Wnt-receiving cells within the blastema.

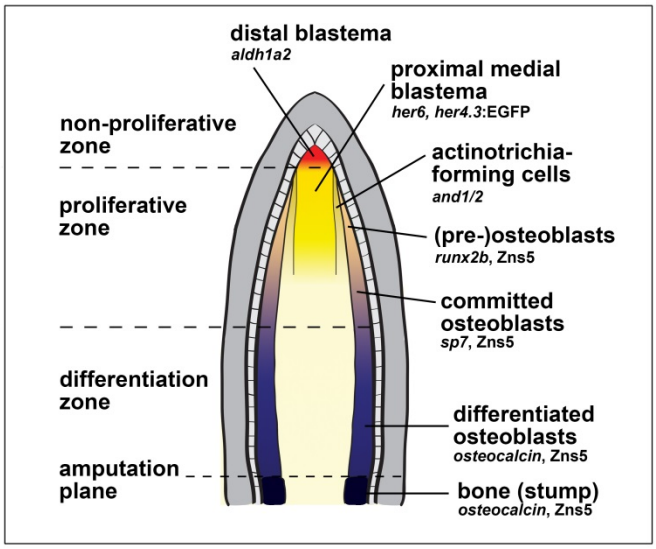

Fig. 4.10. Tissue compartments in a caudal fin regenerate at 72 hpa. Cartoon summarizing relevant anatomical structures and expression domains of a caudal fin regenerate during the outgrowth phase. Longitudinal section view is shown.

In *6xTCF*:dGFP regenerates reporter activity was robustly detected in the distal blastema plus in lateral domains of the proximal blastema (arrowheads in Fig. 4.11A-C), while these proximal domains were difficult to detect in *7xTCF*:mCherry regenerates (arrowhead in Fig. 4.11B), indicating that the *6xTCF*:dGFP reporter is more sensitive and that β–catenin signaling activity is strongest in the distal blastema. The proximal *gfp* expression was confined to thin lateral domains of approximately 2-3 cells medial to the basal layer of the epidermis and medial to the osteoblast progenitors further proximally (asterisk in Fig. 4.11C, Fig. 4.11E). The mesenchymal expression domains of *and1*, a marker for actinotrichia-forming cells (Zhang *et al*., 2010) appeared very similar to those of *6xTCF*:dGFP (Fig. 4.11D), and double ISH indicated that *6xTCF*:dGFP expressing cells

were also positive for *and1* (asterisk in 4.11E, F). In contrast, no overlap of *6xTCF*:dGFP or *7xTCF*:mCherry reporter activity with the osteoblast marker Zns5, which labels all osteoblasts irrespectively of their differentiation state (Fig. 4.11G) (Johnson and Weston, 1995), or the (pre-)osteoblast markers *runx2b* (Fig. 4.11H-I) or *sp7* (Fig. 4.11J) was observed. Thus, Wnt/β–catenin signaling is active in the presumptive actinotrichia-forming cells lining the osteoblasts, but cannot be detected in the bone lineage itself.

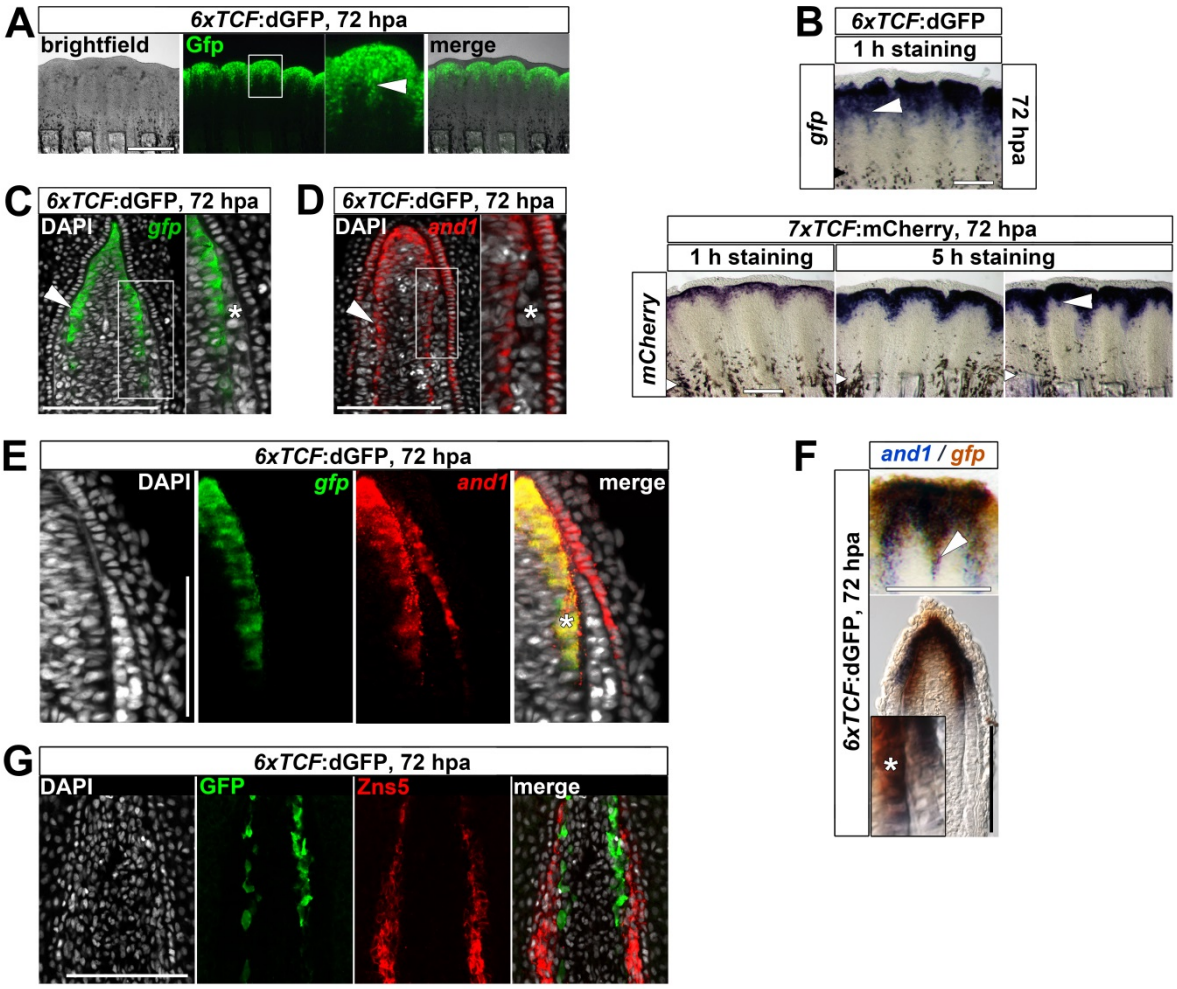

Fig. 4.11. Wnt activity in the proximal blastema is confined to the actinotrichia-forming cells. (A) Whole mount view of GFP fluorescence in *6xTCF*:dGFP transgenic regenerates. Arrowhead points to expression extending further proximally in the center of each blastema. **(B)** Reporter activity in proximally located blastemal regions, as robustly detected in *6xTCF*:dGFP transgenic regenerates (big white arrowhead), can only be detected in *7xTCF*:mCherry transgenics in a minority of samples after prolonged staining (big white arrowhead, 1/8 regenerates). **(C)** *gfp* RNA in *6xTCF*:dGFP transgenic regenerates is expressed in cells medial to the (pre-)osteoblasts (asterisk) in the proximal blastema (arrowhead). **(D)** *and1* expression is detected in the basal layer of the wound epidermis and in the blastema, where it resembles *6xTCF*:GFP reporter activity shown in (C). Arrowhead: actinotrichia-forming cells. Asterisk: (pre-)osteoblasts. **(E-F)** *gfp* transcripts are co-expressed with *and1* in the distal and proximal blastema of *6xTCF*:dGFP transgenics (arrowhead, asterisk). **(G)** Antibody staining shows that proximal GFP-positive cells are located adjacent to Zns5-postives osteoblasts in *6xTCF*:dGFP transgenic regenerates. **(C-E, G)** Confocal images of a longitudinal section are shown. **Continued on the next page.**

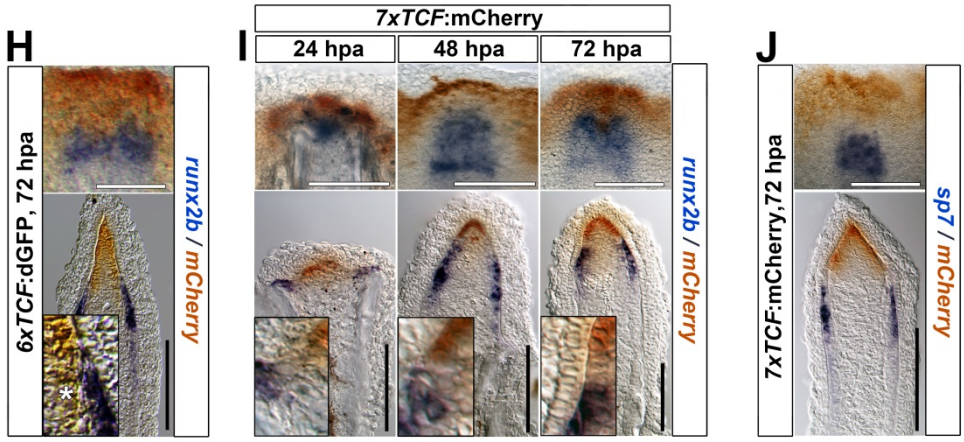

Fig. 4.11. continued. (H) *gfp* expression (brown, asterisk) is detected medial to *runx2b* transcripts (blue) in *6xTCF*:dGFP transgenic regenerates. **(I-J)** *runx2b* or *sp7* (blue) and *mCherry* transcripts (brown) do not co-localize in *7xTCF* mCherry transgenic regenerates at any stage analyzed. **(A-J)** Small arrowheads: amputation plane. Scale bars: whole mounts, 200 µm (A-B) and 100 µm (E-H); sections, 100 µm and 50 µm (E).

In addition to these mediolateral proximal domains reporter expression of both transgenic lines was strongly detected in the distal blastema (arrow in Fig. 4.13A). *7xTCF*:mCherry reporter expression co-localized with *aldh1a2* and *msxB*, which in whole mount stainings label the distal-most blastema (Fig. 4.12A-B). In contrast, in *7xTCF*:mCherry; *her4.3*:EGFP double transgenic fish, *mCherry* expression was detected distally to *egfp* expression marking the proximal medial blastema (Fig. 4.12C-D).

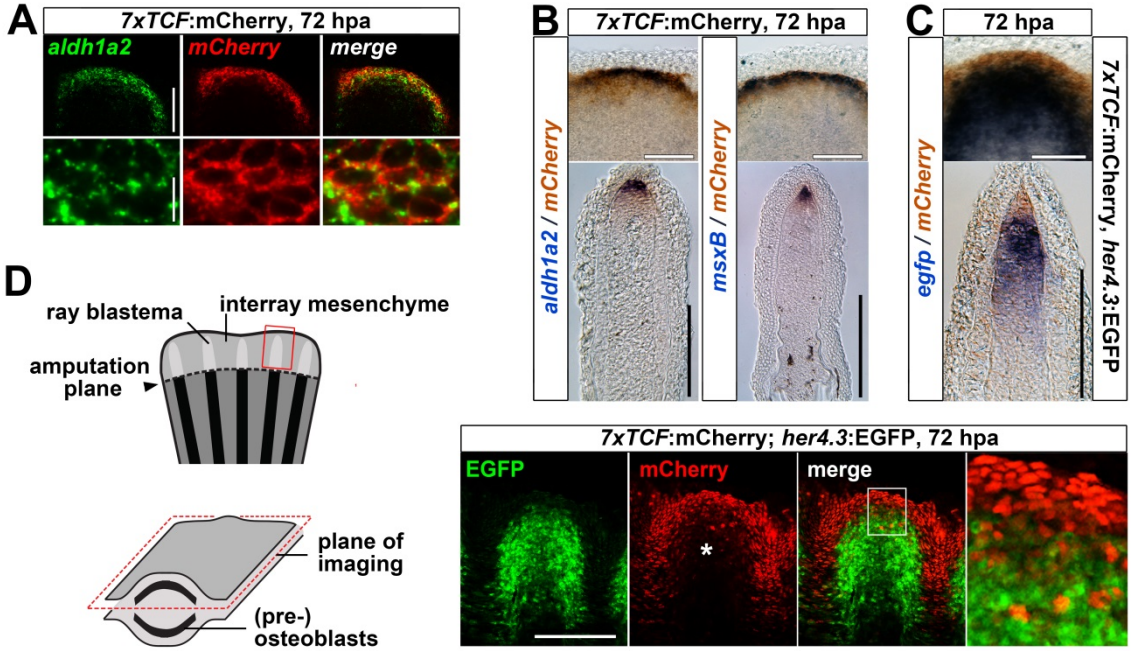

Fig. 4.12. Wnt/β–catenin signaling is active in the distal-most blastema. (A) Double ISH shows co-expression of the *7xTCF:mCherry* reporter and *aldh1a2* in the same cells in the distal-most blastema. Confocal image through the center of a blastema. **(B)** *aldh1a2* and *msxB* co-localize with *mCherry* transcripts in the distal-most blastema in *7xTCF*:mCherry transgenic regenerates. Note that samples were stained for mCherry expression only shortly, so

that only the strongest expression domain in the distal blastema was detected. **(C)** *mCherry* transcripts are detected distally to *egfp* transcripts in *7xTCF* mCherry; *her4.3*:EGFP double transgenic regenerates. **(D)** mCherry fluorescence is detected distally to the EGFP fluorescence-positive proximal blastema in *7xTCF*:mCherry; *her4.3*:EGFP double transgenic regenerates. Cartoon showing the plane of imaging and an optical section through the center of a blastema is shown. **(A-D)** Scale bars: whole mounts, 100 µm and 10 µm (A); sections, 100 µm.

The distal-most blastemal domain has been shown to consist of largely non-proliferative cells during regenerative outgrowth, while cells of proximal domains proliferate at a high rate (Nechiporuk and Keating, 2002). Indeed, I found that the distal expression domains of the *6xTCF*:dGFP and *7xTCF*:mCherry transgenics did hardly overlap with proliferative cell nuclear antigen (Pcna) activity (arrow in Fig. 4.13A-B). Furthermore, a number of *7xTCF*:mCherry reporter-positive cells located in the distal-most row of blastemal cells did not incorporate the S-phase marker bromodeoxyuridine (BrdU) even when treated for 48 h (arrowheads in Fig. 4.13C). Thus, Wnt/β–catenin signaling is active in the scarcely proliferative distal-most blastema.

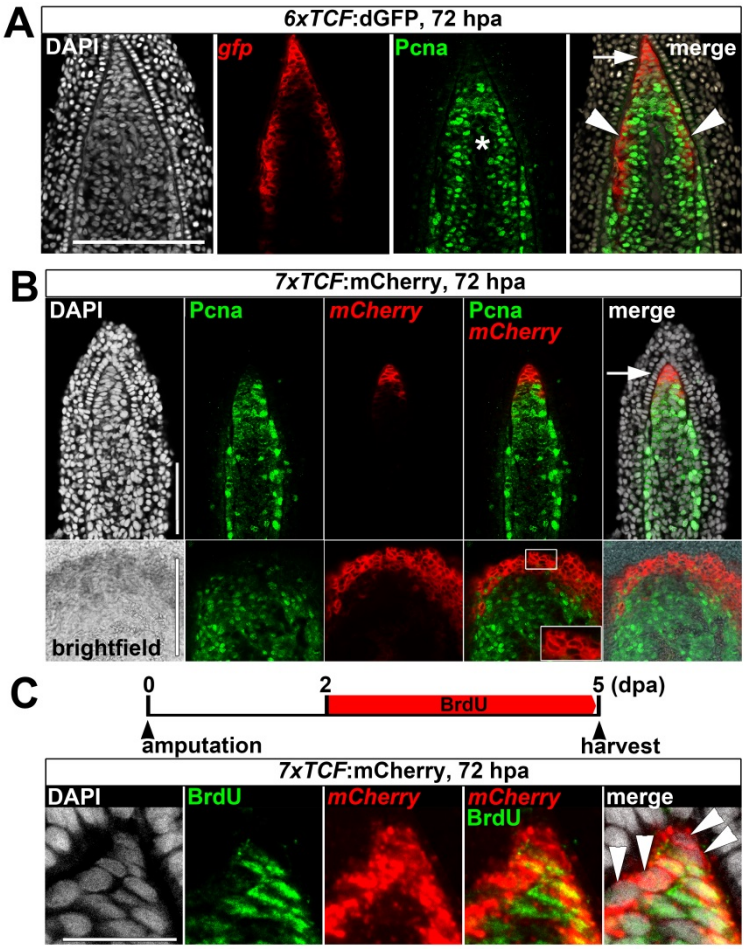

Fig. 4.13. The Wnt-receiving cells in the distal-most blastema define a scarcely-proliferative cell population. (A) *gfp* RNA in *6xTCF*:dGFP regenerates is detected in the distal-most, Pcna-negative blastema (arrow) and in a subpopulation of the Pcna-positive proximal blastema (arrowheads). Confocal image of a longitudinal section is shown. Asterisk: lack of Pcna staining due to a blood vessel. **(B)** *7xTCF* mCherry reporter activity is detected in the Pcna-negative distal-most blastema (arrow). Confocal images of a longitudinal section and a whole mount regenerate stained for *mCherry* transcripts and Pcna protein are shown. **(C)** A number of *7xTCF* mCherry reporter-positive cells remain BrdU-negative even when treated for 48 h (arrowheads). BrdU treatment was performed according to the schematic timeline. Confocal image of a longitudinal section is shown. **(A-C)** Scale bars: whole mounts, 100 µm and 20 µm (C); sections, 100 µm

Short-term fate mapping of the distal-most row of blastemal cells using a transgenic line expressing the photoconvertible fluorescent protein Kaede under control of the *7xTCF siamois* promoter (*7xTCF*:3xKaede; Fig. 4.14A-B) showed that some of these cells maintained their distal positions for 48 h after photoconversion (arrowhead in Fig. 4.14C) despite the marked increase in regenerate size (approximately 400 µm) that occurred within this time (Fig. 4.14D). These data support a model in which the distal Wnt-receiving cells maintain their position during regenerative growth and hardly contribute progenitors to the process of tissue restoration.

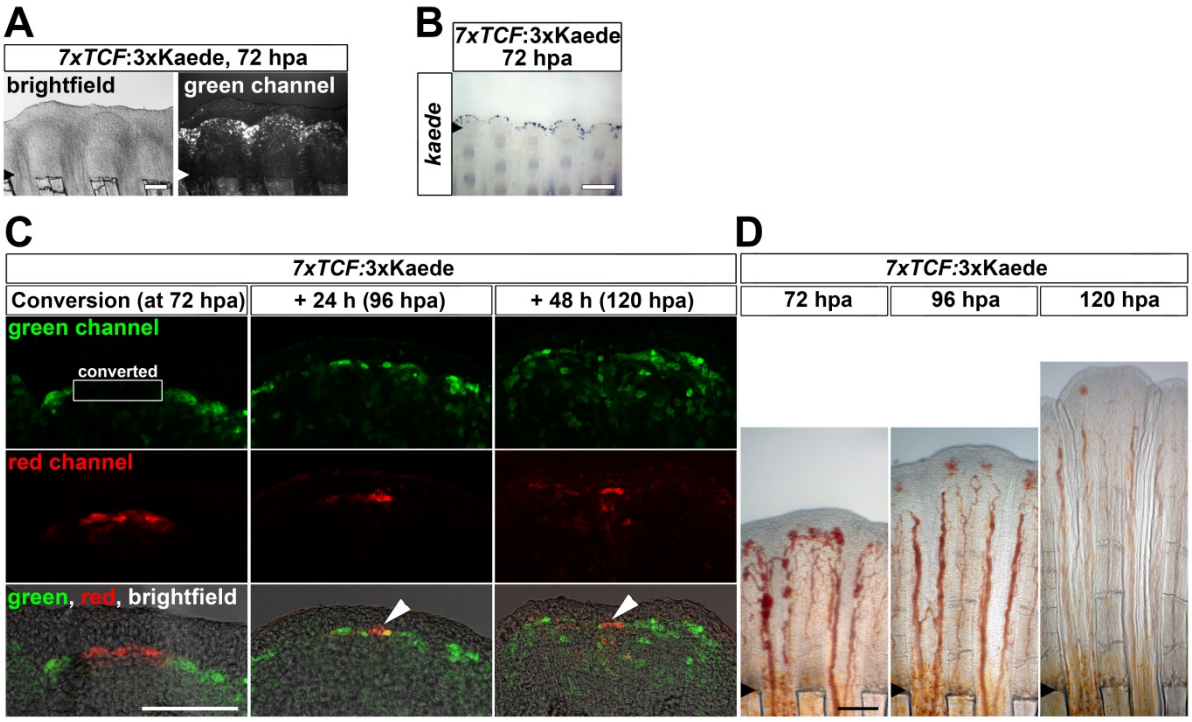

Fig. 4.14. The Wnt-receiving cells in the distal-most blastema retain their relative localization during regenerative growth. (A-B) Kaede fluorescence (A) and transcripts (B) in *7xTCF*:3xKaede transgenic regenerates resembles *7xTCF* mCherry reporter activity. **(C-D)** Kaede-positive Wnt-receiving cells located in the distal-most row of mesenchymal cells of a 72 hours-old *7xTCF*:3xKaede transgenic blastema were photoconverted from green to red fluorescence and traced for two consecutive days using a confocal microscope. Cells containing the converted Kaede protein were still detected in the distal-most cell row 24 h and 48 h post conversion (white arrowheads in C) despite the substantial regenerative growth that occurred in these fins (D). Small arrowheads: amputation plane. Scale bars: whole mounts, 100 µm and 20 µm (C); sections, 100 µm.

In contrast to the Wnt-receiving cells located in the distal-most blastema, the proximal Wnt reporter-positive domains were positive for Pcna (arrowheads in Fig. 4.13A). With the exception of these mediolateral domains, the remaining proliferative proximal blastema was found to be largely negative for Wnt reporter activity as revealed in optical stacks of *6xTCF*:dGFP regenerates (asterisk in Fig. 4.15). Interestingly, analysis of

lrp5 and *lrp6* Wnt co-receptor expression revealed similar distinct patterns. *lrp5* transcripts were confined to proximal mediolateral domains and absent from the distal-most blastema (arrowhead in Fig. 4.16) and the (pre-)osteoblast domains (asterisk in Fig. 4.16), while *lrp6* appeared to be predominantly expressed in the distal-most blastema (arrowhead in Fig. 4.16). Thus, during regenerative outgrowth, Wnt/β–catenin signaling is confined to two blastemal domains with distinct proliferative properties and Wnt co-receptor expression: the distal-most, non-proliferative, *lrp6*+ blastema and proximal, mediolateral, proliferative, *lrp5*+ cells that are likely to form actinotrichia.

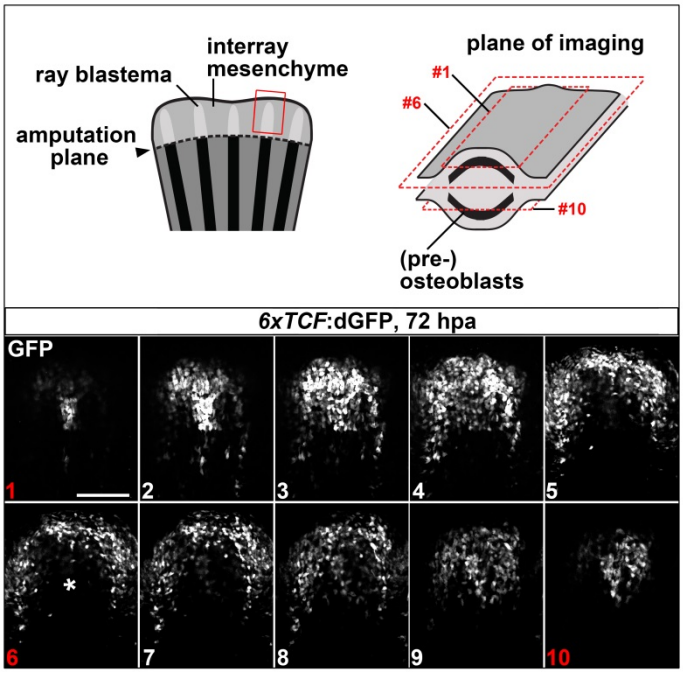

Fig. 4.15. *6xTCF*:dGFP reporter activity in the regenerating caudal fin at 72 hpa. 10 confocal optical sections spanning the entire mesenchymal region of a whole mount *6xTCF*:GFP transgenic regenerate are shown, the distal tip of the regenerate is up. Note that GFP fluorescence is absent from the medial proximal blastema (asterisk in section 6), while expression extends further proximally in the lateral regions of the blastema (*e.g.* in section 2 and 3). Scale bar: 200 µm.

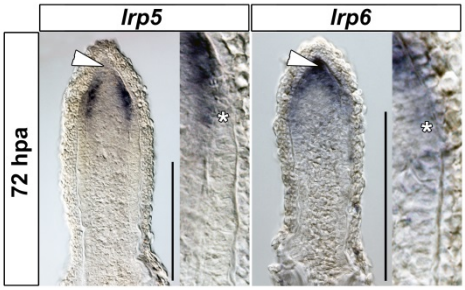

Fig. 4.16. *lrp5 and lrp6* co-receptors are distinctly expressed in the blastema during regenerative outgrowth of the caudal fin. *lrp5* transcripts are confined to proximal mediolateral domains and absent in the distal-most blastema (arrowhead) and the osteoblast progenitors (asterisk). *lrp6* transcripts are predominantly detected in the distal-most blastema (arrowhead). Asterisk: osteoblast progenitors. Scale bars: 100 µm.

4.6 Tissue-Specific Pathway Manipulation Indicates That Wnt/β–catenin Signaling in the Proximal Blastema, in Committed Osteoblasts, or the Wound Epidermis Has no Role in Regulating Regenerative Cell Proliferation

Loss of Wnt/β–catenin signaling as achieved by *dkk1* overexpression in the entire regenerate – including the distal blastema – interferes with blastemal cell proliferation and regenerative growth as reported previously (Stoick-Cooper *et al.*, 2007b). Likewise, systemic overexpression of *axin1* in *hs*:Axin1 fish at 72 hpa strongly reduced Pcna expression in the proximal mesenchyme and blocked further growth when expression was maintained by continuous heat shocks (Fig. 4.17A-C).

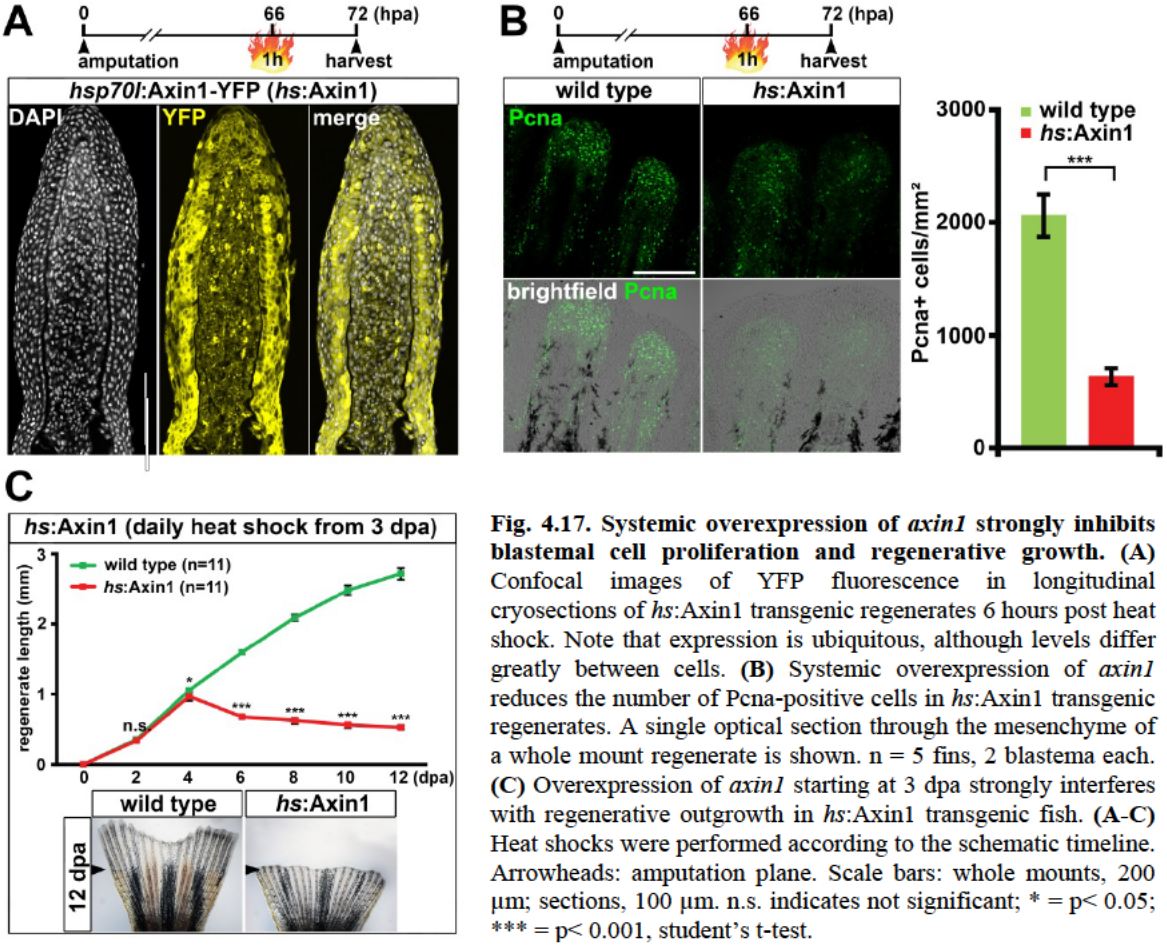

Fig. 4.17. Systemic overexpression of *axin1* strongly inhibits blastemal cell proliferation and regenerative growth. (A) Confocal images of YFP fluorescence in longitudinal cryosections of *hs*:Axin1 transgenic regenerates 6 hours post heat shock. Note that expression is ubiquitous, although levels differ greatly between cells. **(B)** Systemic overexpression of *axin1* reduces the number of Pcna-positive cells in *hs*:Axin1 transgenic regenerates. A single optical section through the mesenchyme of a whole mount regenerate is shown. n = 5 fins, 2 blastema each. **(C)** Overexpression of *axin1* starting at 3 dpa strongly interferes with regenerative outgrowth in *hs*:Axin1 transgenic fish. **(A-C)** Heat shocks were performed according to the schematic timeline. Arrowheads: amputation plane. Scale bars: whole mounts, 200 µm; sections, 100 µm. n.s. indicates not significant; * = p< 0.05; *** = p< 0.001, student's t-test.

Yet, the data presented so far suggest that Wnt/β–catenin signaling is largely absent in proliferating regions of the fin during regenerative outgrowth, namely the osteoblasts, the epidermis, and the majority of the medial proximal blastema, raising the possibility that Wnt signaling regulates cell proliferation in these domains and therewith regenerative growth indirectly. To test this, I specifically interfered with Wnt signaling in these tissues utilizing the TetON system that has recently been adapted for use in zebrafish (Huang *et al*., 2005; Knopf *et al*., 2010). The TetON system comprises a driver line (TetActivator) in which a doxycycline (DOX)-inducible transcriptional activator (TetA; [irtTAM2(3F)]) is under control of a tissue-specific promoter, and a responder line (TetResponder) that harbors a transgene of interest under transcriptional control of a Tet response element (TetRE, Fig. 4.18A). To interfere with Wnt/β–catenin signaling in a cell autonomous manner, I used a *TetRE*:Axin1-YFP^{tud1} TetResponder line that was shown to cause severe Wnt loss-of-function phenotypes when ubiquitously activated during zebrafish gastrulation (Knopf *et al*., 2010). Treatment of *TetRE*:Axin1-YFP single transgenic fish with DOX or EtOH for 12 days starting immediately after amputation did not affect regenerative growth, confirming low DOX toxicity and transgene leakiness (Fig. 4.18B, Knopf *et al*., 2010). I next asked whether overexpression of *axin1* in the entire fin using this system is sufficient to interfere with regenerative growth and thus phenocopies *hs*:Axin1 fish. I created a TetActivator line expressing irtTAM2(3F) and the fluorophore AmCyan under control of the *ubiquitin* promoter (*ubiquitin*:irtTAM2(3F)-p2a-AmCyan [*ubiquitin*:TetA AmCyan]) (Mosimann *et al*., 2011). Although this driver line was not ubiquitously expressed in the regenerating adult fin (Fig. 4.18C), DOX treatment of *ubiquitin*:TetA AmCyan; *TetRE*:Axin1-YFP double transgenics robustly induced *axin1-yfp* transgene expression in the majority of the blastema and in the wound epidermis within 6 hours after start of the treatment (Fig. 4.18E). Administration of DOX for 5 days starting 1 day before amputation efficiently interfered with regeneration initiation (Fig. 4.18D). Similarly, DOX treatment from 3 dpa until 12 dpa strongly inhibited further regenerative growth, while EtOH had no effect (Fig. 4.18E). Furthermore, DOX treatment for 24 hours was sufficient to strongly reduce epidermal *lef1* expression (Fig. 4.18F). Thus, expression levels achievable using the TetON system are suitable for studying the tissue-specific roles of Wnt/β–catenin signaling in adult zebrafish.

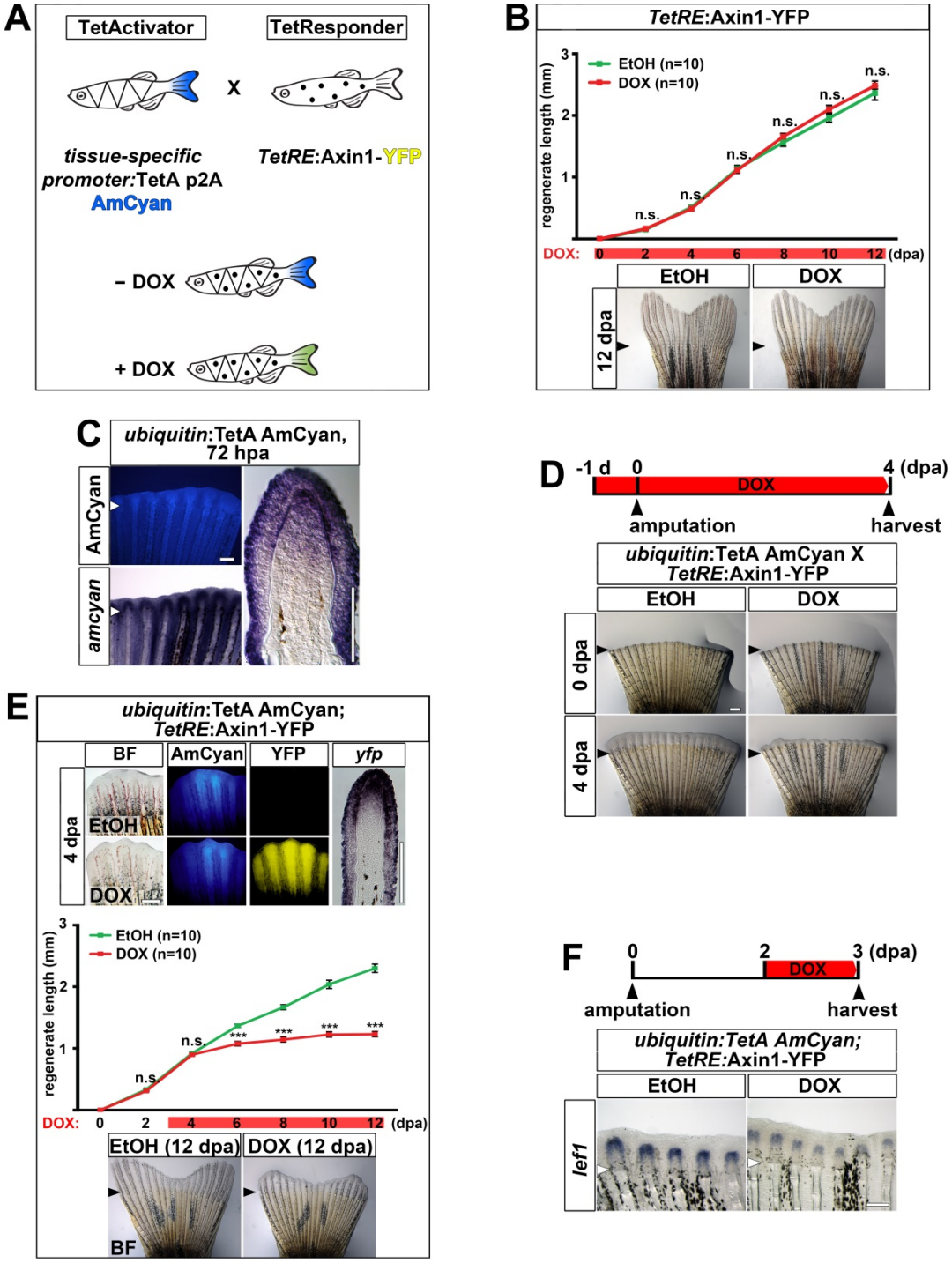

Fig. 4.18. The TetON system is suitable for studying the tissue-specific role of Wnt/β–catenin signaling during caudal fin regeneration. (A) Cartoon showing the strategy for tissue-specific inducible expression of the Wnt inhibitor *axin1* using the TetON system. **(B)** DOX treatment starting immediately after amputation does not affect regenerative growth in *TetRE*:Axin1-YFP transgenic fish compared to EtOH-treated controls. **(C)** AmCyan fluorescence and transcripts in *ubiquitin*:TetA AmCyan transgenic regenerates. Note that expression is quite ubiquitous in the epidermis and the distal blastema, and covers a substantial part of the proximal blastema. **(D-F)** *ubiquitin* promoter-driven *axin1-yfp* overexpression in the wound epidermis and the blastema is sufficient to block regeneration initiation (D) and regenerative growth (E) as well as inhibits *lef1* transcription (F). *lef1*: n(EtOH) = 6/6, n(DOX) = 5/6. **(B-F)** DOX treatments were performed according to the schematic timeline. Arrowheads: amputation plane. Scale bars: whole mounts, 200 µm; sections, 100 µm. n.s. indicates not significant; *** = p< 0.001, student's t-test.

To interfere with β–catenin signaling in a tissue-specific manner, a panel of TetActivator lines was established in collaboration with Christa Haase and Gilbert Weidinger (Technische Universität Dresden; Ulm University). To specifically interfere with Wnt/β–catenin signaling in the epidermis, two TetActivator lines were created using regulatory elements of the *keratin4* (Gong *et al*., 2002) and *keratin18* (Wang *et al*., 2006) genes (*keratin4*:irtTAM2(3F)-p2a-AmCyan [*keratin4*:TetA AmCyan] and *keratin18*: irtTAM2(3F)-p2a-AmCyan [*keratin18*:TetA AmCyan]). While the *keratin4* promoter drove TetActivator expression in all layers of the wound epidermis excluding the basal layer (asterisk in Fig. 4.19A), the *keratin18* driven TetActivator was only expressed in the latter (Fig. 4.19B). Although these drivers robustly induced the *TetRE*:Axin1-YFP transgene in the respective domains of the wound epidermis after DOX treatment (plus ectopically in the proximal medial blastema in case of the *keratin18*:TetA AmCyan line), regenerative growth was not inhibited when fish were treated with DOX for 12 days starting immediately after amputation or 1 day before amputation (Fig. 419C-D and data not shown).

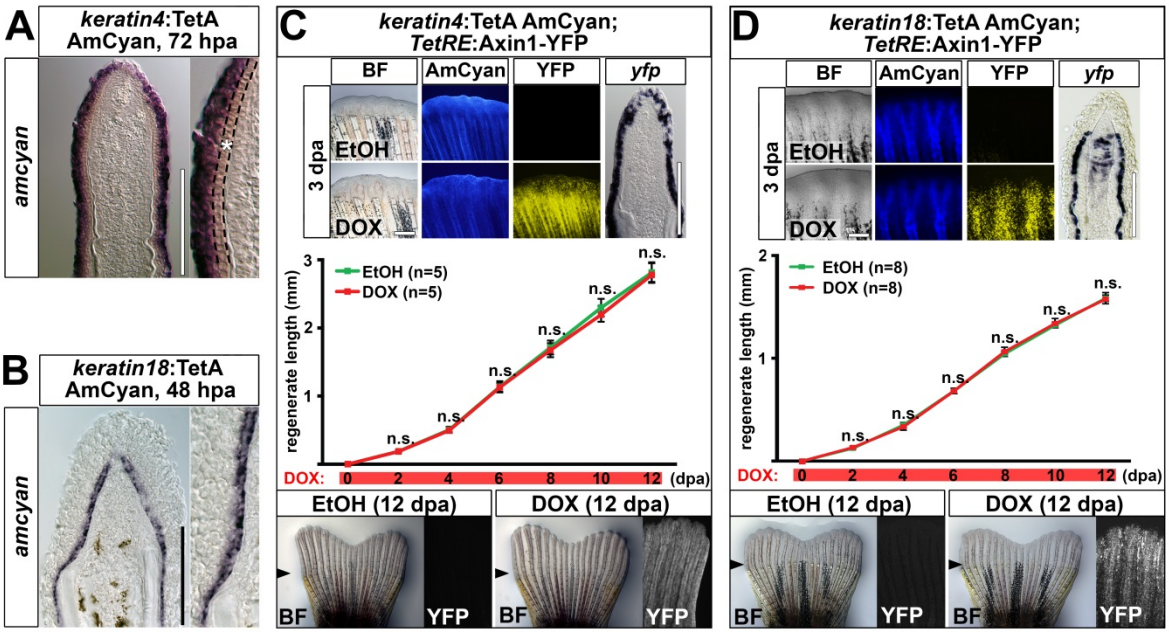

Fig. 4.19. Wnt/β–catenin signaling is not required in the wound epidermis during caudal fin regeneration. **(A)** *amcyan* RNA expression in *keratin4*:TetA AmCyan transgenic regenerates is detected in the epidermis excluding the basal epidermal layer (asterisk). **(B)** *amcyan* RNA expression in *keratin18*:TetA AmCyan transgenic regenerates is confined to the basal epidermal layer. **(C)** *keratin4* promoter-driven *axin1-yfp* expression in the wound epidermis excluding the basal layer does not interfere with regenerative growth. **(D)** *keratin18* promoter-driven *axin1-yfp* expression in the basal epidermal layer (plus ectopic expression in the proximal medial blastema) does not interfere with regenerative growth. **(A-D)** DOX-treatments were performed according to the schematic timelines. Arrowheads: amputation plane. Scale bars: whole mounts, 200 µm; sections, 100 µm. n.s. indicates not significant, student's t-test.

Similarly, continuous overxpression of *axin1-yfp* specifically in committed osteoblasts mediated by a *sp7*:irtTAM2(3F)-p2a-Cerulean driver (*sp7*:TetA Cerulean), whose expression pattern in the fin at 72 hpa resembled that of endogenous *sp7*/*osx* did not reduce regenerate growth (Fig. 4.20A-B). In contrast, *axin1-yfp* ovexpression in the proximal medial blastema (including the *and1*+ cells) driven by a *her4.3*:irtTAM2(3F)-p2a-AmCyan Activator line (*her4.3*:TetA AmCyan, Fig. 4.21A-C) was able to slow, but not block regenerative growth (Fig. 4.21C). Intriguingly, despite this effect on regenerate length, ovexpression of *axin1-yfp* in the *her4.3* domain for 48 hours was not sufficient to significantly reduce mesenchymal cell proliferation as determined by confocal imaging of anti-phospho-histone 3 (H3P)-stained whole mount regenerates (Fig. 4.22). In contrast, proliferation was severely reduced (>50 %) in *ubiquitin*:TetA AmCyan; *TetRE*:Axin1-YFP double transgenic fish under the same conditions (Fig. 4.22). I conclude that β–catenin signaling must be inhibited in the mediolateral proximal blastema and in the distal-most blastema at the same time, as achieved by the *ubiquitin*:TetA driver, for blastemal proliferation to be blocked. Together, these data suggest that Wnt/β–catenin signaling is not directly required for cell proliferation in the wound epidermis, in committed osteoblasts or in the fibroblasts of the proximal medial blastema during the outgrowth phase of fin regeneration. Rather Wnt signaling in the distal, non-proliferative blastema appears to indirectly regulate cell proliferation in the other compartments of the regenerate.

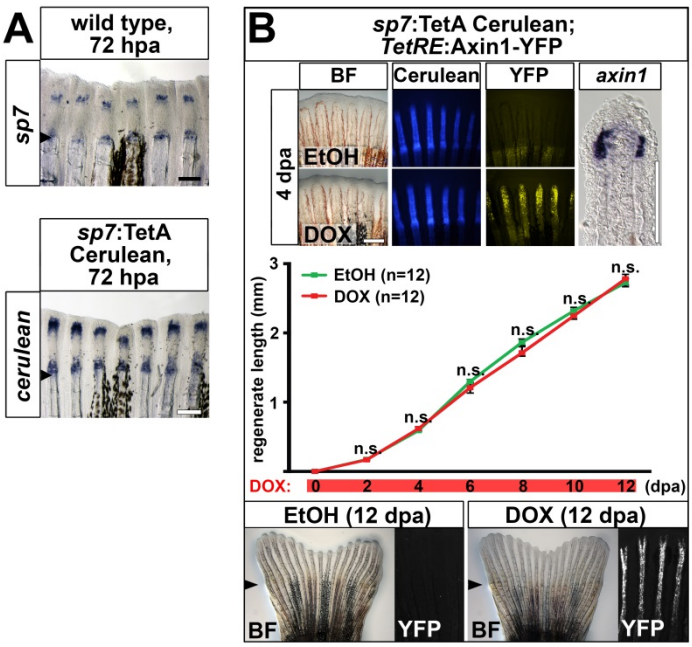

Fig. 4.20. Wnt/β–catenin signaling is not required in committed osteoblasts during caudal fin regeneration. (A) *cerulean* expression recapitulates endogenous *sp7* expression in *sp7*:TetA Cerulean transgenic regenerates. **(B)** *axin1-yfp* overexpression in the committed *sp7*-positive osteoblasts does not interfere with regenerative growth. **(A-B)** DOX treatments were performed according to the schematic timeline. Arrowheads: amputation plane. Scale bars: whole mounts, 200 µm; sections, 100 µm. n.s. indicates not significant, student's t-test.

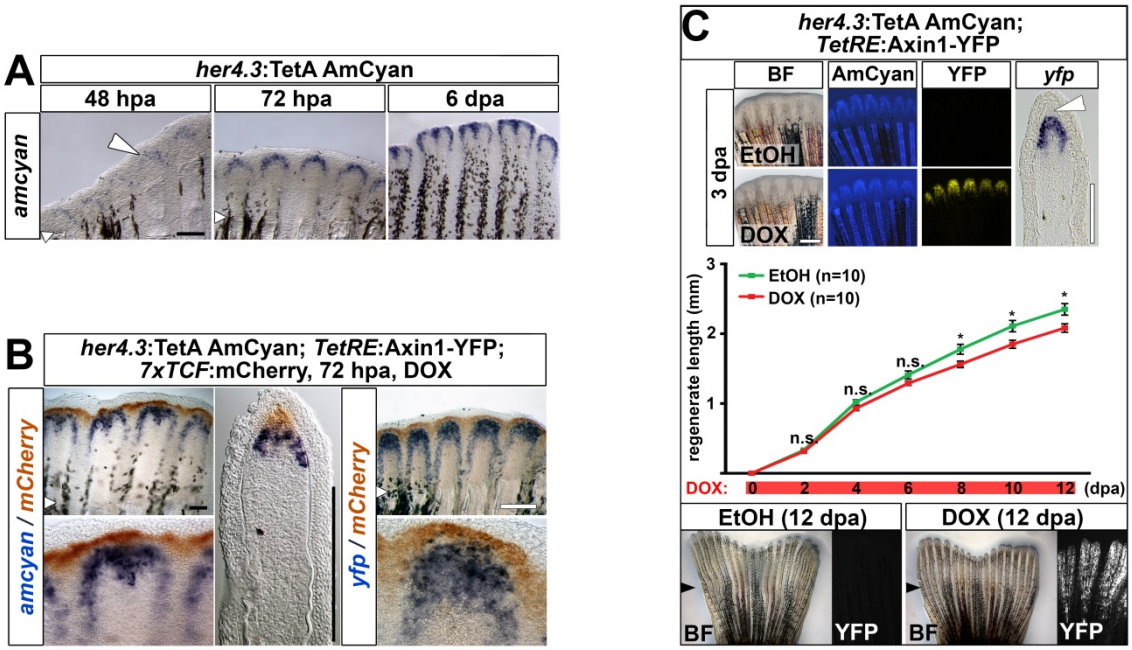

Fig. 4.21. Wnt/β–catenin signaling in the proximal medial blastema is not essential for regenerative growth during caudal fin regeneration. (A) *amcyan* transcripts are detected from 48 hpa (big arrowhead) in *her4.3*:TetA AmCyan transgenic regenerates. **(B)** *amcyan* and *yfp* transcripts are detected proximally to *mCherry* in regenerates of *her4.3*:TetA AmCyan; *TetRE*:Axin1-YFP; *7xTCF*:mCherry triple transgenic fish treated with DOX for 12 hours. **(C)** *axin1-yfp* overexpression in the medial proximal blastema has only little impact on regenerative growth in *her4.3*:TetA AmCyan; *TetRE*:Axin1-YFP double transgenic fish. The big arrowhead marks the distal-most blastema which is devoid of *yfp* transcripts. **(A-C)** Small arrowheads: amputation plane. Scale bars: whole mounts, 200 µm; sections, 100 µm. n.s. indicates not significant; * = p< 0.05, student's t-test.

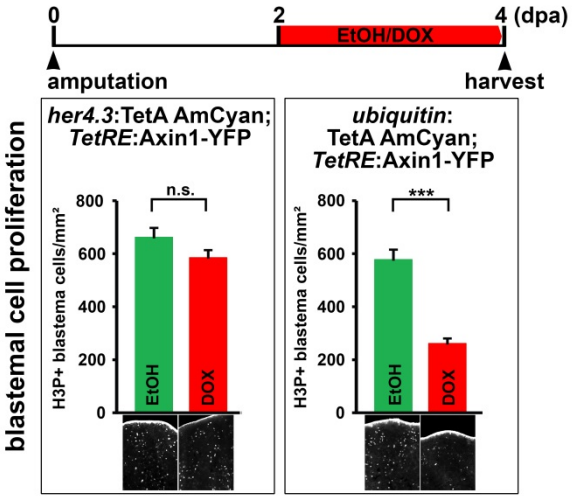

Fig. 4.22. Wnt/β–catenin signaling in the medial proximal blastema has little role in regulating blastemal cell proliferation. *axin1-yfp* overexpression in the medial proximal blastema does not significantly reduce blastemal cell proliferation in *her4.3*:TetA AmCyan; *TetRE*:Axin1-YFP double transgenic fish. The number of H3P+ cells in the blastemal mesenchyme is shown. In contrast, proliferation is strongly reduced when *axin1-yfp* is directed to the distal plus medial proximal blastema using the *ubiquitin* promoter. n = 4 fish, 16 blastemas. DOX treatments were performed according to the schematic timeline. n.s. indicates not significant; *** = p< 0.001, student's t-test.

4.7 Wnt/β–catenin Signaling in the Actinotrichia-Forming Cells is Required for Osteoblast Differentiation

I have recently contributed to the discovery that regenerative outgrowth can be halted under conditions where overall levels of cell proliferation are not reduced but osteoblast differentiation fails, as is the case when Notch signaling is overactivated (Grotek *et al*., 2013). Since inhibition of β–catenin signaling in the proximal blastema also reduced regenerate length without strongly affecting cell proliferation, I asked whether Wnt signaling in this domain regulates osteoblast differentiation. To test this, I examined calcification of regenerating bone as detected by Alizarin Red or Calcein staining in *her4.3*:TetA AmCyan; *TetRE*:Axin1-YFP double transgenic fish following DOX treatment. In fish exposed to DOX for 8 days starting at 2 dpa (Fig. 4.23A) regenerate length was reduced by ~20 % at 10 dpa compared to EtOH controls (Fig. 4.23B). In controls, ~85 % of the regenerate was calcified as detected using either of the staining methods, while upon Wnt inhibition in the proximal medial blastema this fraction was reduced to ~50 % as detected by Alizarin Red staining (Fig. 23C) or ~60 % as detected by Calcein staining (Fig. 4.23D). Importantly, *axin1-yfp* overexpression in committed osteoblasts in *sp7*:TetA Cerulean; *TetRE*:Axin1-YFP double transgenics had no effect on bone calcification (Fig. 4.24C-D). Furthermore, DOX treatment of *her4.3*:TetA AmCyan; *TetRE*:Axin1-YFP double transgenic fish for 24 hours strongly reduced *sp7* expression, a marker for osteoblast commitment (Fig. 23E). Importantly, the reduction in *sp7* expression was not due to enhanced apoptotic cell death as detected by the TUNEL assay (Fig. 23F). I conclude that Wnt/β–catenin signaling in the actinotrichia-forming cells indirectly regulates differentiation of adjacently located osteoblast progenitors.

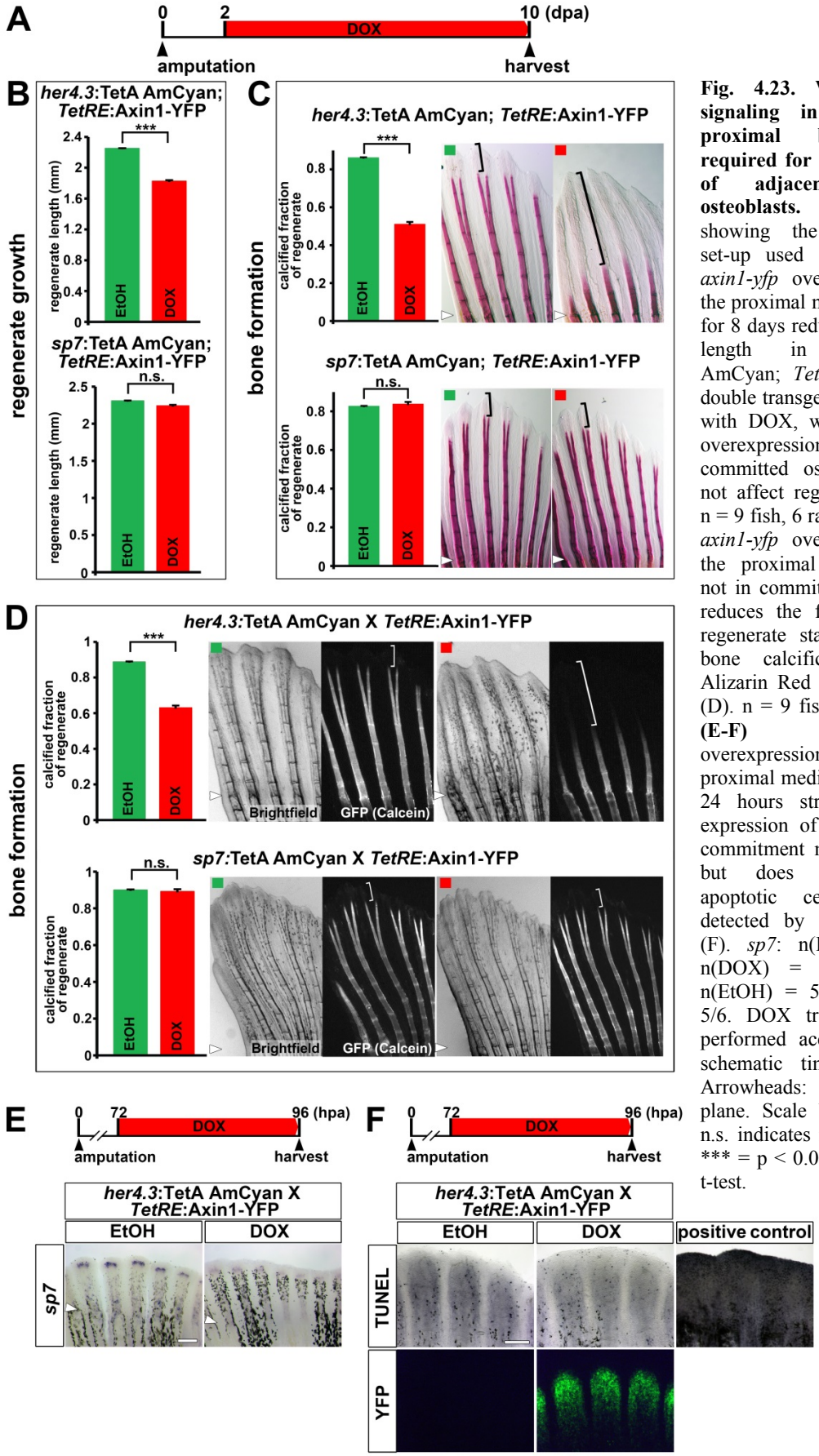

Fig. 4.23. Wnt/β–catenin signaling in the medial proximal blastema is required for differentiation of adjacently located osteoblasts. (A) Scheme showing the experimental set-up used in (B-D). **(B)** *axin1-yfp* overexpression in the proximal medial blastema for 8 days reduces regenerate length in *her4.3*:TetA AmCyan; *TetRE*:Axin1-YFP double transgenic fish treated with DOX, while *axin1*-yfp overexpression in the committed osteoblasts does not affect regenerate length. n = 9 fish, 6 rays each. **(C-D)** *axin1-yfp* overexpression in the proximal blastema but not in committed osteoblasts reduces the fraction of the regenerate stained with the bone calcification marker Alizarin Red (C) or Calcein (D). n = 9 fish, 6 rays each. **(E-F)** *axin1-yfp* overexpression in the proximal medial blastema for 24 hours strongly reduces expression of the osteoblast commitment marker *sp7* (E) but does not enhance apoptotic cell death as detected by TUNEL assay (F). *sp7*: n(EtOH) = 6/6, n(DOX) = 4/6. TUNEL: n(EtOH) = 5/6, n(DOX) = 5/6. DOX treatments were performed according to the schematic timelines. **(B-F)** Arrowheads: amputation plane. Scale bars: 200 µm. n.s. indicates not significant; *** = $p < 0.001$, student's t-test.

4.8 Identification of the Wnt Targetome in the Regenerating Caudal Fin

The data presented here strongly suggest that Wnt/β–catenin signaling indirectly regulates proliferation, differentiation and gene expression in several territories of the regenerate. To identify signaling pathways that could mediate these effects, I next aimed to characterize the Wnt targetome in the regenerating fin. This analysis was conducted in collaboration with Birgit Kagermeier-Schenk, Mohankrishna Dalvoy Vasudevaro, and Gilbert Weidinger (Technische Universität Dresden; Ulm University). Identification of the Wnt targetome in the fin was performed during wound healing (6 hpa), blastema formation (48 hpa) and regenerative outgrowth (96 hpa) by profiling gene expression after inducible inhibition of Wnt/β–catenin signaling using *hs*:Axin1 and *hs:*dkk1 transgenic lines (see Table 3.10 in chapter '*3.2.14 Microarray Analysis*'). Transgenic fish and their wild type siblings were heat shocked and regenerates were harvested 6 hours post heat shock to enrich for directly regulated targets. In addition, fins were profiled in which *dkk1* or *axin1* had been continuously overexpressed via serial heat shocks from amputation till 48 hpa. To identify genes which showed similar expression dynamics in response to the experimental conditions and thus might be functionally related, a supervised co-expression analysis of genes differentially expressed in 48 or 96 hpa samples was performed using weighted gene expression correlation network analysis (WGCNA; Langfelder and Horvath, 2008). Thereby, expression patterns could be grouped into 33 different modules. DAVID Bioinformatics resource-based gene ontology analysis (Huang da *et al*., 2009) revealed that 15 out of these 33 modules were enriched for distinct biological processes (Benjamini corrected p-value <0.05) which were considered for further analysis (see Table 3.11 in chapter '*3.2.15 Weighted Gene Expression Correlation Network Analysis*'). Plotting of the module eigengene value, which represents the weighted average expression of all genes present in a module, revealed that three modules (26, 21 and 3) showed reduced expression under conditions of Wnt inhibition (Fig. 4.24A). Module 26 contained genes whose expression in wild type fish is increased at 48 hpa and 96 hpa relative to 0 hpa fins and whose expression is reduced by inhibition of Wnt/β–catenin signaling (Fig. 4.24A). It was significantly enriched in genes involved in Wnt signaling, but also in genes associated with Fgf and Hh signaling pathways (Fig. 4.24B, Table 4.1). Modules 21 and 3 contained

critical components of not only Wnt signaling pathways but also Bmp/Tgfβ, Hh, Notch, retinoic acid (RA) and Mapk signaling (Table 4.1). This suggests that Wnt/β–catenin signaling regulates key signaling pathway involved in regeneration.

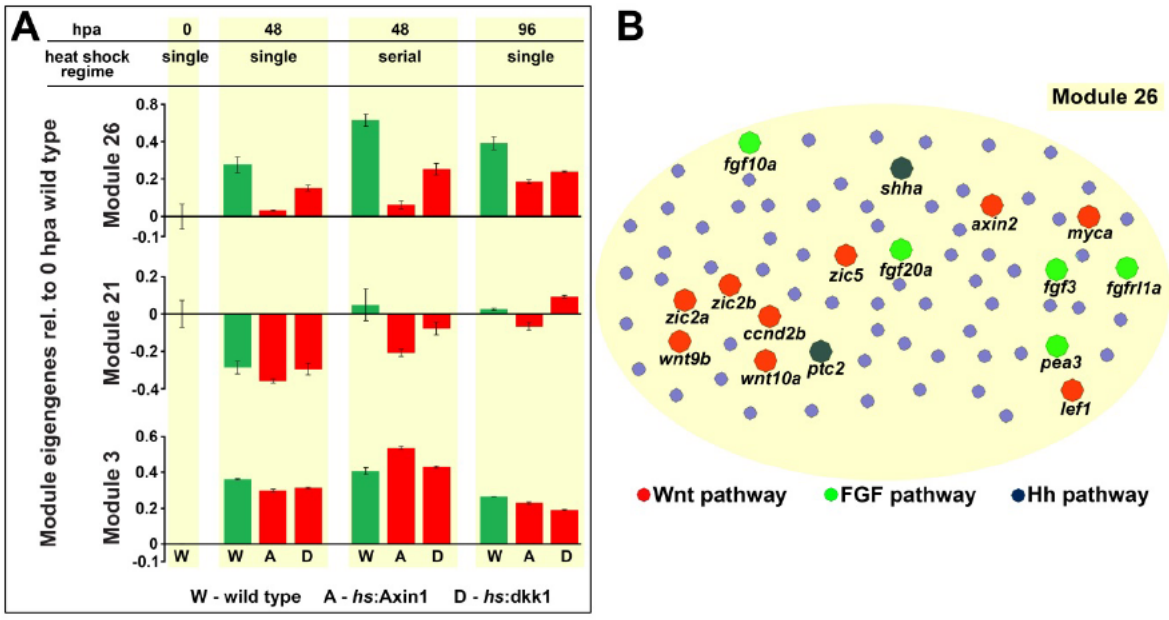

Fig. 4.24. Genes of WGCNA modules 26, 21 and 3 are co-expressed under conditions of Wnt inhibition. (A) Eigengene values of three correlated WGCNA modules, representing the average relative expression values of all genes in the module, in 10 experimental conditions. Values shown are the average of triplicate samples relative to 0 hpa wild type samples. **(B)** Cartoon of genes found in module 26 with a selection of genes highlighted that are associated with Wnt, Fgf and Hh signaling. The above shown figure was generated in collaboration with Mohankrishna Dalvoy Vasudevaro (Ulm University).

Table 4.1. Gene composition of WGCNA modules 26, 21 and 3. (Genes associated with signaling pathways are listed). Table was generated in collaboration with Mohankrishna Dalvoy Vasudevaro (Ulm University).

Signaling pathway	Module 26	Module 21	Module 3
Wnt	*wnt9b, wnt10a, axin2, lef1 ,myca, ccnd2b*	*wnt6, sost, prickle1a, kremen1, notum, sfrp1*	*wnt4a, fn1b*
Hedgehog	*shha, ptch2, zic2a, zic5, scube2*	*hhip, ihh*	*smo, sufu, gli2a, fbxw11a*
Fgf	*fgf10a, fgf20a, fgf3, fgfrl1a, pea3*	*fgf18, fgfr1a, fgfr4*	*none*
Notch	*heyl*	*None*	*jag1a*
Bmp	*bmp7a, bambia*	*bmp2a, bmp4, bmp8a, inhβb, bambib*	*bmp2b,inhβAa, smad5*
Retinoic acid	*None*	*rxrg, rxrbb*	*aldh1a2*
Mapk	*None*	*igf2a*	*igf2b, hbegf*

4.9 Wnt/β–catenin Signaling is Required for Expression of Ligands, Pathway Components and Target Genes of numerous Signaling Pathways Involved in Regeneration

ISH revealed that expression of the Wnt pathway components *axin2*, *lef1, sost* and *wnt10a* was indeed strongly dependent on Wnt/β–catenin signaling supporting the usefulness of the WGCNA analysis and suggesting that these genes are under feedback control (Fig. 4.2A, 4.5, 4.25).

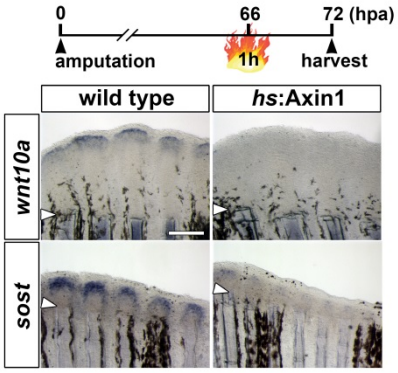

Fig. 4.25. *wnt10a* and *sost* expression depends on Wnt/β–catenin signaling during caudal fin regeneration. *sost and wnt10a* expression is strongly reduced upon *axin1* overexpression for 6 hours in *hs*:Axin1 transgenic regenerates. *sost*: n(wild type) = 7/8, n(*hs*:Axin) = 8/9; *wnt10a*: n(wild type) = 6/7, n(*hs*:Axin1) = 6/7. Heat shocks were performed according to the schematic timeline. Arrowheads: amputation plane. Scale bar: 200 µm.

Consistent with the co-expression analysis I found that overexpression of *dkk1* or *axin1* suppressed expression of ligands, target genes and pathway components of a large number of signaling pathways that have been reported to be required for fin regeneration. Specifically, I found that Hh signaling was dependent on Wnt/β–catenin signaling, since expression of Hh ligands (*ihha* and *shha*), the target gene *ptc2* as well as the pathway component *scube2* were reduced upon *dkk1* or *axin1* overexpression (Fig. 4.26B). Hh signaling has been shown to be important for regenerative growth, differentiation of the regenerating osteoblasts and patterning of the bony fin rays (Laforest *et al*., 1998; Quint *et al*., 2002). Wnt/β–catenin signaling was also required for expression of the Bmp family members *gdf6a/bmp13*, *bmp2a*, *bmp4,* as well as the Bmp pathway feedback inhibitor *bambib* (Fig. 4.26C). Bmp signaling is thought to regulate osteoblast differentiation and patterning of the dermoskeleton (Laforest *et al*., 1998; Smith *et al*., 2006). Interestingly, *bmp4* transcripts co-localized with *7xTCF*:mCherry Wnt reporter activity in the distal-most

blastema suggesting that *bmp4* transcription could be directly controlled by Wnt/β–catenin signaling (arrowhead in Fig. 4.27A). Wnt signaling inhibition also abolished expression of the RA synthesizing enzyme *aldh1a2/raldh2* and of the RA binding protein *crabp1b* (Fig. 4.26D). RA signaling has recently been shown to be essential for blastemal cell proliferation and survival and it also appears to have roles in fin patterning (Blum and Begemann, 2012; Geraudie *et al*., 1995; White *et al*., 1994). Expression of the Igf signaling ligand *igf2b* was dependent on Wnt/β–catenin signaling as well (Fig. 4.26E). Igf ligands are expressed in the mesenchyme and have been shown to activate Igf receptors in the basal wound epidermis, which is thought to be required for maintenance of basal wound epidermis integrity as a prerequisite for formation of the blastema and its maintenance (Chablais and Jazwinska, 2010). I found that a single heat shock in *hs*:Axin1 transgenic fish was sufficient to reduce Igf1 receptor (Igf1r) phosphorylation in the regenerate 6 hours post-heat shock, suggesting that Wnt/β–catenin signaling regulates epidermal Igf signaling through transcriptional control of Igf ligands (Fig. 4.26F).

I have recently contributed to the discovery that Notch signaling is active in the proliferative, proximal medial blastema where it coordinates osteoblast progenitor proliferation with differentiation during regenerative outgrowth (Grotek *et al*., 2013). Intriguingly, I found that inhibition of Wnt/β–catenin signaling strongly reduced activity of the Notch-dependent *her4.3* promoter in the *her4.3*:TetA AmCyan transgenic line (Fig. 4.26G) and suppressed expression of the Notch target genes *her12* and *heyl* and the Notch pathway component *lunatic fringe* (*lfng*) (Fig. 4.26H). Finally, a recent study has provided evidence that Wnt signaling regulates Fgf signaling during fin regeneration via transcriptional regulation of the Fgf ligand *fgf20a* (Stoick-Cooper *et al*., 2007b) and here I found that Wnt/β–catenin signaling was required for expression of the Fgf ligand *fgf3* and the Fgf-target genes *spry4*, *pea3* and *erm* as well (Fig. 4.26I). Fgf signaling is essential for fin regeneration since it regulates blastema proliferation and epidermal patterning (Lee *et al*., 2005; Poss *et al*., 2000b; Whitehead *et al*., 2005). Interestingly, I also found expression of *socs3b,* a negative regulator of cytokine signaling, to be dependent on Wnt/β–catenin signaling (Fig. 26J). A role for cytokine signaling in caudal fin regeneration is yet to be described.

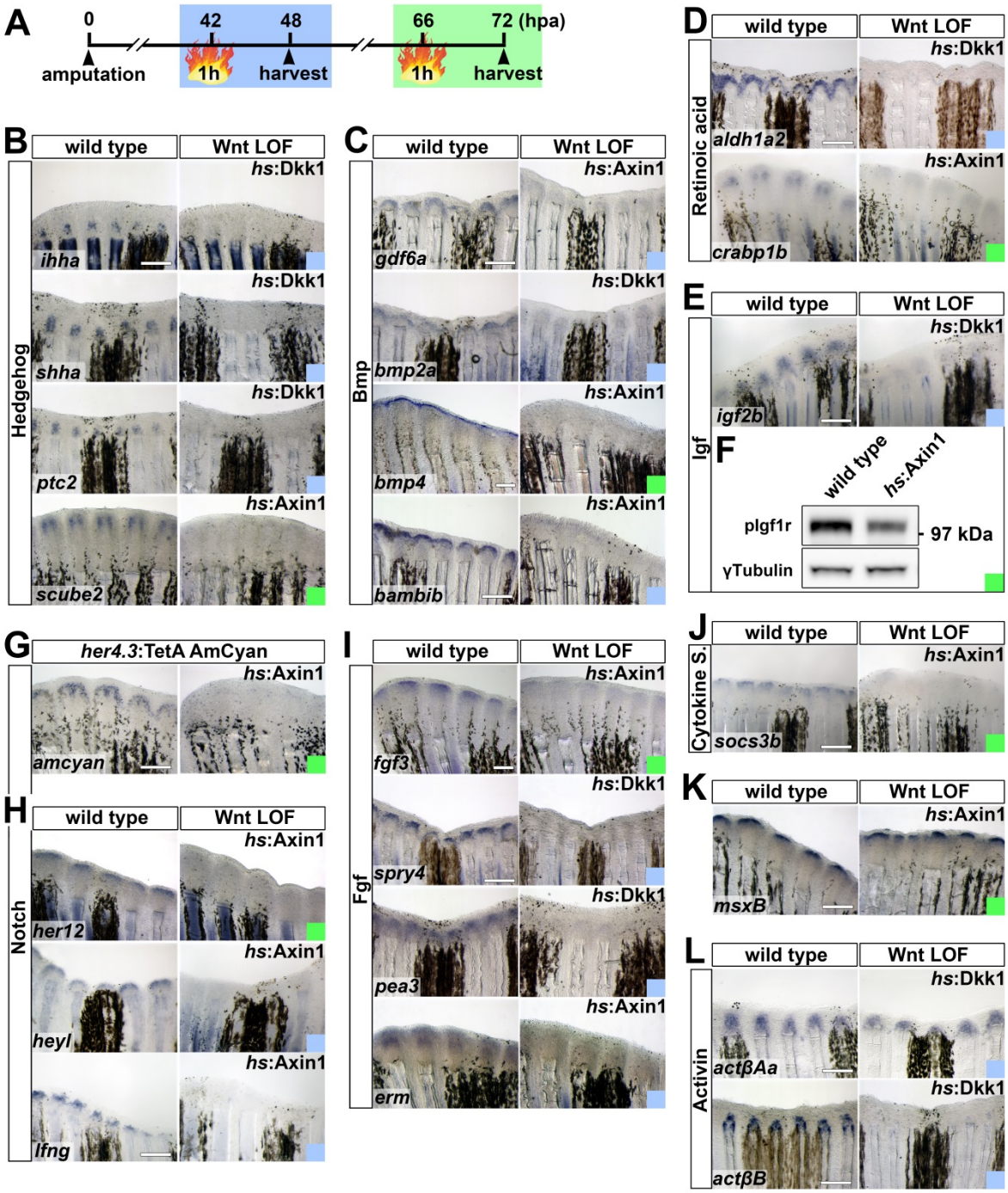

Fig. 4.26. Wnt/β–catenin signaling is required for expression of ligands, pathway components and target genes of many signaling pathways involved in regeneration of the zebrafish caudal fin. (A) Samples in (B-L) were either heat shocked at 42 hpa (blue) or 66 hpa (green) and harvested 6 hours later. **(B-L)** Inhibition of Wnt/β–catenin signaling via *axin1* or *dkk1* overexpression interferes with pathway activity or expression of ligands, pathway components, and target genes of Hh (B), Bmp (C), RA (D), Igf (E-F), Notch (G-H), Fgf (I), and cytokine (J) signaling. Expression of *msxB* and *actβAa* but not *actβB* remains unaffected using the same heat shock protocol (K-L). **(F)** *axin1* overexpression for 6 hours reduces Igf1r phosphorylation as detected in Western blots of whole regenerates at 72 hpa. **(G)** *axin1* overexpression interferes with Notch signaling-dependent *her4.3* promoter activity in *her4.3*:TetA AmCyan fish. *ihha*: n(wild type) = 5/5, n(*hs:*dkk1) = 5/5; *shha*: n(wild type) = 8/8, n(*hs:*dkk1) = 8/8; *ptc2*: n(wild type) = 5/5, n(*hs:*dkk1) = 5/5; *scube2*: n(wild type) = 8/8, n(*hs*:Axin1) = 6/8; *gdf6a*: n(wild type) = 7/7, n(*hs*:Axin1) = 5/7; *bmp2a*: n(wild type) = 7/9, n(*hs:*dkk1) = 7/9; *bmp4*: n(wild type) = 7/7, n(*hs:*dkk1) = 7/7; *bambib*: n(wild type) = 8/8, n(*hs*:Axin1) = 8/8; *aldh1a2*: n(wild type) = 7/7, n(*hs:*dkk1) = 7/7; *crabp1b*: n(wild type) = 7/8, n(*hs*:Axin1) = 6/8; *igf2b*: n(wild type) = 8/8, n(*hs:*dkk1) = 7/7; n(*her4.3*:TetA

AmCyan) = 7/7, n(*her4.3*:TetA AmCyan; *hs*:Axin1) = 6/8; *her12*: n(wild type) = 6/7, n(*hs*:Axin1) = 6/7; *heyl*: n(wild type) = 6/7, n(*hs*:Axin1) = 6/7, *lfng*: n(wild type) = 9/10, n(*hs*:Axin1) = 9/10; *fgf3*: n(wild type) = 6/7, n(*hs:*dkk1) = 6/7; *spry4*: n(wild type) = 8/9, n(*hs:*dkk1) = 6/8; *pea3*: n(wild type) = 8/8, n(*hs:*dkk1) = 9/9; *erm*: n(wild type) = 8/8, (*hs*:Axin1) = 7/7; *socs3b*; n(wild type) = 7/8, n(*hs:*Axin1) = 5/8; *msxB*: n(wild type) = 7/7, n(*hs*:Axin1) = 7/7; *actβAa*: n(wild type) = 6/6, n(*hs:*dkk1) = 7/8; *actβB*: n(wild type) = 8/8, n(*hs*:Axin1) = 6/8. Scale bars: 200µm. Heat shocks were performed according to the schematic timeline.

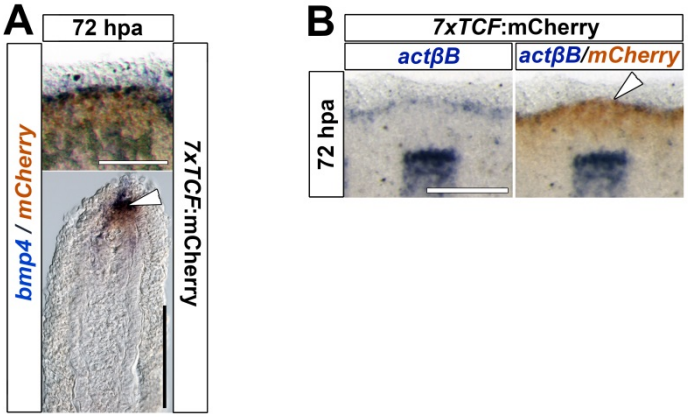

Fig. 4.27. *bmp4* and *actβB* are expressed in the Wnt-receiving cells. (A) *bmp4* and *mCherry* transcripts co-localize in the distal-most blastema (arrowhead) in *7xTCF* mCherry transgenic regenerates. **(B)** *actβB* and *mCherry* transcripts co-localize in the distal most blastema in *7xTCF*:mCherry transgenic regenerates **(A-B)** Note that samples were stained for mCherry expression only shortly, so that only the strongest expression domain in the distal blastema was detected. Scale bars: whole mounts, 100 µm; sections, 100 µm.

Importantly, some factors required for fin regeneration were insensitive to inhibition of Wnt/β–catenin signaling using the same heat shock protocol, namely *msxB* (Fig. 4.26K and data not shown) and *actβAa/inhβAa* (Fig. 4.26L and data not shown), indicating that gene expression is not non-specifically suppressed in *axin1* or *dkk1* expressing fins. Activin signaling has been shown to promote blastemal proliferation (Jazwinska *et al*., 2007). Interestingly, while *actβAa/inhβAa* was not dependent on Wnt/β–catenin signaling, *actβB/inhβB* expression, which co-localized with *7xTCF*:mCherry in the distal-most blastema, was (Fig. 4.26L, arrowhead in Fig. 4.27B).

Together, these data strongly suggest that Wnt/β–catenin signaling regulates the activity of multiple signaling pathways required for fin regeneration including Hh, Bmp, RA, Igf, Notch, Fgf and Activin.

4.10 Wnt/β–catenin Signaling Receives Little Reciprocal Input from the Signaling Pathways it Regulates

The data presented here indicate that Wnt/β–catenin signaling regulates many other signaling pathways required for fin regeneration. To determine whether these pathways also reciprocally control β–catenin signaling, I assayed *7xTCF:*mCherry reporter activity or expression of the endogenous Wnt target *axin2* after genetic or pharmacological inhibition of a number of these pathways. Yet, the Wnt reporter was hardly reduced after continuous inhibition of Igf signaling using the Igf1r inhibitor NVP-AEW541 or Fgf signaling by overexpression of a dominant negative *zebrafish FGF receptor 1* (*dnfgfr1*) in *hsp70l:*dnfgfr1-EGFP^{pd1} (*hs:*dnfgfr1; Lee *et al*., 2005); *7xTCF:*mCherry double transgenics for 3 days starting prior to amputation (Fig. 4.28A-B), although regenerative growth was severely reduced by both treatments. Reporter expression was reduced but still robustly detected in the severely diminished regenerates produced by continuous interference with Notch signaling using the γSecretase inhibitor LY411575 (Fig. 4.28C), with Activin signaling using the Activin receptor-like kinase receptor 4 (Alk4) inhibitor SB431542 (Fig. 4.28D) or with RA signaling using overexpression of zebrafish *cyp26* in *hsp70l*:cyp26a1^{kn1} (*hs*:cyp26a1; Blum and Begemann, 2012); *7xTCF:*mCherry double transgenics (arrowhead in Fig. 4.28E). Furthermore, expression of the direct Wnt target *axin2* was hardly reduced after interference for 6 hours with Activin signaling using the Alk4 receptor inhibitor SB431542 (Fig. 4.28F), with Igf signaling using the Igf1r inhibitor NVP-AEW541 (Fig. 4.28G), with Hh signaling using the Smoothened antagonist Cyclopamine (Fig. 4.28H), or with Notch signaling using the γSecretase inhibitor LY411575 (Fig. 4.28I). *axin2* expression was likewise robustly detected 6 hours after heat shock-induced overexpression of the *dnfgfr1* in *hs:*dnfgfr1 transgenics (Fig. 4.28J), of *cyp26a1* in *hs*:cyp26a1 transgenics (Fig. 4.28K), or of the Bmp inhibitor *noggin3* in *hsp70l*:noggin3^{fr14} transgenics (*hs*:nog3; Chocron *et al*., 2007) (Fig. 4.28L). Importantly, *axin2* expression was strongly reduced 6 hours after a single heat shock in *hs*:Axin1 transgenics (Fig. 4.2A) or when fish were treated for 6 hours with IWR-1, a pharmacological compound that inhibits Wnt/β–catenin signaling through stabilization of Axin (Fig. 4.28M). Thus, while interference with β–catenin signaling severely reduced or abolished expression of ligands or readouts of Activin, Bmp, Fgf, Hh, Igf, Notch and RA pathways within hours, inhibition of these

pathways to a level that severely affected regeneration was not sufficient to completely abolish Wnt signaling activation in the remaining blastemal tissue even after prolonged pathway interference. I conclude that Wnt/β–catenin signaling acts upstream of these pathways, but receives little reciprocal input.

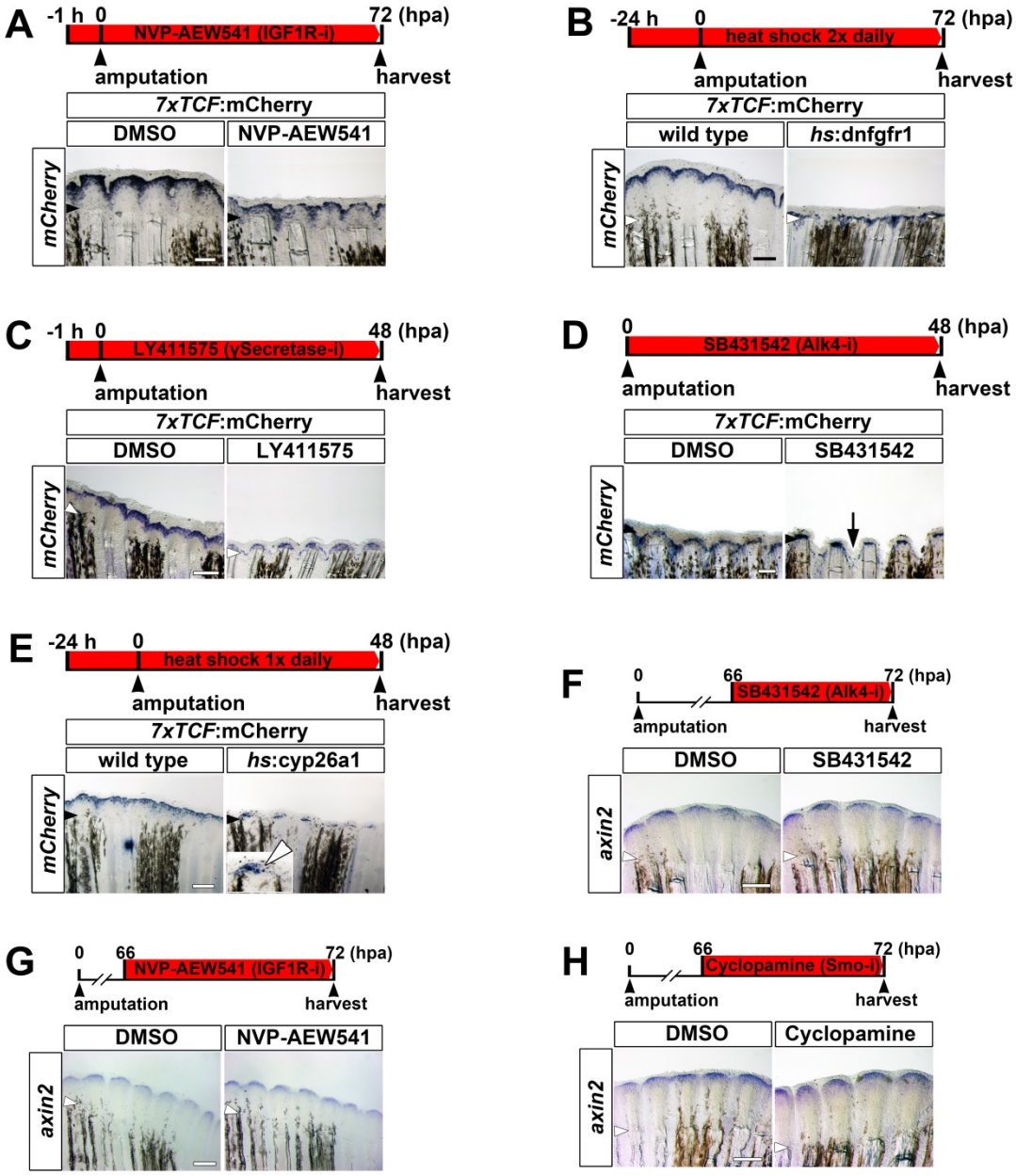

Fig. 4.28. Wnt/β–catenin signaling receives little reciprocal input from other developmental signaling pathways during caudal fin regeneration. (A-E) *7xTCF*:mCherry reporter expression is robustly detectable in severely reduced regenerates obtained after prolonged inhibition of Igf (A), Fgf (B), Notch (C), Activin (D) or RA (E) signaling for 48 or 72 hours using pharmacological compounds or heat shock-induced overexpression of pathway inhibitors. **Continued on the next page.**

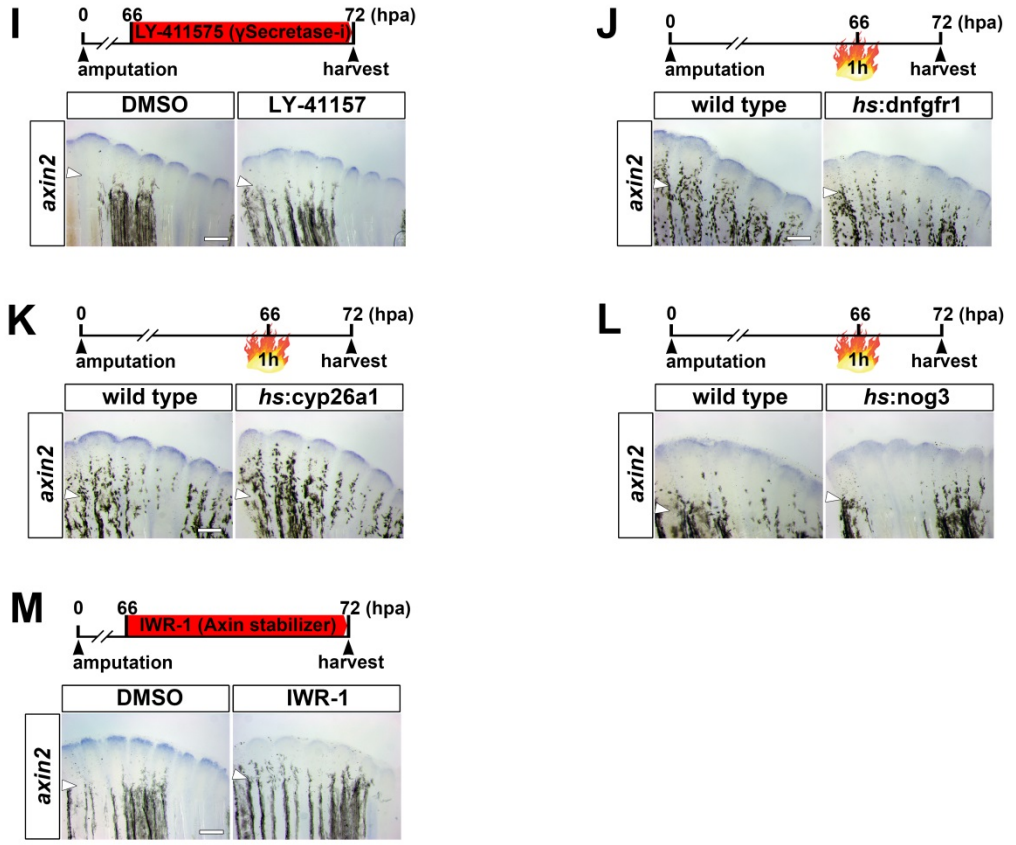

Fig. 4.28. continued. (F-L) Expression of the endogenous Wnt target *axin2* is robustly detected after inhibition of Activin (F), Igf (G), Hh (H), Notch (I), Fgf (J), RA (K) or Bmp (L) signaling for 6 hours, while it is strongly reduced when Wnt/β–catenin signaling (M) is inhibited for 6 hours. Drug treatments or heat shocks were performed according to the schematic timeline. Small arrowheads: amputation plane. Scale bar: whole mounts, 200 µm. ***7xTCF*:mCherry**: NVP-AEW541: n(DMSO) = 6/6, n(NVP-AEW541) = 6/6; *hs:*dnfgfr1: n(*7xTCF*:mCherry) = 6/6, n(*7xTCF*:mCherry; *hs:*dnfgfr1) = 6/6; LY-411575: n(DMSO) = 5/6, n(LY-411575) = 4/6; SB431542: n(DMSO) = 6/6, n(SB431542) = 6/6; *hs*:cyp26a1: n(*7xTCF*:mCherry) = 4/4, n(*7xTCF*:mCherry; *hs*:cyp26a1) = 4/4. ***axin2***: SB431542: n(DMSO) = 7/7, n(SB431542) = 7/7; NVP-AEW541: n(DMSO) = 6/6, n(NVP-AEW541) = 6/6; Cyclopamine: n(DMSO) = 6/6, n(Cyclopamine) = 6/6; LY-411575: n(DMSO) = 6/6, n(LY-411575) = 5/6; *hs:*dnfgfr1: n(wild type) = 8/8, n(*hs*:dnfgfr1) = 7/8; *hs*:cyp26a1: n(wild type) = 8/9, n(*hs*:cyp26a1) = 7/9; *hs:*nog3: n(wild type) = 5/5, n(*hs*:nog3) = 4/5, IWR-1: n(DMSO) = 7/7, n(IWR-1) = 6/7.

4.11 Wnt/β–catenin Signaling Indirectly Regulates Epidermal Patterning Through Fgf and Bmp Signaling

I have provided evidence that cell proliferation in several compartments of the regenerating fin appears to be indirectly regulated by Wnt/β–catenin signaling. Likewise, epidermal *lef1* expression cannot be directly controlled by the pathway. Consistent with this hypothesis we found that *mCherry* expression was already abolished 3 hours after a single heat shock in *7xTCF*:mCherry; *hs:*dkk1 double transgenic regenerates (arrow in Fig. 4.29A) while in the same fins epidermal *lef1* expression was unaffected (asterisk in Fig.4.29A). I thus

looked for candidate signals that could act downstream of β–catenin signaling to mediate its effects in the epidermis. In other systems, *lef1* expression has been shown to be regulated by Bmp signaling (Kratochwil *et al*., 1996). I found that epidermal *lef1* expression was strongly reduced 6 hours following heat shock-driven overexpression of the Bmp inhibitor *noggin3* in the *hs*:nog3 transgenic line (Fig. 4.29B-C), while Wnt reporter activity was hardly altered in *7xTCF*:mCherry; *hs*:nog3 double transgenics (Fig. 4.29C). Thus, the Bmp pathway regulates epidermal *lef1* expression independently of β–catenin signaling. *lef1* has also been shown to be regulated by Fgf signaling in the regenerating fin (Lee *et al*., 2009). I found that *lef1* expression was strongly diminished 6 hours after activation of *dnfgfr1* expression in *hs:*dnfgfr1; *7xTCF*:mCherry double transgenics, while in the same fin rays the Wnt reporter was unaffected (Fig. 4.29D). Together with the finding that Bmp and Fgf signaling are regulated by the Wnt/β–catenin pathway, these data suggest that these pathways control epidermal *lef1* expression downstream of β–catenin signaling.

Interestingly, as shown in Fig. 4.26I, I have found that expression of the Fgf target genes *spry4*, *pea3* and *erm,* which are all expressed in distal domains of the basal epidermal layer (Lee *et al*., 2005; Lee *et al*., 2009), likewise depends on Wnt/β–catenin signaling. While Fgf ligands regulate *erm* and *pea3* expression via the Ras/Mapk pathway, *lef1* expression is controlled via a Ras-independent route in the regenerating fin (Lee *et al*., 2009). Thus, Wnt/β–catenin signaling might regulate *pea3* and *erm* expression through the Fgf/Ras pathway. To test this, we asked whether Ras activation could rescue *erm* and *pea3* expression in Wnt-inhibited fins using *hs*:Axin1; *hsp70l*:vHRAS,cryaa:DsREDEx^{pd8} (*hs*:v-ras; Lee *et al*., 2009) double transgenics. In agreement with published data (Lee *et al*., 2009) a single heat shock was sufficient to upregulate *pea3* and *erm* expression in *hs*:v-ras transgenic regenerates 6 hours post heat shock, while their expression was abolished in *hs*:Axin1 transgenics (Fig. 4.30A). Intriguingly, upon simultaneous overexpression of *axin1* and *v-ras*, *erm* and *pea3* expression was restored (Fig. 4.30B). Thus, I conclude that Wnt/β–catenin signaling in the distal blastema regulates *pea3* and *erm* transcription in the adjacent wound epidermis via activation of Fgf/Ras signaling. *fgf3* is a candidate Fgf ligand mediating this interaction between tissues, since its expression co-localizes with β–catenin activity in the distal-most blastema (arrowhead in Fig. 4.30B), where it is dependent on β–catenin signaling (Fig. 4.26I).

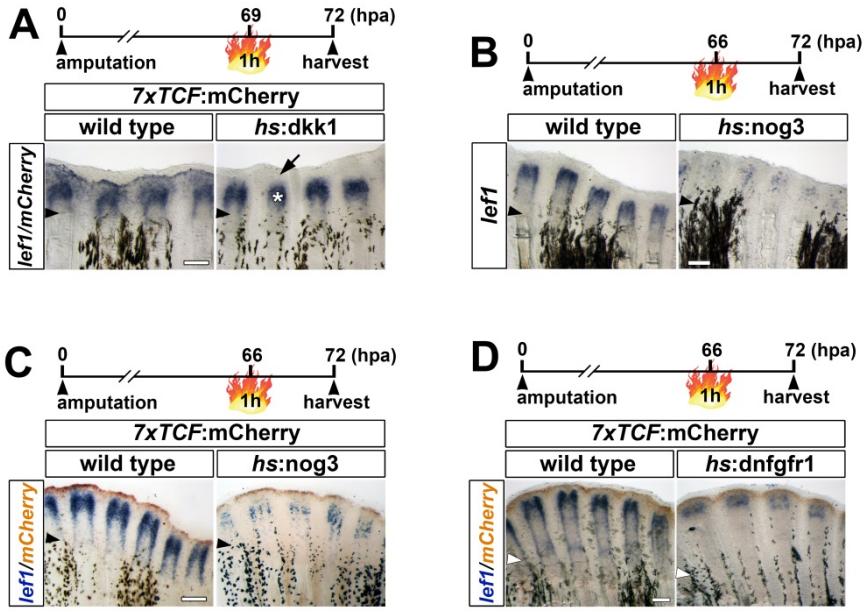

Fig. 4.29. Epidermal *lef1* expression is regulated via Bmp and Fgf signaling independently of Wnt/β-catenin signaling. (A) *dkk1* overexpression interferes with *mCherry* (arrow) but not *lef1* (asterisk) expression 3 hours after a single heat shock in *7xTCF*:mCherry; *hs:*dkk1 double transgenic regenerates. n(*7xTCF* mCherry) = 7/8, n(*7xTCF*:mCherry*; hs:*dkk1) = 6/8. **(B)** Overexpression of the Bmp inhibitor *noggin3* for 6 hours interferes with *lef1* expression in *hs* nog3 transgenic regenerates at 72 hpa. n(wild type) = 7/7, n(*hs* nog3) = 5/7. **(C)** *noggin3* overexpression reduces *lef1* (blue) but not *mCherry* (brown) expression in *7xTCF* mCherry; *hs*:nog3 double transgenic regenerates. n(*7xTCF* mCherry) = 6/6, n(*7xTCF*:mCherry*; hs*:nog3) = 5/6. **(D)** Overexpression of a dominant negative *fgf receptor 1* reduces *lef1* (blue) but not *mCherry* (brown) expression in *7xTCF*:mCherry; *hs:*dnfgfr1 double transgenic regenerates. (*7xTCF*:mCherry) = 6/7, n(*7xTCF*:mCherry*; hs:*dnfgfr1) = 5/7. **(A-D)** Heat shocks were performed according to the schematic timeline. Small arrowheads: amputation plane. Scale bar: whole mounts, 200 µm.

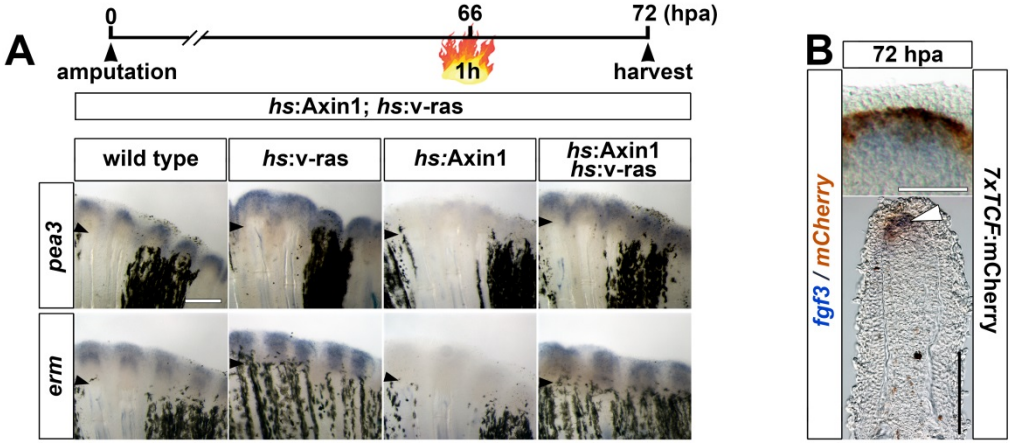

Fig. 4.30. Wnt/β-catenin signaling regulates epidermal *pea3* and *erm* expression via Fgf/Ras signaling. (A) *axin1* overexpression inhibits expression of the Fgf targets *pea3* and *erm* which is rescued by concomitant activation of Fgf/Ras signaling via overexpression of *v-ras*. *pea3*: n(wild type) = 7/7, n(*hs*:v-Ras) = 7/7, n(*hs*:Axin1) = 7/7, n(*hs*:Axin1; *hs*:v-ras) = 6/7; *erm*: n(wild type) = 8/8, n(*hs*:v-ras) = 7/7, n(*hs*:Axin1) = 7/7, n(*hs*:Axin1; *hs*:v-ras) = 6/7. Heat shocks were performed according to the schematic timeline. **(B)** *fgf3* and *mCherry* transcripts co-localize in the distal-most blastema (arrowhead) in *7xTCF*:mCherry transgenic regenerates Note that samples were stained for mCherry expression only shortly, so that only the strongest expression domain in the distal blastema was detected. **(A-B)** Small arrowheads: amputation plane. Scale bar: whole mounts, 200 µm (A) and 100 µm (B); section, 100 µm.

4.12 Wnt/β–catenin Signaling regulates Maintenance of the Wound Epidermis via a Retinoic Acid/Igf Signaling Axis

A recent study has proposed a model in which Igf signaling from the blastemal mesenchyme to the basal epidermal layer is essential for maintaining the integrity of the basal wound epidermis as a prerequisite for regeneration (Chablais and Jazwinska, 2010). Similarly, Wnt/β–catenin signaling is required for specification of the basal wound epidermis (Kawakami *et al*., 2006; Stoick-Cooper *et al*., 2007b). As shown in Fig. 4.26E-F one of the pathways regulated by Wnt signaling in the regenerating fin is Igf, suggesting that Wnt/β–catenin signaling regulates maintenance of the wound epidermis via activating epidermal Igf signaling. However, *igf2b* transcripts were found to be largely absent in regions of the regenerate with active Wnt/β–catenin signaling, namely the distal-most blastema and the actinotrichia-forming cells (Fig. 4.31A), indicating that it is not a direct target of the pathway. Interestingly, a recent study has provided evidence for RA signaling controlling *igf2b* transcription (Blum and Begemann, 2012) and I found that expression of the rate-limiting enzyme in RA synthesis *aldh1a2* depends on Wnt/β–catenin signaling (Fig. 4.26D). Thus I asked whether Wnt/β–catenin signaling regulates *igf2b* indirectly via RA pathway activation. I inhibited Wnt/β–catenin signaling using *hs:*dkk1 transgenic fish and concomitantly injected RA. Consistent with my previous results and those of others (Blum and Begemann, 2012), RA injections slightly enhanced, while *dkk1* overexpression blocked *igf2b* expression. Intriguingly, upon RA administration I could again detect *igf2b* transcripts in *hs:*dkk1 transgenic regenerates (arrows in Fig. 4.31B). Thus Wnt/β–catenin signaling regulates at least in part *igf2b* expression indirectly via RA signaling. Together these data suggest that Wnt/β–catenin signaling possibly regulates maintenance of the wound epidermis via sequential activation of RA and Igf signaling.

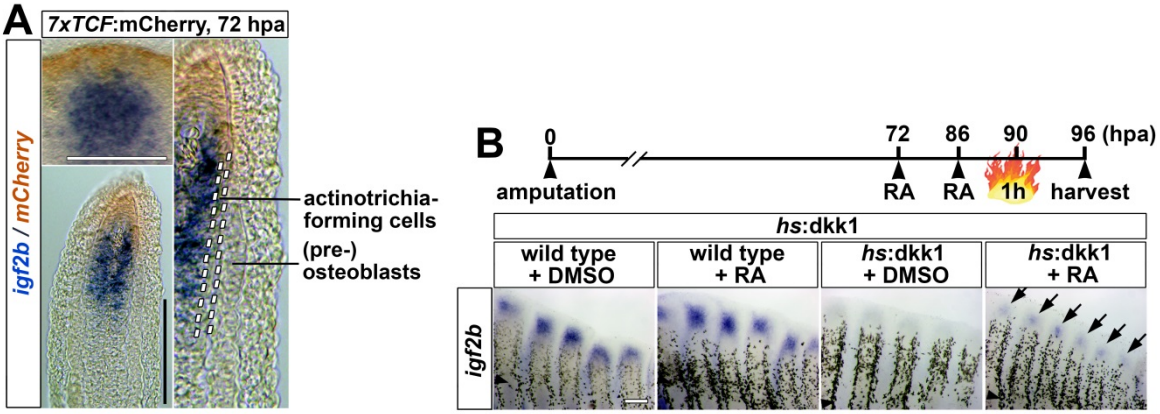

Fig. 4.31. Wnt/β–catenin signaling regulates Igf signaling via retinoic acid signaling. (A) *igf2b* transcripts are detected proximally to the mCherry expression domain and also medially to the actinotrichia-forming cells in 7xTCF:mCherry transgenic regenerates. **(B)** *dkk1* overexpression inhibits *igf2b* expression which is partially rescued (arrows) by repetitive injections of RA. n(wild type, DMSO) = 5/6, n(*hs:*dkk1, DMSO) = 5/6, n(wild type, RA) = 6/6, n(*hs:*dkk1, RA) = 4/6. Heat shocks and drug treatments were performed according to the schematic timeline. **(A-B)** Small arrowheads: amputation plane. Scale bar: whole mount, 200 µm; section, 100 µm.

4.13 Blastemal Cell Proliferation is Regulated by the Wnt/β–catenin Pathway via Hedghehog and Retinoic Acid Signaling

Hh signaling is a candidate pathway that could act downstream of β–catenin to mediate its mitogenic effects in the blastemal mesenchyme, since Hh ligands are transcriptionally regulated by β–catenin signaling (see Fig. 4.26B) and the pathway has been shown to be required for blastema proliferation (Quint *et al*., 2002). Activation of Hh signaling using the Smoothened agonist SAG could rescue epidermal and blastemal expression of the direct Hh target gene *ptc2* in *hs*:Axin1 transgenic fins (Fig. 4.32A-B), indicating that this treatment can restore Hh signaling lost after inhibition of β–catenin signaling. Thus, I asked whether Hh signaling could rescue blastemal proliferation upon Wnt pathway inhibition. *hs*:Axin1 transgenic fish and their wild type siblings were subjected to a single heat shock, treated with SAG or vehicle control and anti-phospho-histone 3 (H3P)-positive blastemal cells were quantified using confocal imaging. Consistent with previous reports *axin1* overexpression significantly decreased, while SAG-treatment increased the number of H3P+ cells in the blastemal mesenchyme (Fig. 4.33A) (Lee *et al*., 2009; Stoick-Cooper *et al*., 2007b). Importantly, SAG treatment rescued the number of H3P+ cells in *hs*:Axin1 transgenic fish back to wild type levels (Fig. 4.33A). In contrast, activation of

Wnt/β–catenin signaling through overexpression of *wnt8* in *hs:*wnt8 transgenic fish failed to rescue blastemal proliferation that was reduced upon inhibition of Hh signaling using Cyclopamine (Fig. 4.33B). Thus, Wnt/β–catenin signaling regulates blastemal proliferation through Hh signaling.

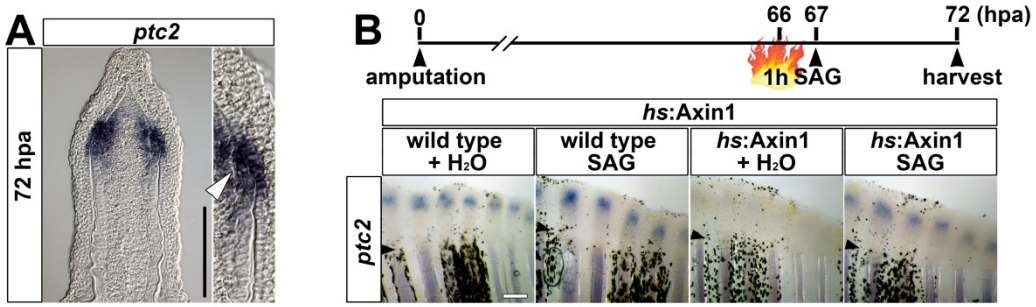

Fig. 4.32. Wnt/β-catenin signaling regulates Hedgehog signaling. (A) *ptc2* expression is detected in the basal epidermal layer and in osteoblasts (arrowhead). **(B)** *axin1* overexpression inhibits expression of the Hh target *ptc2* which is rescued by concomitant activation of Hh signaling using the pharmacological compound SAG. n(wild type) = 5/6, n(wild type, SAG) = 5/6, n(*hs*:Axin1) = 6/6, n(*hs*:Axin1, SAG) = 4/6. Heat shocks and drug treatments were performed according to the schematic timeline. **(A-B)** Small arrowheads: amputation plane; scale bar: whole mount, 200 µm; section, 100 µm.

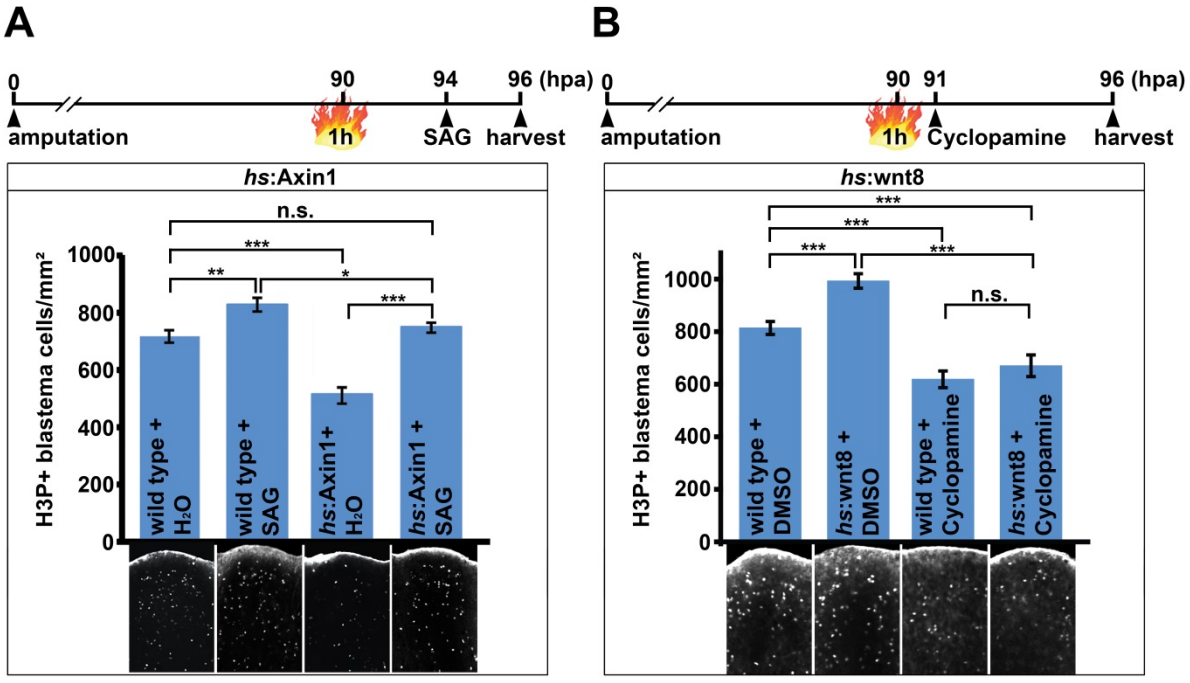

Fig. 4.33. Wnt/β–catenin signaling regulates blastemal cell proliferation via Hedgehog signaling. (A) *axin1* overexpression reduces the number of H3P+ cells in the blastema which is rescued by concomitant activation of Hh signaling using the Smoothened Agonist SAG. n = 5 fish, 20 blastemas. **(B)** Inhibition of Hh signaling through exposure to the Smoothened antagonist Cyclopamine reduces the number of H3P+ cells in the blastema which is not rescued by concomitant activation of Wnt signaling following *wnt8* overexpression. n = 5 fish, 20 blastemas. **(A-B)** Heat shocks and drug treatments were performed according to the schematic timeline.

Another candidate pathway that could mediate the mitotic effects of Wnt/β–catenin signaling in the proximal blastema is RA signaling, which has recently been shown to be essential for blastema formation and proliferation (Blum and Begemann, 2012). Expression of the RA synthesizing enzyme *aldh1a2* is largely confined to the Wnt/β–catenin signaling-positive distal-most blastema, where its expression depends on the Wnt pathway (Fig. 4.12A-B, 4.26D). In contrast, the *retinoic acid receptor γa* (*rarγa*) was mainly expressed in the *7xTCF*:mCherry negative (pre-)osteoblast domain in the lateral blastema, indicating that these cells are competent to respond to the distally synthesized RA (Fig. 4.34A, Blum and Begemann, 2012). To test whether RA acts downstream of Wnt/β–catenin signaling in regulation of blastemal cell proliferation, I assayed blastema mitosis in *hs*:Axin1 transgenic fish that were injected with RA. Consistent with previous results, RA increased the number of H3P+ mesenchymal cells, while overexpression of *axin1* suppressed proliferation (Blum and Begemann, 2012; Stoick-Cooper *et al*., 2007b) (Fig. 4.34B). Intriguingly, I found that proliferation was rescued back to wild type levels in RA-treated, *axin1* expressing fins, indicating that RA signaling regulates blastemal proliferation downstream of Wnt/β–catenin signaling during regenerative outgrowth (Fig. 4.34B). Although repetitive administration of RA rescued blastemal cell proliferation when Wnt/β–catenin signaling was concomitantly inhibited, it was not sufficient to rescue regenerative growth in *hs:*dkk1 transgenic fish (Fig. 4.34C), supporting the finding that Wnt/β–catenin signaling orchestrates fin regeneration through regulation of multiple signaling pathways. Together, these data indicate that Wnt/β–catenin signaling regulates blastemal cell proliferation indirectly through Hh and RA pathways.



Fig. 4.34. Wnt/β–catenin signaling regulates blastemal cell proliferation via retinoic acid signaling. (A) Transcripts of the RA receptor *rarγa* are detected proximally to *mCherry* expression in the distal-most blastema in *7xTCF*:mCherry transgenic regenerates. Longitudinal sections reveal that *rarγa* expression is confined to the lateral blastema containing (pre-)osteoblasts. **Continued on the next page.**

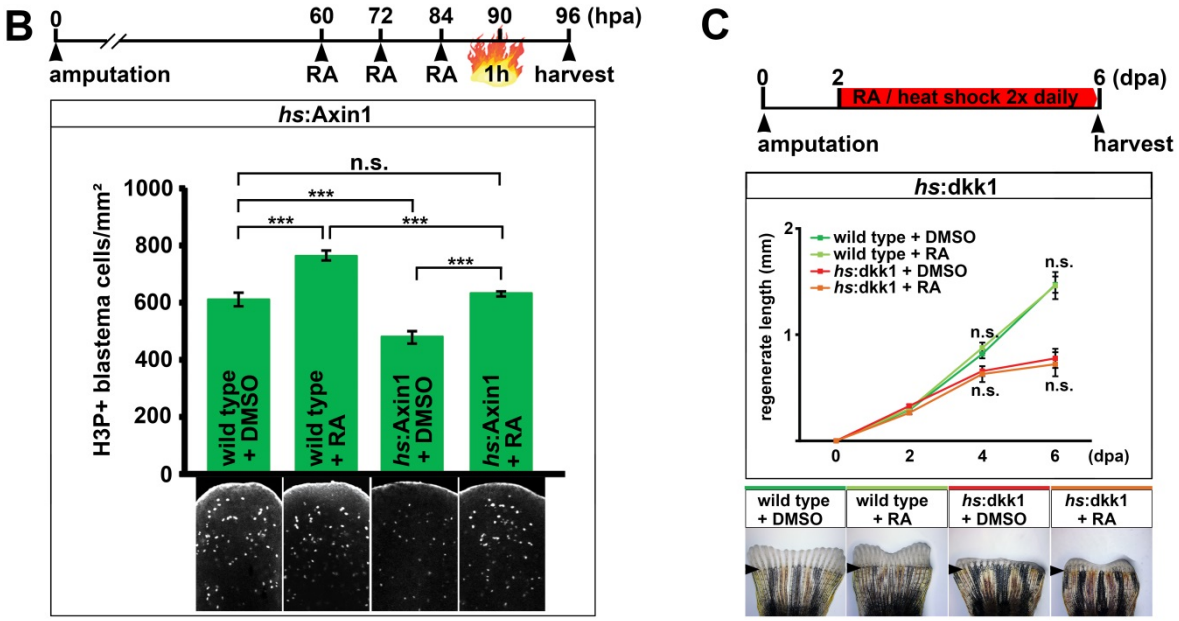

Fig. 4.34. continued. (B) *axin1* overexpression reduces the number of H3P+ cells in the blastema which is rescued by concomitant activation of retinoic acid signaling through administration of RA. n = 5 fish, 20 blastemas. **(C)** *dkk1* overexpression strongly inhibits regenerative growth which is not rescues by concomitant activation of retinoic acid signaling through administration of RA. n = 5 fish. **(A-C)** Heat shocks and drug treatments were performed according to the schematic timeline. Arrowheads: amputation plane. Scale bar: 100 µm.

4.14 Amputation-Induced Jnk Activity, ROS Production or Immune System Activation is Dispensable for Wnt/β–catenin Pathway Activation During Caudal Fin Regeneration

The data presented strongly suggest that the β–catenin pathway acts upstream of many other signaling pathways required for regeneration, indicating that Wnt signaling acts early in the hierarchy of signals. Thus, an important question arises: what signal acts upstream of Wnt/β–catenin signaling, that is, which wounding-induced signals activate Wnt ligand expression and thus β–catenin signaling? Potential candidate signals that have been shown to be activated very soon after wounding and are essential for initiation of adult fin or larval finfold regeneration are redox signaling via generation of reactive oxygen species (ROS) such as H_2O_2, activation of cytokine and chemokine-secreting immune cells, and c-Jun-N-terminal kinase/stress-activated proteinase kinase (Jnk/Sapk)-mediated activation of gene transcription (Ishida *et al*., 2010; Kyritsis *et al*., 2012; Niethammer *et al*., 2009; Yoo *et al*., 2012; Gauron *et al*., 2013). To test whether any of the aforementioned signals act upstream of β–catenin pathway activation I assayed *7xTCF:*mCherry reporter expression

following immunosuppression or pharmacological inhibition of ROS production or Jnk signaling. *7xTCF:*mCherry reporter expression was robustly detected after continuous inhibition of Jnk activity using the pharmacological compound SP60125 although regeneration was severely inhibited (Fig. 4.35A). Similarly, *7xTCF:*mCherry reporter expression was detectable upon inhibition of NADPH oxidase-mediated H_2O_2 production using the pharmacological compound VAS-2780 (arrows in Fig. 4.35B) even though treated fish failed to form a wound epidermis. Finally, immunosuppression via sub-lethal irradiation (40 Gy; Traver *et al*., 2004), which was performed in collaboration with Nona Shayegi (CRTD, Dresden), completely blocked fin regeneration but did not inhibit *7xTCF*:mCherry reporter activity (Fig. 4.35C). Together, these data suggest that redox signaling, Jnk/Sapk signaling and immune system-induced inflammation is dispensable for activation of Wnt/β–catenin signaling during caudal fin regeneration.

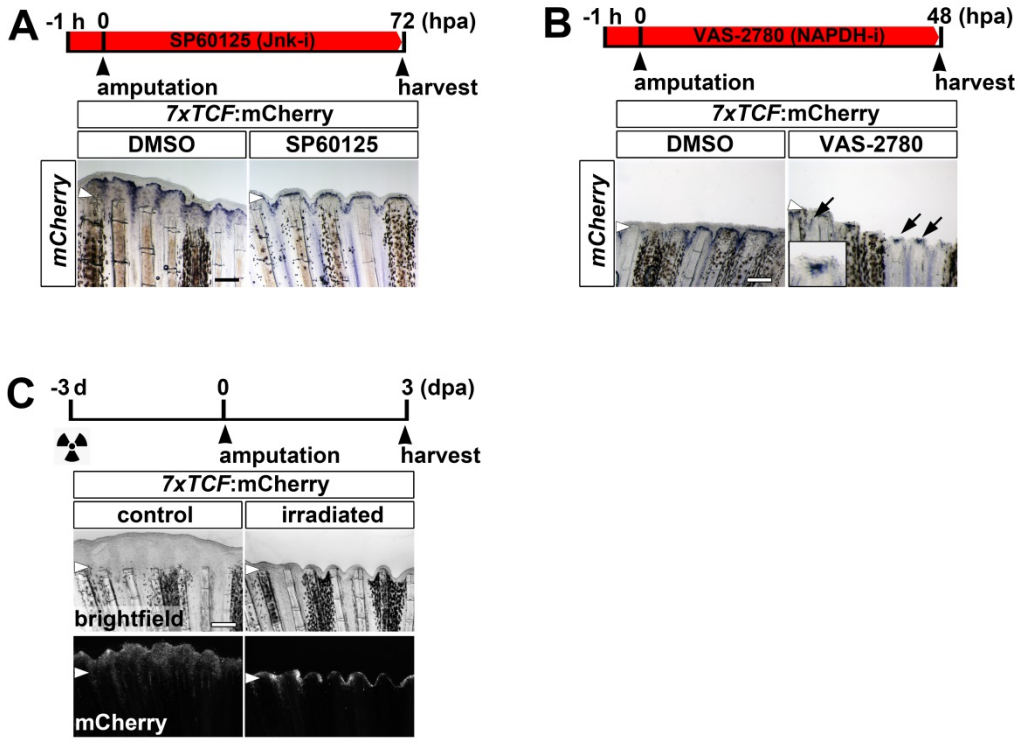

Fig. 4.35. Amputation-induced Jnk activity, ROS production or immune system activation is dispensable for activation of Wnt/β–catenin signaling during caudal fin regeneration. (A-C) *7xTCF*:mCherry reporter expression is robustly detectable in severely reduced regenerates obtained after prolonged inhibition of Jnk signaling (A), ROS production (B), or in immunosuppressed fins (C). Jnk: n(DMSO): 6/6, n(SP60125) = 6/6; ROS: n(DMSO) = 5/5, n(VAS-2780) = 5/5; Immunosuppression: n(control) = 7/7, n(irradiated) = 8/8. Fish were treated according to the schematic timeline. Scale bars: 200 µm.

5 Discussion

5.1 A Model for Wnt/β–catenin Signaling Functions During Caudal Fin Regeneration

The work presented here significantly advances our understanding of the mechanisms underlying vertebrate appendage regeneration. The results presented here suggest that the blastema, the population of undifferentiated mesenchymal cells characteristic of regenerating appendages, displays previously unrecognized functional diversity, since it contains signaling centers that orchestrate growth and differentiation of the regenerate. I propose that Wnt/β–catenin signaling has essential functions in defining these organizing centers, and that it acts upstream of a large number of other developmental signaling pathways that mediate the effects of these organizers on surrounding tissues. Specifically, my data support the following model of Wnt/β–catenin pathway action during fin regeneration (Fig. 5.1):

Wnt/β–catenin signaling is activated already during wound re-epithelialization (at 6 hpa) in the interray mesenchyme, making β–catenin pathway activation one of the earliest known responses to fin amputation (Fig. 5.1A). Pathway activation at 6 hpa is consistent with the induction of *wnt10a* expression at this time point, which has been reported previously (Stoick-Cooper *et al*., 2007b). Pathway activity is maintained in interray mesenchyme throughout regeneration but the functional significance of this site of β–catenin signaling remains to be determined. Here, I have concentrated on Wnt functions in the ray blastema, where pathway activation starts around 24 hpa. Subsequently, the blastema is compartmentalized into several subregions with distinct proliferative properties and cell fate (Fig. 5.1B). Wnt-receiving cells localize to the distal-most compartment where they remain largely quiescent and retain their distal position until regeneration is completed. Additionally, Wnt activity is detectable in a subregion of the proliferative proximal blastema, namely the presumptive actinotrichia-forming cells that lie medial to the osteoblast progenitors. No β–catenin pathway activation appears to occur in the highly

proliferative wound epidermis, osteoblasts or the majority of the proximal medial blastema.

Surprisingly, the data obtained using tissue-specific Wnt signaling inhibition suggest that signaling in the non-proliferative distal-most blastema is required for proliferation of other blastemal domains, while signaling in the proliferative proximal blastema has little role in regulating cell division, but in directing differentiation of adjacent osteoblast progenitors (Fig. 5.1C). Furthermore, β–catenin signaling regulates the maintenance of gene expression domains in the wound epidermis and thus, likely its regionalization indirectly as well (Fig. 5.1C). Thus, I conclude that β–catenin signaling controls regenerate growth, differentiation and patterning largely indirectly. I found that almost all signaling pathways that have previously been shown to be involved in controlling fin regeneration are regulated by Wnt/β–catenin signaling and that Hh and RA signals act downstream of β–catenin in the promotion of blastemal cell proliferation, while Fgf and possibly Igf and Bmp signaling mediate its effects on the epidermis (Fig. 5.1C-D).

Interestingly, the data presented here indicate that Wnt/β–catenin signaling receives little reciprocal input from the signals it regulates. These findings support a model in which Wnt/β–catenin signaling acts on top of a likely cooperative signaling network that instructs fin regeneration (Fig. 5.1D). In contrast, a recent study has proposed that RA signaling promotes Fgf and Wnt/β–catenin signaling and that these pathways cooperatively regulate regeneration (Blum and Begemann, 2012). While the rescue experiments shown point towards a role of the Wnt pathway upstream of RA, Fgf and Hh signaling, epistatic relationships are difficult to assess in hypomorphic knock-down conditions. Thus, definitive conclusions about the hierarchical relationships between pathways regulating regeneration probably need to await the development of inducible genetic loss-of-function techniques in zebrafish.

In summary, I propose that Wnt signaling sets up two signaling centers, one in the distal-most blastema and one in the presumptive actinotrichia forming cells in the mediolateral proximal blastema, from which other signals, either diffusible or via cell-cell contact, emanate that direct growth, differentiation and patterning of the regenerating zebrafish caudal fin.

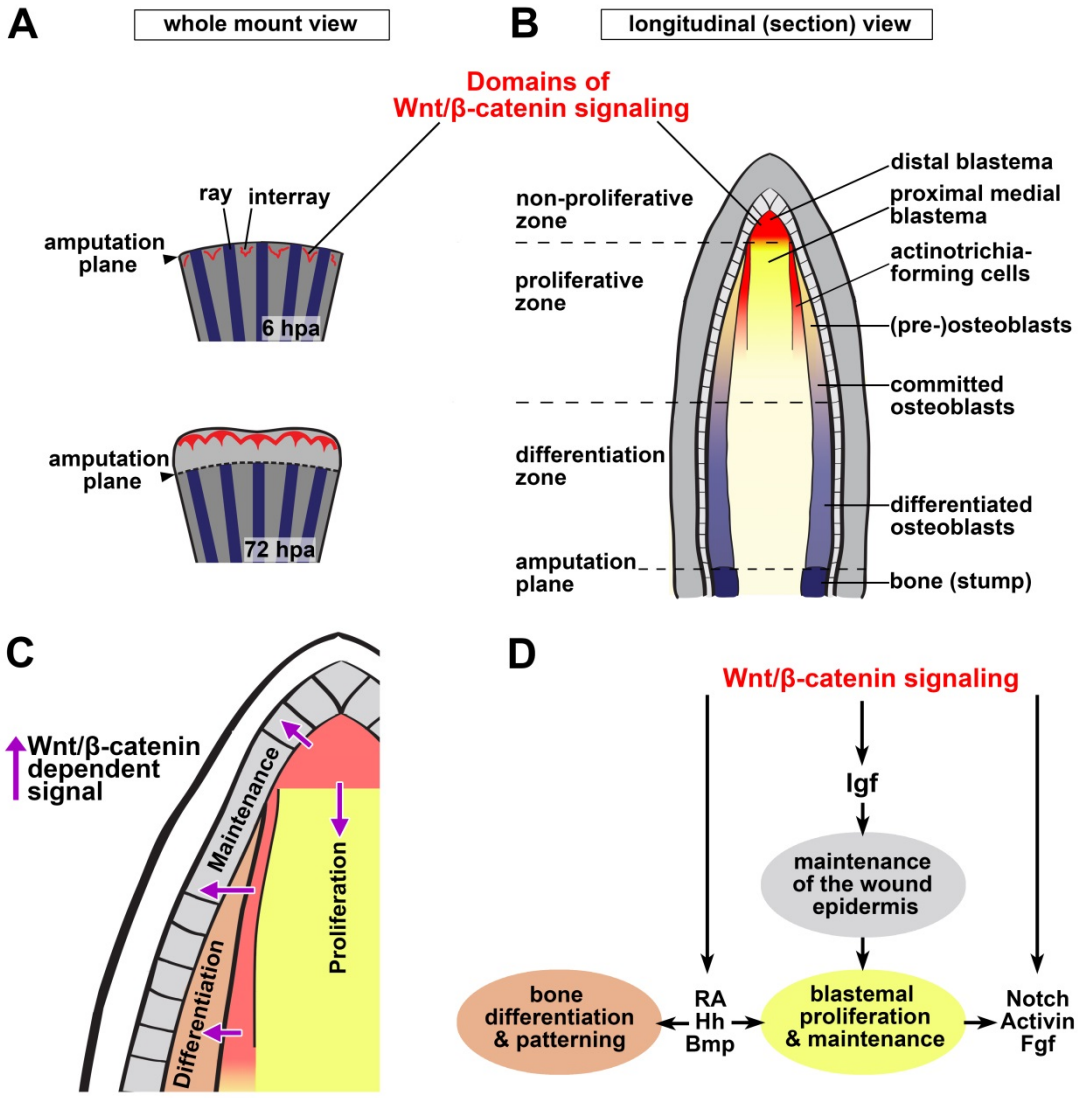

Fig. 5.1. A model for Wnt/β–catenin function during caudal fin regeneration. (A-B) Schematic summary of the Wnt/β–catenin activity domains (in red color) during caudal fin regeneration. Whole mount (A) and longitudinal section views (B) are shown. **(C)** Wnt pathway activity is required for production of (diffusible) signals that regulate proliferation of proximal blastemal regions, differentiation of osteoblasts, and maintenance of gene expression domains in the epidermis. **(D)** Schematic summary of the hierarchical position of Wnt/β–catenin signaling within the molecular signaling network controlling caudal fin regeneration. Arrows indicate direct or indirect regulation.

An interesting aspect of this study is that these signaling centers not only show differences in proliferative properties and, according to the proposed model, exert distinct functions, but can also be defined by their Wnt co-receptor expression. The Wnt-receiving cells located in the distal-most blastema are rather quiescent and positive for *lrp6* transcripts. In contrast, the Wnt-receiving cells that are found in mediolateral domains of the blastema, adjacent to the osteoblast progenitors, are highly proliferative and positive

for *lrp5* transcripts. A question thus arises: does the difference in *lrp5* and *lrp6* co-receptor expression account for the distinct proliferative potential and/or for the functional difference of these domains? A recent study provided evidence that Lrp6 exhibits stronger signaling activity as compared to Lrp5 and thus providing a possible mode of achieving differential signaling outputs (MacDonald *et al*., 2011). Consistent with this, I found that Wnt reporter activity is most strongly detected in the distal-most *lrp6*+ blastema. Thus, it would be interesting to test whether the difference in *lrp5* and *lrp6* co-receptor expression determines the functionality and proliferative properties of the blastemal signaling centers described here using genetic loss-of-function approaches.

5.2 Signaling Pathway Interactions During Vertebrate Appendage Regeneration

While many signaling pathways have been identified to be required for complete vertebrate appendage regeneration, their hierarchical relationships are poorly understood. This study provides for the first time a more detailed insight into the complex interaction network of signaling pathways that guide vertebrate appendage regeneration. Loss-of-function experiments revealed that expression of ligands for Fgf, Hh and RA signaling pathways depend on Wnt/β–catenin signaling and the rescue experiments performed indicate, that Wnt/β–catenin signaling acts upstream of Fgf, Hh and RA signaling in the regulation of blastemal cell proliferation and epidermal patterning. Interestingly, interaction of Wnt/β–catenin signaling with Hh or Fgf signaling pathways has also been reported for appendage regeneration in frogs and newts. In frog tadpole limbs, expression of the Fgf ligand family member *fgf8* depends on Wnt/β–catenin signaling (Yokoyama et al., 2007). This suggests, that Wnt/β–catenin signaling regulates Fgf signaling, similar to fin regeneration, through transcriptional control of Fgf ligands. Furthermore, it has been shown that both, Wnt/β–catenin and Fgf signaling are required for *Xenopus* tadpole tail regeneration, and that Fgf acts downstream of Wnt/β–catenin signaling (Lin and Slack, 2008). Interestingly, in both regenerating systems, the fish fin and the frog tadpole tail, expression of the Fgf ligand *fgf20a* is regulated by Wnt/β–catenin signaling, suggesting conserved mechanisms of appendage regeneration (Stoick-Copper *et al*., 2007; Lin and

Slack, 2008). In contrast to the zebrafish fin however, Bmp signaling appears to act upstream of Wnt/β–catenin signaling in the regenerating *Xenopus* tadpole tail (Lin and Slack, 2008). During newt limb regeneration, activation of the Wnt or Hh pathway promotes proliferation of blastemal cells (Singh et al., 2012). However, in contrast to the regenerating fin, Wnt signaling appears to acts downstream of Hh signaling during newt limb regeneration. Thus, Wnt and Fgf or Wnt and Hh signaling pathway interactions are conserved between different appendage regeneration systems, yet the hierarchy of events differs in some cases. Further studies are required to gain a more detailed insight into the hierarchical relationships of signaling pathways in these systems, which will allow for more substantial comparison.

5.3 Wound Signals Activating Wnt/β–catenin Signaling During Caudal Fin Regeneration

In response to tissue injury signals are provided by the wound which, depending on the regenerative capacity of the organisms, lead to scarring of the wound or initiate a regenerative program. Activation of Wnt/β–catenin signaling, possibly via Wnt10a, occurs within 6 hours after fin amputation and appears to regulate many other signaling pathways required for regeneration. Thus, it would be interesting to identify the wound signal acting upstream of Wnt/β–catenin pathway activation. The data presented here suggest that key early wound signals of regenerative processes in fish and frogs, including redox signaling (Gauron *et al*., 2013; Love *et al*., 2013; Niethammer *et al*., 2009; Yoo *et al*., 2012), Jnk signaling (Ishida *et al*., 2010) and activation of immune cells (Kyritsis *et al*., 2012), are dispensable for amputation-induced Wnt/β–catenin pathway activation, leaving the identity of the signal bridging injury and Wnt/β–catenin pathway activation undiscovered. Further studies will be required to unravel this important mechanism, which will aid the understanding why mammals fail to initiate a regenerative response after severe injury while lower vertebrates do. An excellent candidate signal that remains to be tested is apoptosis. In many regenerating systems, including the *Xenopus* larval tail (Tseng *et al*., 2007), the zebrafish caudal fin (Gauron *et al*., 2013), planarians (Pellettieri *et al*., 2010), and the head of the freshwater water polyp *Hydra* (Chera *et al*., 2009), injury-induced

apoptosis has been identified to be a crucial event that precedes regeneration. Interestingly, *Hydra* head regeneration requires Wnt3 which is released by apoptotic cells (Chera *et al*., 2009). Thus it would be interesting to test whether apoptotic cells in the fin stump likewise provide a source of Wnt ligands and thereby activate the β–catenin pathway.

5.4 Tcf1/Lef1 Function in the Wound Epidermis

The data presented here indicate that the wound epidermis of the regenerating fin is not competent to respond to Wnt ligands activating β–catenin signaling. Yet, *tcf1* and *lef1* expression is robustly detected in the proximal basal epidermal layer. Thus, Tcf1 and Lef1 transcription factors in the wound epidermis must regulate gene transcription independently of Wnt/β–catenin signaling. Indeed, a number of examples are known where Lef/Tcf proteins together with co-activators can activate target gene transcription independently of β–catenin: 1) Lef1 (and also weakly Tcf1) can interact with Ets1, Runx1, Cbf and Aly at the T-cell receptor α enhancer to activate transcription (Bruhn *et al*., 1997; Hsu *et al*., 1998; Mayall *et al*., 1997), 2) during mouse palate development and *Xenopus* embryogenesis Lef1 and Smad factors cooperatively activate transcription of Tgfβ target genes (Labbe *et al*., 2000; Nawshad and Hay, 2003), and 3) *in vitro* evidence has also been provided for an interaction of the Notch intracellular domain (Nicd) or the Igf1r with Lef1 in regulation of target genes (Ross and Kadesch, 2001; Warsito *et al*., 2012). In addition to binding transcriptional co-activators, Lef/Tcf transcription factors are able to induce a strong bend in the DNA which facilitates gene expression (Koopman, 2010). Thus, beside for their function in Wnt/β–catenin signaling Lef/Tcf transcription factors have distinct roles in activation of target genes expression of other signaling pathways.

5.5 Parallels and Differences to Amniote Limb Development

A common feature of amniote limb development is the establishment of signaling centers, which provide instructive cues to pattern the forming appendage along three axes. Signals controlling elongation and patterning along the proximal-distal axis are mainly provided by

the apical ectodermal ridge (AER), a thickened epithelium covering the distal tip of the growing limb (Fernandez-Teran and Ros, 2008). Wnt/β–catenin pathway activation via ectodermally-derived Wnt3 is essential for induction and maintenance of the AER signaling center (Fernandez-Teran and Ros, 2008). Importantly, Wnt ligands activating the β–catenin pathway that emanate from surface ectoderm, including the AER, are essential for limb outgrowth by maintaining proliferation and concomitantly preventing differentiation of the underlying mesenchyme (ten Berge *et al*., 2008). Although development of pectoral fins, which are homologous to amniote limbs in zebrafish, is less well understood, many molecular signals and their interaction network are shared with limb organogenesis in mouse and chicken (Zeller *et al*., 2009). *wnt3l* is expressed in the AER of pectoral fin buds (Norton *et al*., 2005), and Lef1 and Tcf1-mediated Wnt/β–catenin signaling in the AER and the underlying mesenchyme is required for AER maintenance and pectoral fin growth (Nagayoshi *et al*., 2008; Shimizu *et al*., 2012; Veien *et al*., 2005).

During regenerative outgrowth of the zebrafish fin, I found Wnt/β–catenin signaling to be activated in the distal blastemal mesenchyme underneath the wound epidermis and that pathway activation is essential for maintaining proliferation of the mesenchymal progenitors in the proximal blastema and therewith distally-oriented regenerate growth. While the ligand responsible for β–catenin pathway activation remains to be elucidated, *wnt3a* has been reported to be expressed in the basal epidermis that abuts the distal blastemal mesenchyme, hinting at parallels between distally-oriented growth of developing limbs and regenerating fins (Poss *et al*., 2000a). However, more substantial comparisons between development and regeneration require a better characterization of the development of the adult caudal zebrafish fin – whose molecular regulation is essentially unknown.

5.6 Wnt Signaling in Osteoblast Differentiation

During mammalian development, Wnt/β–catenin signaling is well accepted to have essential roles in promoting osteoblast differentiation (Long, 2012; Regard *et al*., 2012). The data presented here indicate that β–catenin signaling likewise is required for bone maturation in the regenerating fin. Surprisingly however, my results suggest, that in

contrast to mammals, Wnt signaling does not directly regulate osteoblast differentiation during fin regeneration. Instead, I find β–catenin signaling not to be active or required in osteoblasts but rather in adjacent presumptive actinotrichia-forming cells. Thus, Wnt/β–catenin signaling likely promotes osteoblast maturation via stimulation of diffusible factors that are yet to be determined. An alternative explanation could be that Wnt/β–catenin signaling in the presumptive actinotrichia-forming cells directs osteoblast maturation by creating a local permissive environment based on the extracellular matrix (ECM) composition. It is well established that the ECM plays a central role in controlling cell behavior and that the degree of ECM stiffness based on its composition directs lineage specification and cellular differentiation (Engler *et al*., 2006; Izu *et al*., 2011; Mason, 2012). The actinotrichia-forming cells are known to express different collagens that form rigid hyperpolymerized collagen macrofibrils (Duran *et al*., 2011). Notably, it has been shown that rigid, collagenous matrices promote osteogenic lineage specification of mesenchymal stem cells and type XII Collagen has been shown to regulate osteoblast differentiation and maturation in mice (Engler *et al*., 2006; Izu *et al*., 2011). Indeed, genetic loss of *col1a1a* function, a Collagen predominantly expressed in the actinotrichia-forming cells, results in aberrant lepidotrichia pattern and reduced ossification during caudal fin regeneration (Duran *et al*., 2011). Therefore, Wnt/β–catenin signaling in the actinotrichia-forming cells might indirectly direct osteoblasts maturation via regulation of the ECM composition.

While I cannot rule out a role of Wnt/β–catenin signaling in osteoblasts, the dermal bone found in fish fins has been suggested to be distinct from other skeletal tissues based on morphological and gene expression characteristics (Mari-Beffa *et al*., 2007). Furthermore, little is known about the role of Wnt signaling in skeletogenesis during fish embryonic development. Thus, it remains to be determined whether lack of a direct role of β–catenin signaling in osteoblasts observed here reflects a general difference in skeletal development between fish and mammals, is a special feature of the fin ray bones during development and regeneration, or occurs only during regeneration. Yet, I suggest that Wnt/β–catenin signaling exerts a dual role during fin regeneration similar to limb development where the distal domain of Wnt signaling promotes proliferation of mesenchymal progenitors, while the proximal domains induce osteoblast maturation.

In summary, the study presented here greatly expands our knowledge about the molecular mechanisms regulating zebrafish appendage regeneration, since it

1) uncovers previously unknown organizing centers that direct cellular behavior of adjacent tissues in the regenerating caudal fin
2) identifies Wnt/β–catenin signaling as a crucial signal in specifying these signaling centers by regulating most other developmental signaling pathway known to be required for regeneration
3) hints at parallels, yet interesting differences in the role of Wnt signaling in bone formation between regeneration and development.

These findings may have implications in regenerative medicine.

6 References

Akimenko, M.A., Johnson, S.L., Westerfield, M., and Ekker, M. (1995). Differential induction of four msx homeobox genes during fin development and regeneration in zebrafish. Development *121*, 347-357.

Ando, R., Hama, H., Yamamoto-Hino, M., Mizuno, H., and Miyawaki, A. (2002). An optical marker based on the UV-induced green-to-red photoconversion of a fluorescent protein. Proc Natl Acad Sci U S A *99*, 12651-12656.

Angers, S., and Moon, R.T. (2009). Proximal events in Wnt signal transduction. Nature reviews Molecular cell biology *10*, 468-477.

Arce, L., Yokoyama, N.N., and Waterman, M.L. (2006). Diversity of LEF/TCF action in development and disease. Oncogene *25*, 7492-7504.

Azevedo, A.S., Grotek, B., Jacinto, A., Weidinger, G., and Saude, L. (2011). The regenerative capacity of the zebrafish caudal fin is not affected by repeated amputations. PLoS One *6*, e22820.

Banziger, C., Soldini, D., Schutt, C., Zipperlen, P., Hausmann, G., and Basler, K. (2006). Wntless, a conserved membrane protein dedicated to the secretion of Wnt proteins from signaling cells. Cell *125*, 509-522.

Bartscherer, K., and Boutros, M. (2008). Regulation of Wnt protein secretion and its role in gradient formation. EMBO Rep *9*, 977-982.

Bartscherer, K., Pelte, N., Ingelfinger, D., and Boutros, M. (2006). Secretion of Wnt ligands requires Evi, a conserved transmembrane protein. Cell *125*, 523-533.

Blum, N., and Begemann, G. (2012). Retinoic acid signaling controls the formation, proliferation and survival of the blastema during adult zebrafish fin regeneration. Development *139*, 107-116.

Bode, H.R. (2009). Axial patterning in hydra. Cold Spring Harb Perspect Biol *1*, a000463.

Boulter, L., Govaere, O., Bird, T.G., Radulescu, S., Ramachandran, P., Pellicoro, A., Ridgway, R.A., Seo, S.S., Spee, B., Van Rooijen, N.*, et al.* (2012). Macrophage-derived Wnt opposes Notch signaling to specify hepatic progenitor cell fate in chronic liver disease. Nature medicine *18*, 572-579.

Brack, A.S., Conboy, I.M., Conboy, M.J., Shen, J., and Rando, T.A. (2008). A temporal switch from notch to Wnt signaling in muscle stem cells is necessary for normal adult myogenesis. Cell stem cell *2*, 50-59.

Broun, M., Gee, L., Reinhardt, B., and Bode, H.R. (2005). Formation of the head organizer in hydra involves the canonical Wnt pathway. Development *132*, 2907-2916.

Brown, A.M., Fisher, S., and Iovine, M.K. (2009). Osteoblast maturation occurs in overlapping proximal-distal compartments during fin regeneration in zebrafish. Dev Dyn *238*, 2922-2928.

Bruhn, L., Munnerlyn, A., and Grosschedl, R. (1997). ALY, a context-dependent coactivator of LEF-1 and AML-1, is required for TCRalpha enhancer function. Genes Dev *11*, 640-653.

Chablais, F., and Jazwinska, A. (2010). IGF signaling between blastema and wound epidermis is required for fin regeneration. Development *137*, 871-879.

Chera, S., Ghila, L., Dobretz, K., Wenger, Y., Bauer, C., Buzgariu, W., Martinou, J.C., and Galliot, B. (2009). Apoptotic cells provide an unexpected source of Wnt3 signaling to drive hydra head regeneration. Dev Cell *17*, 279-289.

Chocron, S., Verhoeven, M.C., Rentzsch, F., Hammerschmidt, M., and Bakkers, J. (2007). Zebrafish Bmp4 regulates left-right asymmetry at two distinct developmental time points. Dev Biol *305*, 577-588.

Clevers, H., and Nusse, R. (2012). Wnt/beta-catenin signaling and disease. Cell *149*, 1192-1205.

Cruciat, C.M., and Niehrs, C. (2013). Secreted and transmembrane Wnt inhibitors and activators. Cold Spring Harbor perspectives in medicine *3*, a015081.

Dorsky, R.I., Sheldahl, L.C., and Moon, R.T. (2002). A transgenic Lef1/beta-catenin-dependent reporter is expressed in spatially restricted domains throughout zebrafish development. Dev Biol *241*, 229-237.

Du, S.J., Purcell, S.M., Christian, J.L., McGrew, L.L., and Moon, R.T. (1995). Identification of distinct classes and functional domains of Wnts through expression of wild-type and chimeric proteins in Xenopus embryos. Mol Cell Biol *15*, 2625-2634.

Duncan, A.W., Dorrell, C., and Grompe, M. (2009). Stem cells and liver regeneration. Gastroenterology *137*, 466-481.

Duran, I., Mari-Beffa, M., Santamaria, J.A., Becerra, J., and Santos-Ruiz, L. (2011). Actinotrichia collagens and their role in fin formation. Dev Biol *354*, 160-172.

Engler, A.J., Sen, S., Sweeney, H.L., and Discher, D.E. (2006). Matrix elasticity directs stem cell lineage specification. Cell *126*, 677-689.

Fernandez-Teran, M., and Ros, M.A. (2008). The Apical Ectodermal Ridge: morphological aspects and signaling pathways. Int J Dev Biol *52*, 857-871.

Filali, M., Cheng, N., Abbott, D., Leontiev, V., and Engelhardt, J.F. (2002). Wnt-3A/beta-catenin signaling induces transcription from the LEF-1 promoter. The Journal of biological chemistry *277*, 33398-33410.

Fung, Y.K., Shackleford, G.M., Brown, A.M., Sanders, G.S., and Varmus, H.E. (1985). Nucleotide sequence and expression in vitro of cDNA derived from mRNA of int-1, a provirally activated mouse mammary oncogene. Mol Cell Biol *5*, 3337-3344.

Gauron, C., Rampon, C., Bouzaffour, M., Ipendey, E., Teillon, J., Volovitch, M., and Vriz, S. (2013). Sustained production of ROS triggers compensatory proliferation and is required for regeneration to proceed. Scientific reports *3*, 2084.

Geraudie, J., Monnot, M.J., Brulfert, A., and Ferretti, P. (1995). Caudal fin regeneration in wild type and long-fin mutant zebrafish is affected by retinoic acid. Int J Dev Biol *39*, 373-381.

Gierer, A., Berking, S., Bode, H., David, C.N., Flick, K., Hansmann, G., Schaller, H., and Trenkner, E. (1972). Regeneration of hydra from reaggregated cells. Nature: New biology *239*, 98-101.

Gong, Z., Ju, B., Wang, X., He, J., Wan, H., Sudha, P.M., and Yan, T. (2002). Green fluorescent protein expression in germ-line transmitted transgenic zebrafish under a stratified epithelial promoter from keratin8. Dev Dyn *223*, 204-215.

Goodman, R.M., Thombre, S., Firtina, Z., Gray, D., Betts, D., Roebuck, J., Spana, E.P., and Selva, E.M. (2006). Sprinter: a novel transmembrane protein required for Wg secretion and signaling. Development *133*, 4901-4911.

Grotek, B., Wehner, D., and Weidinger, G. (2013). Notch signaling coordinates cellular proliferation with differentiation during zebrafish fin regeneration. Development *140*, 1412-1423.

Gurley, K.A., Rink, J.C., and Sanchez Alvarado, A. (2008). Beta-catenin defines head versus tail identity during planarian regeneration and homeostasis. Science *319*, 323-327.

He, X., Semenov, M., Tamai, K., and Zeng, X. (2004). LDL receptor-related proteins 5 and 6 in Wnt/beta-catenin signaling: arrows point the way. Development *131*, 1663-1677.

Hofmann, K. (2000). A superfamily of membrane-bound O-acyltransferases with implications for wnt signaling. Trends Biochem Sci *25*, 111-112.

Holstein, T.W. (2012). The evolution of the Wnt pathway. Cold Spring Harb Perspect Biol *4*, a007922.

Hoppler, S., and Kavanagh, C.L. (2007). Wnt signalling: variety at the core. Journal of cell science *120*, 385-393.

Hovanes, K., Li, T.W., Munguia, J.E., Truong, T., Milovanovic, T., Lawrence Marsh, J., Holcombe, R.F., and Waterman, M.L. (2001). Beta-catenin-sensitive isoforms of lymphoid enhancer factor-1 are selectively expressed in colon cancer. Nat Genet *28*, 53-57.

Hsu, S.C., Galceran, J., and Grosschedl, R. (1998). Modulation of transcriptional regulation by LEF-1 in response to Wnt-1 signaling and association with beta-catenin. Mol Cell Biol *18*, 4807-4818.

Huang, C.J., Jou, T.S., Ho, Y.L., Lee, W.H., Jeng, Y.T., Hsieh, F.J., and Tsai, H.J. (2005). Conditional expression of a myocardium-specific transgene in zebrafish transgenic lines. Dev Dyn *233*, 1294-1303.

Huang da, W., Sherman, B.T., and Lempicki, R.A. (2009). Systematic and integrative analysis of large gene lists using DAVID bioinformatics resources. Nature protocols *4*, 44-57.

Ishida, T., Nakajima, T., Kudo, A., and Kawakami, A. (2010). Phosphorylation of Junb family proteins by the Jun N-terminal kinase supports tissue regeneration in zebrafish. Dev Biol *340*, 468-479.

Izu, Y., Sun, M., Zwolanek, D., Veit, G., Williams, V., Cha, B., Jepsen, K.J., Koch, M., and Birk, D.E. (2011). Type XII collagen regulates osteoblast polarity and communication during bone formation. J Cell Biol *193*, 1115-1130.

Jazwinska, A., Badakov, R., and Keating, M.T. (2007). Activin-betaA signaling is required for zebrafish fin regeneration. Curr Biol *17*, 1390-1395.

Jho, E.H., Zhang, T., Domon, C., Joo, C.K., Freund, J.N., and Costantini, F. (2002). Wnt/beta-catenin/Tcf signaling induces the transcription of Axin2, a negative regulator of the signaling pathway. Mol Cell Biol *22*, 1172-1183.

Johnson, S.L., and Weston, J.A. (1995). Temperature-sensitive mutations that cause stage-specific defects in Zebrafish fin regeneration. Genetics *141*, 1583-1595.

Jopling, C., Sleep, E., Raya, M., Marti, M., Raya, A., and Izpisua Belmonte, J.C. (2010). Zebrafish heart regeneration occurs by cardiomyocyte dedifferentiation and proliferation. Nature *464*, 606-609.

Kadowaki, T., Wilder, E., Klingensmith, J., Zachary, K., and Perrimon, N. (1996). The segment polarity gene porcupine encodes a putative multitransmembrane protein involved in Wingless processing. Genes Dev *10*, 3116-3128.

Kagermeier-Schenk, B., Wehner, D., Ozhan-Kizil, G., Yamamoto, H., Li, J., Kirchner, K., Hoffmann, C., Stern, P., Kikuchi, A., Schambony, A*., et al.* (2011). Waif1/5T4 inhibits Wnt/beta-catenin signaling and activates noncanonical Wnt pathways by modifying LRP6 subcellular localization. Dev Cell *21*, 1129-1143.

Kawakami, Y., Rodriguez Esteban, C., Raya, M., Kawakami, H., Marti, M., Dubova, I., and Izpisua Belmonte, J.C. (2006). Wnt/beta-catenin signaling regulates vertebrate limb regeneration. Genes Dev *20*, 3232-3237.

King, R.S., and Newmark, P.A. (2012). The cell biology of regeneration. J Cell Biol *196*, 553-562.

Knopf, F., Hammond, C., Chekuru, A., Kurth, T., Hans, S., Weber, C.W., Mahatma, G., Fisher, S., Brand, M., Schulte-Merker, S.*, et al.* (2011). Bone regenerates via dedifferentiation of osteoblasts in the zebrafish fin. Dev Cell *20*, 713-724.

Knopf, F., Schnabel, K., Haase, C., Pfeifer, K., Anastassiadis, K., and Weidinger, G. (2010). Dually inducible TetON systems for tissue-specific conditional gene expression in zebrafish. Proc Natl Acad Sci U S A *107*, 19933-19938.

Komekado, H., Yamamoto, H., Chiba, T., and Kikuchi, A. (2007). Glycosylation and palmitoylation of Wnt-3a are coupled to produce an active form of Wnt-3a. Genes Cells *12*, 521-534.

Koopman, P. (2010). HMG Domain Superfamily of DNAbending Proteins: HMG, UBF, TCF, LEF, SOX, SRY and Related Proteins. Encyclopedia of Life Sciences (ELS) *John Wiley & Sons, Ltd: Chichester.*

Kratochwil, K., Dull, M., Farinas, I., Galceran, J., and Grosschedl, R. (1996). Lef1 expression is activated by BMP-4 and regulates inductive tissue interactions in tooth and hair development. Genes Dev *10*, 1382-1394.

Kurayoshi, M., Yamamoto, H., Izumi, S., and Kikuchi, A. (2007). Post-translational palmitoylation and glycosylation of Wnt-5a are necessary for its signalling. Biochem J *402*, 515-523.

Kusserow, A., Pang, K., Sturm, C., Hrouda, M., Lentfer, J., Schmidt, H.A., Technau, U., von Haeseler, A., Hobmayer, B., Martindale, M.Q.*, et al.* (2005). Unexpected complexity of the Wnt gene family in a sea anemone. Nature *433*, 156-160.

Kyritsis, N., Kizil, C., Zocher, S., Kroehne, V., Kaslin, J., Freudenreich, D., Iltzsche, A., and Brand, M. (2012). Acute inflammation initiates the regenerative response in the adult zebrafish brain. Science *338*, 1353-1356.

Labbe, E., Letamendia, A., and Attisano, L. (2000). Association of Smads with lymphoid enhancer binding factor 1/T cell-specific factor mediates cooperative signaling by the transforming growth factor-beta and wnt pathways. Proc Natl Acad Sci U S A *97*, 8358-8363.

Laforest, L., Brown, C.W., Poleo, G., Geraudie, J., Tada, M., Ekker, M., and Akimenko, M.A. (1998). Involvement of the sonic hedgehog, patched 1 and bmp2 genes in patterning of the zebrafish dermal fin rays. Development *125*, 4175-4184.

Langfelder, P., and Horvath, S. (2008). WGCNA: an R package for weighted correlation network analysis. BMC bioinformatics *9*, 559.

Lee, Y., Grill, S., Sanchez, A., Murphy-Ryan, M., and Poss, K.D. (2005). Fgf signaling instructs position-dependent growth rate during zebrafish fin regeneration. Development *132*, 5173-5183.

Lee, Y., Hami, D., De Val, S., Kagermeier-Schenk, B., Wills, A.A., Black, B.L., Weidinger, G., and Poss, K.D. (2009). Maintenance of blastemal proliferation by functionally diverse epidermis in regenerating zebrafish fins. Dev Biol *331*, 270-280.

Lehoczky, J.A., Robert, B., and Tabin, C.J. (2011). Mouse digit tip regeneration is mediated by fate-restricted progenitor cells. Proc Natl Acad Sci U S A *108*, 20609-20614.

Li, T.W., Ting, J.H., Yokoyama, N.N., Bernstein, A., van de Wetering, M., and Waterman, M.L. (2006). Wnt activation and alternative promoter repression of LEF1 in colon cancer. Mol Cell Biol *26*, 5284-5299.

Lin, G., and Slack, J.M. (2008). Requirement for Wnt and FGF signaling in Xenopus tadpole tail regeneration. Dev Biol *316*, 323-335.

Logan, C.Y., and Nusse, R. (2004). The Wnt signaling pathway in development and disease. Annu Rev Cell Dev Biol *20*, 781-810.

Long, F. (2012). Building strong bones: molecular regulation of the osteoblast lineage. Nature reviews Molecular cell biology *13*, 27-38.

Love, N.R., Chen, Y., Ishibashi, S., Kritsiligkou, P., Lea, R., Koh, Y., Gallop, J.L., Dorey, K., and Amaya, E. (2013). Amputation-induced reactive oxygen species are required for successful Xenopus tadpole tail regeneration. Nat Cell Biol *15*, 222-228.

Lu, J., Ma, Z., Hsieh, J.C., Fan, C.W., Chen, B., Longgood, J.C., Williams, N.S., Amatruda, J.F., Lum, L., and Chen, C. (2009). Structure-activity relationship studies of small-molecule inhibitors of Wnt response. Bioorganic & medicinal chemistry letters *19*, 3825-3827.

Lustig, B., Jerchow, B., Sachs, M., Weiler, S., Pietsch, T., Karsten, U., van de Wetering, M., Clevers, H., Schlag, P.M., Birchmeier, W.*, et al.* (2002). Negative feedback loop of Wnt signaling through upregulation of conductin/axin2 in colorectal and liver tumors. Mol Cell Biol *22*, 1184-1193.

MacDonald, B.T., Semenov, M.V., Huang, H., and He, X. (2011). Dissecting molecular differences between Wnt coreceptors LRP5 and LRP6. PLoS One *6*, e23537.

MacDonald, B.T., Tamai, K., and He, X. (2009). Wnt/beta-catenin signaling: components, mechanisms, and diseases. Dev Cell *17*, 9-26.

Mari-Beffa, M., Santamaria, J.A., Murciano, C., Santos-Ruiz, L., Andrades, J.A., Guerado, E., and Becerra, J. (2007). Zebrafish fins as a model system for skeletal human studies. TheScientificWorldJournal *7*, 1114-1127.

Mason, B.N.C., J. P. and Reinhart-King, C. A (2012). Matrix Stiffness: A Regulator of Cellular Behavior and Tissue Formation

Novel Technologies for Clinical Applications. In Engineering Biomaterials for Regenerative Medicine, S.K. Bhatia, ed. (Springer), pp. 19-37.

Mathew, L.K., Sengupta, S., Franzosa, J.A., Perry, J., La Du, J., Andreasen, E.A., and Tanguay, R.L. (2009). Comparative expression profiling reveals an essential role for raldh2 in epimorphic regeneration. The Journal of biological chemistry *284*, 33642-33653.

Mayall, T.P., Sheridan, P.L., Montminy, M.R., and Jones, K.A. (1997). Distinct roles for P-CREB and LEF-1 in TCR alpha enhancer assembly and activation on chromatin templates in vitro. Genes Dev *11*, 887-899.

McMahon, A.P., and Moon, R.T. (1989). Ectopic expression of the proto-oncogene int-1 in Xenopus embryos leads to duplication of the embryonic axis. Cell *58*, 1075-1084.

Moro, E., Ozhan-Kizil, G., Mongera, A., Beis, D., Wierzbicki, C., Young, R.M., Bournele, D., Domenichini, A., Valdivia, L.E., Lum, L.*, et al.* (2012). In vivo Wnt signaling tracing through a transgenic biosensor fish reveals novel activity domains. Dev Biol.

Morrison, J.I., Loof, S., He, P., and Simon, A. (2006). Salamander limb regeneration involves the activation of a multipotent skeletal muscle satellite cell population. J Cell Biol *172*, 433-440.

Mosimann, C., Kaufman, C.K., Li, P., Pugach, E.K., Tamplin, O.J., and Zon, L.I. (2011). Ubiquitous transgene expression and Cre-based recombination driven by the ubiquitin promoter in zebrafish. Development *138*, 169-177.

Mulligan, K.A., Fuerer, C., Ching, W., Fish, M., Willert, K., and Nusse, R. (2012). Secreted Wingless-interacting molecule (Swim) promotes long-range signaling by maintaining Wingless solubility. Proc Natl Acad Sci U S A *109*, 370-377.

Munch, J., Gonzalez-Rajal, A., and de la Pompa, J.L. (2013). Notch regulates blastema proliferation and prevents differentiation during adult zebrafish fin regeneration. Development.

Nagayoshi, S., Hayashi, E., Abe, G., Osato, N., Asakawa, K., Urasaki, A., Horikawa, K., Ikeo, K., Takeda, H., and Kawakami, K. (2008). Insertional mutagenesis by the Tol2 transposon-mediated enhancer trap approach generated mutations in two developmental genes: tcf7 and synembryn-like. Development *135*, 159-169.

Nawshad, A., and Hay, E.D. (2003). TGFbeta3 signaling activates transcription of the LEF1 gene to induce epithelial mesenchymal transformation during mouse palate development. J Cell Biol *163*, 1291-1301.

Nechiporuk, A., and Keating, M.T. (2002). A proliferation gradient between proximal and msxb-expressing distal blastema directs zebrafish fin regeneration. Development *129*, 2607-2617.

Nejak-Bowen, K.N., and Monga, S.P. (2011). Beta-catenin signaling, liver regeneration and hepatocellular cancer: sorting the good from the bad. Seminars in cancer biology *21*, 44-58.

Nichols, S.A., Dirks, W., Pearse, J.S., and King, N. (2006). Early evolution of animal cell signaling and adhesion genes. Proc Natl Acad Sci U S A *103*, 12451-12456.

Niethammer, P., Grabher, C., Look, A.T., and Mitchison, T.J. (2009). A tissue-scale gradient of hydrogen peroxide mediates rapid wound detection in zebrafish. Nature *459*, 996-999.

Nikaido, M., Law, E.W., and Kelsh, R.N. (2013). A systematic survey of expression and function of zebrafish frizzled genes. PLoS One *8*, e54833.

Norton, W.H., Ledin, J., Grandel, H., and Neumann, C.J. (2005). HSPG synthesis by zebrafish Ext2 and Extl3 is required for Fgf10 signalling during limb development. Development *132*, 4963-4973.

Nusse, R., and Varmus, H.E. (1982). Many tumors induced by the mouse mammary tumor virus contain a provirus integrated in the same region of the host genome. Cell *31*, 99-109.

Otto, A., Schmidt, C., Luke, G., Allen, S., Valasek, P., Muntoni, F., Lawrence-Watt, D., and Patel, K. (2008). Canonical Wnt signalling induces satellite-cell proliferation during adult skeletal muscle regeneration. Journal of cell science *121*, 2939-2950.

Pellettieri, J., Fitzgerald, P., Watanabe, S., Mancuso, J., Green, D.R., and Sanchez Alvarado, A. (2010). Cell death and tissue remodeling in planarian regeneration. Dev Biol *338*, 76-85.

Poss, K.D. (2010). Advances in understanding tissue regenerative capacity and mechanisms in animals. Nature reviews Genetics *11*, 710-722.

Poss, K.D., Keating, M.T., and Nechiporuk, A. (2003). Tales of regeneration in zebrafish. Dev Dyn *226*, 202-210.

Poss, K.D., Nechiporuk, A., Hillam, A.M., Johnson, S.L., and Keating, M.T. (2002). Mps1 defines a proximal blastemal proliferative compartment essential for zebrafish fin regeneration. Development *129*, 5141-5149.

Poss, K.D., Shen, J., and Keating, M.T. (2000a). Induction of lef1 during zebrafish fin regeneration. Dev Dyn *219*, 282-286.

Poss, K.D., Shen, J., Nechiporuk, A., McMahon, G., Thisse, B., Thisse, C., and Keating, M.T. (2000b). Roles for Fgf signaling during zebrafish fin regeneration. Dev Biol *222*, 347-358.

Quint, E., Smith, A., Avaron, F., Laforest, L., Miles, J., Gaffield, W., and Akimenko, M.A. (2002). Bone patterning is altered in the regenerating zebrafish caudal fin after ectopic expression of sonic hedgehog and bmp2b or exposure to cyclopamine. Proc Natl Acad Sci U S A *99*, 8713-8718.

Reddien, P.W., and Sanchez Alvarado, A. (2004). Fundamentals of planarian regeneration. Annu Rev Cell Dev Biol *20*, 725-757.

Regard, J.B., Zhong, Z., Williams, B.O., and Yang, Y. (2012). Wnt signaling in bone development and disease: making stronger bone with Wnts. Cold Spring Harb Perspect Biol *4*.

Rinkevich, Y., Lindau, P., Ueno, H., Longaker, M.T., and Weissman, I.L. (2011). Germ-layer and lineage-restricted stem/progenitors regenerate the mouse digit tip. Nature *476*, 409-413.

Ross, D.A., and Kadesch, T. (2001). The notch intracellular domain can function as a coactivator for LEF-1. Mol Cell Biol *21*, 7537-7544.

Salo, E. (2006). The power of regeneration and the stem-cell kingdom: freshwater planarians (platyhelminthes). BioEssays : news and reviews in molecular, cellular and developmental biology *28*, 546-559.

Shimizu, H., Julius, M.A., Giarre, M., Zheng, Z., Brown, A.M., and Kitajewski, J. (1997). Transformation by Wnt family proteins correlates with regulation of beta-catenin. Cell Growth Differ *8*, 1349-1358.

Shimizu, N., Kawakami, K., and Ishitani, T. (2012). Visualization and exploration of Tcf/Lef function using a highly responsive Wnt/beta-catenin signaling-reporter transgenic zebrafish. Dev Biol *370*, 71-85.

Singh, B.N., Doyle, M.J., Weaver, C.V., Koyano-Nakagawa, N., and Garry, D.J. (2012). Hedgehog and Wnt coordinate signaling in myogenic progenitors and regulate limb regeneration. Dev Biol *371*, 23-34.

Smith, A., Avaron, F., Guay, D., Padhi, B.K., and Akimenko, M.A. (2006). Inhibition of BMP signaling during zebrafish fin regeneration disrupts fin growth and scleroblasts differentiation and function. Dev Biol *299*, 438-454.

Smyth, G.K., Michaud, J., and Scott, H.S. (2005). Use of within-array replicate spots for assessing differential expression in microarray experiments. Bioinformatics *21*, 2067-2075.

Sousa, S., Afonso, N., Bensimon-Brito, A., Fonseca, M., Simoes, M., Leon, J., Roehl, H., Cancela, M.L., and Jacinto, A. (2011). Differentiated skeletal cells contribute to blastema formation during zebrafish fin regeneration. Development *138*, 3897-3905.

Spoorendonk, K.M., Peterson-Maduro, J., Renn, J., Trowe, T., Kranenbarg, S., Winkler, C., and Schulte-Merker, S. (2008). Retinoic acid and Cyp26b1 are critical regulators of osteogenesis in the axial skeleton. Development *135*, 3765-3774.

Stoick-Cooper, C.L., Moon, R.T., and Weidinger, G. (2007a). Advances in signaling in vertebrate regeneration as a prelude to regenerative medicine. Genes Dev *21*, 1292-1315.

Stoick-Cooper, C.L., Weidinger, G., Riehle, K.J., Hubbert, C., Major, M.B., Fausto, N., and Moon, R.T. (2007b). Distinct Wnt signaling pathways have opposing roles in appendage regeneration. Development *134*, 479-489.

Suster, M.L., Kikuta, H., Urasaki, A., Asakawa, K., and Kawakami, K. (2009). Transgenesis in zebrafish with the tol2 transposon system. Methods Mol Biol *561*, 41-63.

Takeo, M., Chou, W.C., Sun, Q., Lee, W., Rabbani, P., Loomis, C., Taketo, M.M., and Ito, M. (2013). Wnt activation in nail epithelium couples nail growth to digit regeneration. Nature.

ten Berge, D., Brugmann, S.A., Helms, J.A., and Nusse, R. (2008). Wnt and FGF signals interact to coordinate growth with cell fate specification during limb development. Development *135*, 3247-3257.

Thermes, V., Grabher, C., Ristoratore, F., Bourrat, F., Choulika, A., Wittbrodt, J., and Joly, J.S. (2002). I-SceI meganuclease mediates highly efficient transgenesis in fish. Mech Dev *118*, 91-98.

Traver, D., Winzeler, A., Stern, H.M., Mayhall, E.A., Langenau, D.M., Kutok, J.L., Look, A.T., and Zon, L.I. (2004). Effects of lethal irradiation in zebrafish and rescue by hematopoietic cell transplantation. Blood *104*, 1298-1305.

Tseng, A.S., Adams, D.S., Qiu, D., Koustubhan, P., and Levin, M. (2007). Apoptosis is required during early stages of tail regeneration in Xenopus laevis. Dev Biol *301*, 62-69.

Tu, S., and Johnson, S.L. (2011). Fate restriction in the growing and regenerating zebrafish fin. Dev Cell *20*, 725-732.

van Amerongen, R. (2012). Alternative Wnt pathways and receptors. Cold Spring Harb Perspect Biol *4*.

van den Heuvel, M., Harryman-Samos, C., Klingensmith, J., Perrimon, N., and Nusse, R. (1993). Mutations in the segment polarity genes wingless and porcupine impair secretion of the wingless protein. EMBO J *12*, 5293-5302.

Veien, E.S., Grierson, M.J., Saund, R.S., and Dorsky, R.I. (2005). Expression pattern of zebrafish tcf7 suggests unexplored domains of Wnt/beta-catenin activity. Dev Dyn *233*, 233-239.

Wang, Y.H., Chen, Y.H., Lin, Y.J., and Tsai, H.J. (2006). Spatiotemporal expression of zebrafish keratin 18 during early embryogenesis and the establishment of a keratin 18:RFP transgenic line. Gene expression patterns : GEP *6*, 335-339.

Warsito, D., Sjostrom, S., Andersson, S., Larsson, O., and Sehat, B. (2012). Nuclear IGF1R is a transcriptional co-activator of LEF1/TCF. EMBO Rep *13*, 244-250.

Wehrli, M., Dougan, S.T., Caldwell, K., O'Keefe, L., Schwartz, S., Vaizel-Ohayon, D., Schejter, E., Tomlinson, A., and DiNardo, S. (2000). arrow encodes an LDL-receptor-related protein essential for Wingless signalling. Nature *407*, 527-530.

Weidinger, G., Thorpe, C.J., Wuennenberg-Stapleton, K., Ngai, J., and Moon, R.T. (2005). The Sp1-related transcription factors sp5 and sp5-like act downstream of Wnt/beta-catenin signaling in mesoderm and neuroectoderm patterning. Curr Biol *15*, 489-500.

Westerfield, M. (2000). The zebrafish book : a guide for the laboratory use of zebrafish (Danio rerio), 4th edn (Univ. of Oregon Press, Eugene, OR: M. Westerfield).

White, J.A., Boffa, M.B., Jones, B., and Petkovich, M. (1994). A zebrafish retinoic acid receptor expressed in the regenerating caudal fin. Development *120*, 1861-1872.

Whitehead, G.G., Makino, S., Lien, C.L., and Keating, M.T. (2005). fgf20 is essential for initiating zebrafish fin regeneration. Science *310*, 1957-1960.

Whyte, J.L., Smith, A.A., and Helms, J.A. (2012). Wnt signaling and injury repair. Cold Spring Harb Perspect Biol *4*, a008078.

Willert, K., Brown, J.D., Danenberg, E., Duncan, A.W., Weissman, I.L., Reya, T., Yates, J.R., 3rd, and Nusse, R. (2003). Wnt proteins are lipid-modified and can act as stem cell growth factors. Nature *423*, 448-452.

Willert, K., and Nusse, R. (2012). Wnt proteins. Cold Spring Harb Perspect Biol *4*, a007864.

Wong, G.T., Gavin, B.J., and McMahon, A.P. (1994). Differential transformation of mammary epithelial cells by Wnt genes. Mol Cell Biol *14*, 6278-6286.

Yamamoto, H., Sakane, H., Yamamoto, H., Michiue, T., and Kikuchi, A. (2008). Wnt3a and Dkk1 regulate distinct internalization pathways of LRP6 to tune the activation of beta-catenin signaling. Dev Cell *15*, 37-48.

Yeo, S.Y., Kim, M., Kim, H.S., Huh, T.L., and Chitnis, A.B. (2007). Fluorescent protein expression driven by her4 regulatory elements reveals the spatiotemporal pattern of Notch signaling in the nervous system of zebrafish embryos. Dev Biol *301*, 555-567.

Yokoyama, H., Ogino, H., Stoick-Cooper, C.L., Grainger, R.M., and Moon, R.T. (2007). Wnt/beta-catenin signaling has an essential role in the initiation of limb regeneration. Dev Biol *306*, 170-178.

Yoo, S.K., Freisinger, C.M., LeBert, D.C., and Huttenlocher, A. (2012). Early redox, Src family kinase, and calcium signaling integrate wound responses and tissue regeneration in zebrafish. J Cell Biol *199*, 225-234.

Zeller, R., Lopez-Rios, J., and Zuniga, A. (2009). Vertebrate limb bud development: moving towards integrative analysis of organogenesis. Nature reviews Genetics *10*, 845-858.

Zhang, J., Wagh, P., Guay, D., Sanchez-Pulido, L., Padhi, B.K., Korzh, V., Andrade-Navarro, M.A., and Akimenko, M.A. (2010). Loss of fish actinotrichia proteins and the fin-to-limb transition. Nature *466*, 234-237.

Zhang, R., Han, P., Yang, H., Ouyang, K., Lee, D., Lin, Y.F., Ocorr, K., Kang, G., Chen, J., Stainier, D.Y.*, et al.* (2013). In vivo cardiac reprogramming contributes to zebrafish heart regeneration. Nature.

7 Acknowledgements

At this point I would like to use the opportunity to thank the following persons for their commitment and support. I wish to express my gratitude to **Prof. Dr. Gilbert Weidinger** for the chance to join his excellent research laboratory, his supervision, and his support throughout this (and other) project(s). I truly learned a lot! I also would like to acknowledge him for his contribution to the generation of the *sp7*, *her4.3 and keratin4* TetActivator lines and the microarray & WGCNA analysis. I am grateful to **Prof. Dr. Michael Kühl** and **Prof. Dr. Thomas Wirth** for reviewing my thesis. I would like to acknowledge **Christa Haase** for the generation of the *sp7*, *her4.3 and keratin4* TetActivator lines as well as for generation of the *keratin18* TetActivator construct, **Dr. Birgit Kagermeier-Schenk** for the microarray analysis and **Mohankrishna Dalvoy Vasudevaro** for his contribution to the WGCNA analysis and for providing me with Figures and Tables associated with the WGCNA analysis. I am very thankful to **Ellen Geibelt, Markus Burkhardt** and **Carmen Hauser** who have provided support and guidance during light and laser scanning microscopy experiments. Many thanks to **Nicole Rund** for assistance during the flow cytometry, to the **Dresden Genome Center** for the deep-sequencing-based gene expression profiling and to **Dr. Nona Shayegi** for irradiation of the adult zebrafish. Thanks to all former and present **members of the Gilbert Weidinger** and **Christopher Antos laboratory**, especially **Dr. Günes Özhan** and **René Bernitz** for fruitful discussions and consistently aiding my progress. Many thanks also to **all members of the Institute for Biochemistry and Molecular Biology at the Ulm University** and also to **Prof. Dr. Michael Brand**, **Dr. Stefan Hans**, **Peggy Jungke** and **Vanessa Carlos** from the Technische Universität Dresden for their support. Finally I would like to thank **my family**, **partner** and **friends** for supporting me throughout the last years and their infinite endurance in listening to my major and minor problems that arose during this time.

8 Curriculum Vitae

Der Lebenslauf wurde aus datenschutzrechtlichen Gründen aus diesem Dokument entfernt.

9 Erklärung (Statement of Original Contribution)

•I herewith declare that I have produced this thesis without the prohibited assistance of third parties and without making use of aids other than those specified; notions taken over directly or indirectly from other sources have been identified as such. This paper has not previously been presented in identical or similar form to any other German or foreign examination board.

The thesis work was conducted from November 2009 to July 2013 under the supervision of Prof. Dr. Michael Kühl in the research group of Prof. Dr. Gilbert Weidinger, at the Biotechnology Center of the Technische Universität Dresden and at the Institute for Biochemistry and Molecular Biology of the Ulm University.

I declare that I have not undertaken any previous unsuccessful doctorate proceedings.

I declare that I recognize the doctorate regulations of the Fakultät für Naturwissenschaften of the Ulm University.

•Ich versichere hiermit, dass ich die Arbeit selbständig angefertigt habe und keine anderen als die angegebenen Quellen und Hilfsmittel benutzt sowie die wörtlich oder inhaltlich übernommenen Stellen als solche kenntlich gemacht habe. Die Arbeit wurde bisher weder im Inland noch im Ausland in gleicher oder ähnlicher Form einer anderen Prüfungsbehörde vorgelegt.

Die Dissertation wurde von Prof. Dr. Michael Kühl, Institut für Biochemie und Molekularbiologie, Universität Ulm, in der Arbeitsgruppe von Prof. Dr. Gilbert Weidinger am Biotechnologischen Zentrum, Technische Universität Dresden und am Institut für Biochemie und Molekularbiologie, Universität Ulm, betreut und im Zeitraum vom 11/2009 bis 07/2013 verfasst.

Meine Person betreffend erkläre ich hiermit, dass keine früheren erfolglosen Promotionsverfahren stattgefunden haben.

Ich erkenne die Promotionsordnung der Fakultät für Naturwissenschaften, Universität Ulm an.

10 Supplemental Information

Suppl. file *1_M_values.xlsx (Part 1 & 2)*

Suppl. file *2_Differentially_expressed_genes.xlsx*

Suppl. file *3_Module_membership.xlsx*

Suppl. file *4_Module eigengenes.xlsx*

Suppl. file *5_Eigengene adjacency.xlsx*

The supplemental files were generously provided by Mohankrishna Dalvoy Vasudevaro (Ulm University).